

1 **Review Paper: Enthalpy Relaxation and Recovery in Amorphous Materials**

2 **I.M. Hodge**

3 **Eastman Kodak Company, Imaging Research Laboratories, Rochester, NY 14650-2116**

4 **[FIRST DRAFT]**

5
6 Abstract

7 The field of enthalpy relaxation is reviewed. Current phenomenologies for dealing with the
8 nonlinear and nonexponential character of enthalpy relaxation are presented and their successes
9 and shortcomings are discussed. Qualitative experimental data and quantitative parameterizations
10 are summarized and some directions for future research are suggested.

11
12 TABLE OF CONTENTS

13	1	Introduction	3
14	1.1	Nomenclature	3
15	1.2	Kinetics of the Glass Transition	4
16	1.2.1	General aspects	4
17		Table 1	6
18		Figure One	8
19	1.2.2	Nonexponentiality	9
20	1.2.3	Nonlinearity	12
21		Figure Two	14
22	1.3	Thermodynamic Aspects of the Glass Transition	17
23	1.3.1	The Thermodynamic Case	17
24	1.3.2	Ehrenfest Relations	18
25	1.3.3	Prigogine-Defay Ratio	19
26	1.3.4	Heat Capacity at T_g	20
27	2	Experimental Techniques	21
28	2.1	Scanning Calorimetry	21
29	2.2	AC Calorimetry	23
30	3	Phenomenological Expressions	24
31	3.1	Nonexponentiality	24
32	3.2	Nonlinearity	27
33	3.2.1	Narayanaswamy-Moyhahan Equation	27
34	3.2.2	The KAHR Equation	28
35	3.2.3	Adam-Gibbs Equation	29
36	3.2.4	Free Volume Equations	32
37	3.3	Pre-exponential Factor	34
38	4	Calculation Procedures	34
39	4.1	The KAHR Method	34

40	4.2	Tool-Narayanaswamy Method	35
41	4.3	The Ngai-Rendell Method	37
42	4.4	Evaluation of Parameters from Experimental Data	40
43	4.4.1	Activation Energy	40
44	4.4.2	Pre-exponential Factor	41
45	4.4.3	Nonexponentiality	41
46	4.4.4	Nonlinearity	41
47	4.4.4.1	Annealing Method	41
48	4.4.4.2	Method of Curve Shifting	42
49	4.4.4.3	Temperature Step method	43
50	4.4.4.4	Heating Rate Dependence of T_g	43
51	4.4.4.5	Adam-Gibbs T_2	44
52	4.5	Curve Fitting Techniques	44
53	4.6	Thermal Transfer Effects and High Overshoot Data	46
54	4.7	Nonthermal Histories	46
55	4.7.1	Hydrostatic Pressure	46
56	4.7.2	Mechanical Stress and Vapor Induced Swelling	48
57	5	Experimental Methods	48
58	5.1	Scanning Calorimetry	48
59	5.1.1	Enthalpy Recovery Near T_g	48
60	5.1.2	Isothermal Annealing	49
61	5.1.3	Sub- T_g Endotherms	51
62	5.1.3.1	Thermal Histories	51
63	5.1.3.2	Nonthermal Histories	53
64	6	Enthalpy Relaxation Parameters	54
65	6.1	KAHR Equation	54
66	6.2	Narayanaswamy-Moynihan Equation	55
67		Figure Three	56
68	6.3	Adam-Gibbs-Fulcher Equation	59
69		Figure Four	61
70		Table 2	62
71	6.4	AC Calorimetry	64
72		Table 3	65
73	6.5	Parameter Correlations	65
74		Figure Five	67
75	7	Summary and Future Considerations	68
76		Figure Six	69
77	8	References	72
78			

79 1 Introduction

80 This review summarizes developments in enthalpy relaxation in amorphous materials up
 81 to the end of 1992. The field is intimately associated with the glass transition and an abbreviated
 82 account of the glass transition phenomenon is included. However a comprehensive account of
 83 the glass transition as an independent field of scientific endeavor is not attempted. Excellent
 84 accounts of the glass transition and glassy state are available [1-5].

85 The review is divided into seven sections. The introduction begins with some brief
 86 comments on nomenclature, followed by a summary of those aspects of linear response theory
 87 that provide a foundation for the nonlinear phenomenology of enthalpy relaxation, and a brief
 88 account of the kinetics of the glass transition. An account of experimental techniques is given in
 89 Section 2 with emphasis given to experimental difficulties that can affect data quality.
 90 Phenomenological equations for describing enthalpy relaxation are introduced in Section 3 and
 91 calculation procedures for implementing them are described in Section 4. Experimental results
 92 are summarized in Section 5 and enthalpy relaxation parameters are discussed in Section 6. A
 93 summary and some thoughts for future research are given in Section 7.

94
95 1.1 Nomenclature

96 Many experiments described as enthalpy relaxation would be better described as enthalpy
 97 recovery because it is the enthalpy recovered during heating that is recorded and analyzed.
 98 Enthalpy is also a retardation function rather than a relaxation one (Section 1.2.2). To be
 99 consistent with entrenched usage in the literature, however, the terms enthalpy relaxation or
 100 simply relaxation will be used here in statements of a general nature. The more precise terms
 101 ‘enthalpy recovery’ and ‘retardation times’ are used where these are specifically appropriate.
 102 Relaxation in the glassy state is referred to in the literature as structural relaxation, physical
 103 aging, stabilization or annealing. The phrase ‘structural relaxation’ refers to inferred changes in
 104 atomic arrangement that occur during relaxation, although these are not known in any detail for
 105 most materials. The term ‘physical aging’ was introduced by Struik [6] to distinguish relaxation
 106 effects from those produced by chemical reactions, degradation or changes in crystallinity. The
 107 variety of terminologies reflects the considerable practical importance of glassy state relaxation
 108 to both inorganic and organic high polymer glass science and technology. We choose the term
 109 structural relaxation here and refer to relaxation in the glassy state as annealing. Annealing time
 110 and temperature are written as t_a and T_a respectively. For convenience the supercooled liquid or
 111 rubbery state above the glass transition temperature range is referred to as the equilibrium state
 112 to distinguish it from the nonequilibrium glassy state, even though supercooled liquids and some
 113 rubbers are metastable with respect to the crystalline state (except for most atactic polymers).
 114 Differential scanning calorimetry is referred to as DSC.

115 The thermodynamic or ideal glass temperature at which excess properties such as
 116 entropy vanish is referred to in the literature as T_0 (introduced by Fulcher), T_∞ (introduced by
 117 Vogel and also used by Tamman and Hesse), T_2 (introduced by Gibbs and DiMarzio) and T_K
 118 (identified by Kauzmann). Theoretical and experimental reasons can be given for believing that
 119 T_0 , T_2 and T_K are equal for several materials (discussed below) but this belief is not uniformly
 120 accepted. Here, T_0 denotes the adjustable parameter in the empirical linear Vogel-Tamman-
 121 Fulcher equation, T_2 is the temperature of zero excess entropy in theoretically derived nonlinear
 122 kinetic equations, and T_K is the thermodynamically determined Kauzmann temperature of zero
 123 excess entropy. Sets of subscripted variables or material parameters are enclosed in braces, e.g.

124 $\{T_i\}$. Braces are also used as the highest member in the hierarchy of parentheses, $\{[(...)]\}$.
 125 Average quantities are denoted by $\langle \dots \rangle$.

126

127 1.2 Kinetics of the Glass Transition

128 1.2.1 General Aspects

129 The calorimetrically observed glass transition is a kinetic phenomenon and it is the
 130 kinetics of the transition with which enthalpy relaxation is concerned. The observed glass
 131 transition is essentially a Deborah number (DN) effect, named after the prophetess Deborah who
 132 declared that what appeared to mortals to be stationary, such as non-volcanic mountains and the
 133 size of the oceans, are not necessarily so to an eternal deity. The Deborah number is defined as
 134 the ratio of timescales of the observed and the observer, and the glass transition is seen when
 135 these two timescales for structural relaxation cross over and DN passes through unity. Thus the
 136 glass transition can be studied by changing the timescale of either the experimental probe or the
 137 system under study. The experimental timescale can be varied by changing either the frequency
 138 of an applied sinusoidal perturbation or the observation time for a time-dependent property. The
 139 timescale of structural relaxation can be controlled by temperature or pressure, or by various
 140 applied stresses if the system is nonlinear. In the temperature domain that is explored most
 141 thoroughly a DN of unity that defines an average glass transition temperature T_g can be
 142 expressed in terms of the rate of change of some characteristic timescale τ determined during
 143 cooling:

$$144 \quad DN \equiv \frac{d\tau}{dt} = \frac{d\tau}{dT} \frac{dT}{dt} = \frac{\Delta H_{eff}}{RT_g^2} Q_c \tau \approx 1, \quad (1)$$

145 where ΔH_{eff} is the effective average activation energy at T_g defined as $d \ln \tau / d(1/T)$ (e.g. eq.
 146 (5) below), R is the ideal gas constant and Q_c is the cooling rate. The derivative $d\tau/dt$ has also
 147 been termed the Lillie number by Cooper [7] and has been discussed by Cooper and Gupta [8]
 148 and Scherer [9]. Equating it to unity is implicit in earlier work however and has been used to
 149 estimate $\tau(T_g)$ in terms of the activation energy and scan rate, for example in Ref. [10]. It will
 150 enter again into the discussion of the fictive temperature in Section 1.2.3. It is not advisable to
 151 define DN (and therefore T_g) in terms of the heating rate Q_h alone because the kinetics of
 152 recovery are partly determined by the previous history, such as cooling rate (often not specified,
 153 a practice that is to be discouraged) and annealing. It can be shown from quite general
 154 arguments that T_g increases in proportion to $\log Q_c$ [9,11,12], but the value of $\Delta H_{eff} / R$ near T_g
 155 is usually so large (typically several hundred kK) that T_g is defined to within a few K for
 156 cooling rates that vary over several orders of magnitude. Another definition of DN is

$$157 \quad DN = \tau / \langle t \rangle \quad (2)$$

158 where $\langle t \rangle$ is some average time of observation. If $\langle t \rangle$ is numerically equated to the inverse of
 159 Q_c (i.e. $Q_c \tau \approx 1 \text{ K}$) eqs. (1) and (2) are consistent only when the factor $\Delta H_{eff} / RT_g^2$ is of order
 160 unity. Such consistency is indeed found for a wide variety of glasses (Table 1) although there is
 161 a tendency for some inorganic glasses to have values of $\Delta H_{eff} / RT_g^2$ closer to 0.1. The last
 162 observation is the source of the frequently quoted generalization that $\tau(T_g) = 10^2 \text{ s}$, since from

163 eq. (1) $\tau(T_g) \approx (RT_g^2 / \Delta H_{eff})(1/Q_c) \approx 10/Q_c \approx 60\text{s}$ for a typical cooling rate of 10 K min^{-1} . The
 164 quantity $\Delta H_{eff} / RT_g^2$ is equal to the KAHR parameter θ (Section 3.2.2).

165 In this review T_g is generally used to denote the temperature at which the heat capacity
 166 measured during heating reaches half of its ultimate increase through the glass transition region
 167 (the ‘midpoint’ definition frequently used in DSC scans). More specific definitions and
 168 additional nomenclature are introduced in the discussion of fictive temperature in Section 1.2.3.
 169 The average relaxation time at T_g for typical DSC scans depends on history and on how T_g is
 170 defined from DSC data. Calculations using the Tool-Narayanaswamy phenomenology (Section
 171 4.2) confirm the Lillie number analysis given above: for $Q_c = Q_h = 10\text{ K min}^{-1}$, $\tau(T_g) = 10^2\text{ s}$
 172 for the ‘onset’ definition of T_g (where the heat capacity first starts to rise above the glassy state
 173 background). This onset value is the temperature at which the tangent drawn through the
 174 inflection point in the middle of the transition intersects the extrapolated glass heat capacity. The
 175 ‘onset’ and ‘midpoint’ definitions of T_g are illustrated in Fig. 1(A).

176 In the isobaric liquid or rubbery state above T_g where molecular motion is rapid
 177 compared with experimental observation times, the temperature dependence of the average
 178 relaxation time for many dynamic processes is given by the empirical Vogel-Tamman-Fulcher
 179 (VTF) equation [13-15]

$$180 \langle \tau \rangle = A \exp\left[B / (T - T_0) \right], \quad (3)$$

181 in which A , B and T_0 are positive constants. The VTF equation can be derived from the
 182 configurational entropy theory of Adam and Gibbs [16] (Section 3.2.3) and in terms of free
 183 volume. The free volume version is exemplified by the Williams-Landel-Ferry (WLF) equation
 184 [17] that is ubiquitous in the polymer literature. The WLF equation expresses T_0 as $T_g - C_2$ and
 185 defines a shift factor a_T relative to some reference temperature (usually T_g):

$$186 a_T \equiv \frac{\tau(T)}{\tau(T_g)} = \exp\left[\frac{C_1(T - T_g)}{T - T_g + C_2} \right]. \quad (4)$$

187 An extended discussion of the WLF equation is given in the classic book by Ferry [18], in
 188 which C_1 and C_2 are defined in terms of free volume. Ferry, and many others, have noted that
 189 eq. (3) is more objective than eq. (4) because the values of C_1 and C_2 depend on the choice of
 190 T_g . Accordingly eq. (3) is used here in preference to eq. (4). The effective VTF activation
 191 energy is

$$192 \frac{\Delta H_{eff}}{R} = \frac{d \ln \tau}{d(1/T)} = \frac{BT^2}{(T - T_0)^2} = \frac{B}{(1 - T_0/T)^2}. \quad (5)$$

193 The VTF equation can be fitted to data using reiterative linear least squares or nonlinear
 194 regression techniques. The parameters are usually correlated because changes in B can be partly
 195 compensated by changes in T_0 . These changes can be estimated by exploiting the fact that

196 ΔH_{eff} is tightly constrained by the data so that relative changes in B and T_0 can be determined
 197 from eq. (5). The WLF equation suffers the same problem, as does the extension of the VTF
 198 equation into the glassy state (Section 3.2.3).

199

200 Table 1
201 Tool-Narayanaswamy and KAHR Parameters

Material	$\Delta h^*/R$	x	β	$-\ln(A)$	T_g	$x\Delta h^*/R$	θ	Ref
	(kK)			(s)	(K)	(kK)	K ⁻¹	
PVAc	71	0.35	0.57	224.5	310	25	0.74	[250]
	71	0.41	0.51	223.6		29	0.74	[133]
	88	0.27	0.51	277.5		24	0.92	[130]
PS	80	0.46	0.71	216.0	373	37	0.58	[130,161]
	70	0.48	-	-	373	34	0.56	[91]
	53-71	0.52	0.8	-	373	32	0.44	[153]
	70-110	0.44	0.55	-	373	37	0.60	[246]
PVC	225	0.10	0.23	622.0	353	23	1.74	[130]
PBAPC	150	0.19	0.46	355.8	415	29	0.87	[130]
aPMMA	138	0.19	0.35	357.8	375	26	0.98	[130]
	150	0.20	0.35		375	21	0.75	[162]
iPMMA	80	0.22	0.43		325	18	0.76	[162]
sPMMA	135	0.20	0.35		395	27	0.87	[162]
B ₂ O ₃	45	0.40	0.65	75.6	335	18	0.16	[160]
As ₂ Se ₃	41	0.49	0.67	85.5	450	20	0.20	[257]
5P2E	39	0.40	0.70	153.1	243	16	0.65	[42]
NBS710 ^a	74	0.44	0.63	82.8	840	33	0.105	[129,141]
NBS711 ^b	45	0.65	0.65	57.4	670	29	0.10	[260]
ZBLA	168	0.23	0.43	289.9	580	39	0.50	[112,113,157]
	165	0.19	0.50	282.6		31	0.50	[130]
ZBLALiPb	124	0.23	0.53		510	28	0.48	[112]
ZBLALi	132	0.30	0.55		520	40	0.49	[112]
ZBLAN	112	0.35	0.56		535	39	0.39	[112]
ZBL	184	0.27	0.54		570	50	0.57	[112]
BZnYbTe	137	0.35	0.48		620	48	0.36	[112]
LiAc	200	0.17	0.56	490.7	405	34	1.22	[133]
Glycerol	26	0.29	0.51	490.7	190	7.5	0.73	[113]
EG C (bulk)	12	0.49	0.64	81.5	140	5.9	0.61	[218]
EG ° (gel) "	12	0.46	0.39	75.45	150	5.5	0.53	[218]
LiCl' (bulk)	12	0.68	0.93	82.1	145	8.2	0.57	[218]
LiCl ° (gel)	12	0.67	0.39	70.53	155	8.0	0.50	[218]
40Ca(NO ₃)-60KNO ₃	70	0.31	0.46	202.5	335	22	0.62	[258]

203
204

Table 1 (continued)

Material	$\Delta h^*/R$	x	β	$-\ln(A)$	T_g	$x\Delta h^*/R$	θ	Ref
24.4[yNa ₂ O (1 - y)K ₂ O]- 75.65SiO ₂	49	0.70	0.66	62.8	750	34	0.087	[259]
40AgI-60Ag ₂ MoO ₄	77	0.50	-	-	365	39	0.58	[245]
50AgI-50Ag ₂ MoO ₄	61	0.55	-	-	345	34	0.51	[244]
60AgI-40Ag ₂ MoO ₄	43	0.65	-	-	325	28	0.41	[245]
75AgPO ₃ -25Ag ₂ MoO ₄	61	0.68	-	-	539	41	0.21	[244]
30AgI-52.5AgPO ₃ - 17.5Ag ₂ MoO ₄	49	0.68	-	-	471	33	0.22	[244]
50AgI-37.5AgPO ₃ - 12.5Ag ₂ MoO ₄	54	0.68	-	-	418	37	0.31	[244]

205 ^a Soda-lime-silicate206 ^b Lead silicate207 ^c Ethylene glycol (22 mol% in H₂O)208 ^d Imbided in poly(hydroxyethyl-methacrylate)209 ^e LiCl (16 mol% in H₂O)

210

211 Another expression for $\tau(T)$, deduced from mode coupling theory, is

212
$$\langle \tau \rangle = A'(T/T_c - 1)^{-\gamma} \quad (6)$$

213 where $T_c > T_g$. It is difficult to distinguish between eqs. (3) and (6) for $T > T_g$. Their near

214 equivalence arises from the 'Bardeen identity' discussed briefly by Anderson [19]:

215
$$\exp(-1/x) \approx (2/e)^2 - 0.13. \quad (7)$$

216 Equation (7) is accurate to within a few percent near $x = 0.5$ so that for $T \approx 2T_0$ eqs. (3) and (6)

217 are essentially indistinguishable. However it is not possible to apply eq. (6) to enthalpy

218 relaxation within and below the glass transition temperature range because it would have to be

219 extrapolated through the singularity at $T = T_c$. The relevance of mode coupling theory to the

220 glass transition has been questioned by Angell [20,21] and is discussed in the proceedings of an

221 international discussion meeting [22].

222 The glassy state below T_g is generally a nonequilibrium one [23] and glassy state

223 relaxation results from the thermodynamic driving force towards (metastable) equilibrium. An

224 early discussion of the glass transition and nonequilibrium glassy state was given by Simon

225 [24]. Relaxation in the glassy state below T_g generally has an Arrhenius temperature

226 dependence. Any theory or phenomenology must account for, or describe, the change from VTF

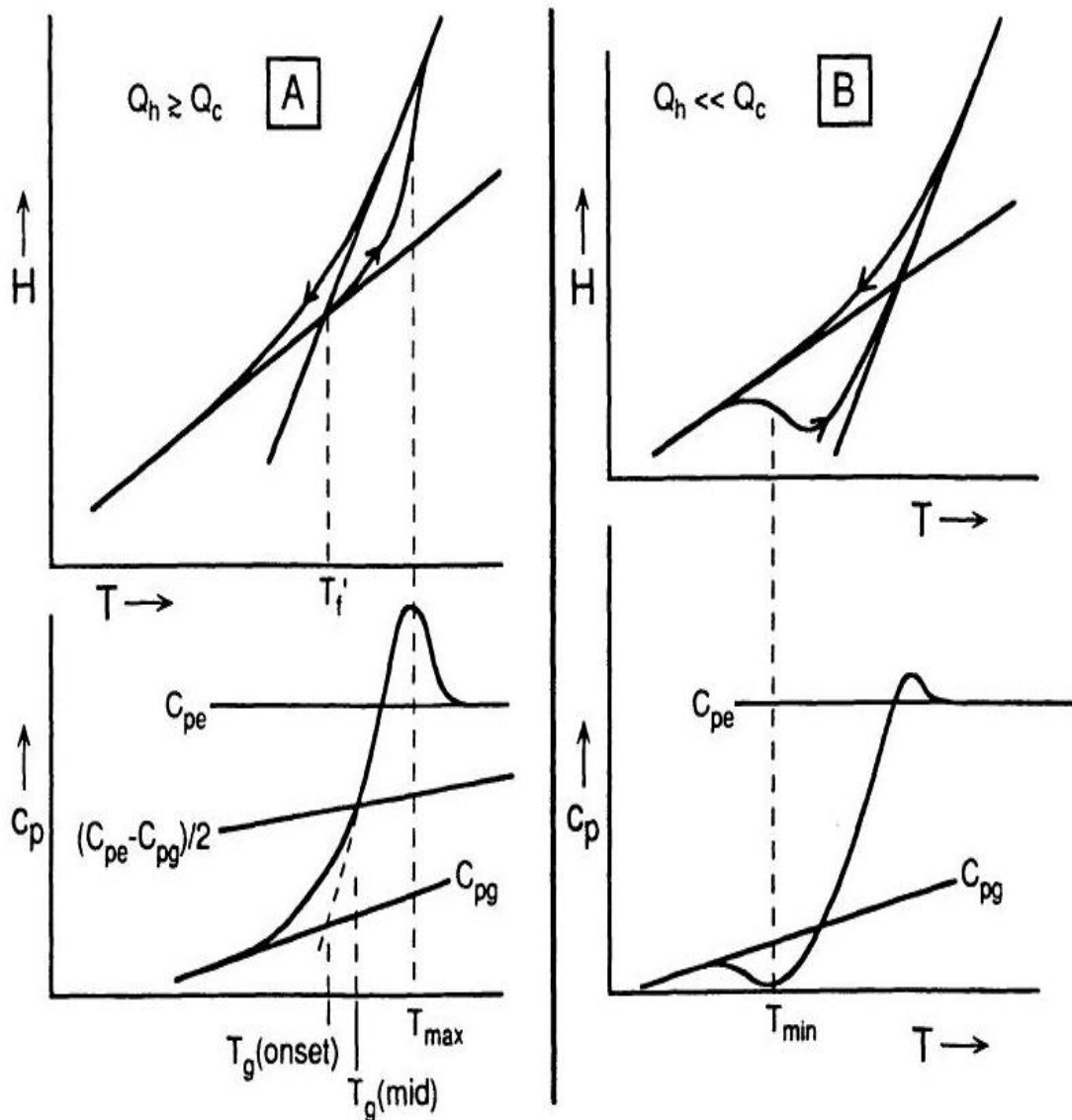
227 behavior above T_g to Arrhenius behavior below T_g . Secondary β relaxations do not affect the

228 glassy heat capacity and there is no evidence that they directly influence enthalpy relaxation.

229 However Goldstein [25,26] has argued that they can affect the change in heat capacity at T_g

230 because of the entropy associated with the corresponding degrees of freedom.

231



232
233

234 Fig. 1 (A) Definition of onset and midpoint values of T_g and of T_f' , for a heating rate
235 comparable with or greater than the cooling rate. (B) Illustration of exothermic excursion below
236

237 1.2.2 Nonexponentiality

238 Most relaxation processes in condensed matter are nonexponential and enthalpy
239 relaxation is no exception. Nonexponentiality produces the memory effect which strongly
240 influences enthalpy recovery after annealing. The memory effect is discussed below but first we
241 consider some aspects of linear response theory for nonexponential decay functions and
242 summarize the more common mathematical expressions used to describe them.

243 A nonexponential decay function $\phi(t)$ is mathematically equivalent to a distribution of
244 relaxation or retardation times $g(\ln \tau)$:

$$245 \quad \phi(\tau) = \int_{-\infty}^{+\infty} g(\ln \tau) \exp(-t/\tau) d \ln \tau, \quad (8)$$

$$246 \quad \int_{-\infty}^{+\infty} g(\ln \tau) d \ln \tau = 1. \quad (9)$$

247 Because of this equivalence it is not possible, in the absence of independent experimental
 248 information, to determine if the essential physics lies in $\phi(t)$ or in $g(\ln \tau)$. Averages of the
 249 relaxation or retardation time $\langle \tau^n \rangle$ are defined by the moments of $g(\ln \tau)$ and $\phi(t)$:

$$250 \quad \langle \tau^n \rangle = \int_{-\infty}^{+\infty} \tau^n g(\ln \tau) \exp(-t/\tau) d \ln \tau \quad (10)$$

$$251 \quad = \frac{1}{\Gamma(n)} \int_0^{+\infty} t^{n-1} \phi(t) dt, \quad (11)$$

252 where Γ is the gamma function. In the frequency domain the corresponding expressions for the
 253 complex retardation function $R_{ret}^*(i\omega)$ are

$$254 \quad R_{ret}^*(i\omega) - R_U = (R_R - R_U) \int_{-\infty}^{+\infty} \frac{1}{1 + i\omega\tau_{ret}} g_{ret}(\ln \tau_{ret}) d \ln \tau_{ret} \quad (12)$$

$$255 \quad = (R_R - R_U) \int_0^{+\infty} -(d\phi/dt) \exp(i\omega t) dt, \quad (13)$$

256 where $i = (-1)^{1/2}$, ω is the angular frequency, $R'(\omega)$ and $R''(\omega)$ are the real and imaginary
 257 components of $R_{ret}^*(i\omega)$ respectively, R_U is the unrelaxed (real) component of $R_{ret}^*(i\omega)$ and
 258 R_R is the relaxed component of $R_{ret}^*(i\omega)$ (also real).

259 The value of R_U corresponds to the limiting high frequency or short time response and
 260 R_R is the limiting low frequency or long time response. For exponential decay functions
 261 $g_{ret}(\ln \tau_{ret})$ is a Dirac delta function $\delta(\tau_{ret} - \tau_0)$ and $R_{ret}^*(i\omega) - R_U$ is proportional to
 262 $1/(1 + i\omega\tau_0)$. The quantity τ_{ret} in eq. (12) is subscripted as a retardation time because in the
 263 time domain it determines the rate of retardation as R increases from R_U to R_R following a step
 264 perturbation:

$$265 \quad R(t) = R_U + (R_R - R_U)[1 - \phi(t)]. \quad (14)$$

266 In eq. (14) the response $R(t)$ corresponds to the change in a measurable property $P(t)$
 267 following an instantaneous increase (Heaviside function) in a forcing perturbation from 0 to F :
 268 $R(t) = P(t)/F$. In the frequency domain this is generalized to $R^*(i\omega) = P^*(i\omega)/F^*(i\omega)$.
 269 Familiar examples of $R_{ret}^*(i\omega)$ are the complex relative permittivity $\varepsilon^*(i\omega)$ and the shear
 270 compliance $J^*(i\omega)$. A less familiar example is the complex isobaric heat capacity $C_p^*(i\omega)$
 271 discussed below. In this last case the forcing function is the temperature and the measured
 272 response is the enthalpy (or isobaric heat, see Section 2.2). Since the limiting high frequency
 273 (short time, low temperature, or glassy) heat capacity is less than the limiting low frequency

274 (long time, high temperature, liquid or rubber) heat capacity, the enthalpic τ is a retardation
275 time.

276 If $R_U > R_R$ the rate of relaxation of $R(t)$ from R_U to R_R is determined by the relaxation
277 time τ_{relax} :

$$278 \quad R(t) = R_U + (R_U - R_R)\phi(t) \quad (15)$$

279 and

$$280 \quad R_{relax}^*(i\omega) - R_R = (R_U - R_R) \int_{-\infty}^{+\infty} \frac{i\omega\tau_{relax}}{1+i\omega\tau_{relax}} g_{relax}(\ln \tau_{relax}) d \ln \tau_{relax}. \quad (16)$$

281 An example of R_{relax}^* is the shear modulus $G^*(i\omega) = 1/J^*(i\omega)$. For properties that are the
282 complex inverses of one another (such as G^* and J^*) specific relations exist between
283 $g_{relax}(\ln \tau_{relax})$ and $g_{ret}(\ln \tau_{ret})$ [18].

284 The distinction between relaxation and retardation times can be important for
285 nonexponential decays because their average values differ substantially if the dispersion
286 $|R_U - R_R|$ is large. For $G^*(i\omega)$ and $J^*(i\omega)$ for example,

$$287 \quad \tau_{ret} = \tau_{relax} (J_R / J_U) \geq \tau_{relax} \quad (17)$$

288 where the factor J_R / J_U increases with increasing nonexponentiality as

$$289 \quad \frac{J_R}{J_U} = \frac{\tau_{ret}}{\tau_{relax}} = \frac{\langle \tau_{relax}^2 \rangle}{\langle \tau_{relax} \rangle^2} \geq 1. \quad (18)$$

290 For strongly nonexponential relaxations, or very broad distributions of relaxation times, the two
291 moments of $g_{relax}(\ln \tau_{relax})$ in eq. (18) can differ by several orders of magnitude. The distinction
292 between retardation and relaxation times also enters into any comparison between the
293 characteristic times of different properties and it is important that a relaxation time for one
294 property not be compared with a retardation time for another. For the rest of this review,
295 however, we omit the subscripts with the understanding that we are discussing enthalpy
296 retardation times.

297 An important consequence of nonexponentiality is the memory effect that arises from
298 Boltzmann superposition of nonexponential response functions (as discussed by Goldstein [27]
299 and others). The memory effect refers to the dependence of relaxation on the path by which the
300 starting state was reached, i.e., the system ‘remembers’ its earlier history. The development of
301 sub- T_g heat capacity peaks in some annealed glasses is due to the memory effect, for example.

302 Another striking manifestation is the initial move away from equilibrium after two temperature
303 steps of opposite sign, followed by the inevitable approach to equilibrium at long times. This
304 results in a maximum in the departure from equilibrium, first observed for volume by Ritland
305 [28] and Kovacs [29], and later by Hofer et al. [30] for enthalpy [31]. It is instructive to analyze
306 these observations, the relevance of which to enthalpy recovery has been discussed by Hodge
307 [32]. Consider a specific example of the thermal history just mentioned: a downward step in
308 temperature from the equilibrium state at T_0 to T_1 at time t_1 followed by an upward step from T_1
309 to T_2 at time t_2 . Boltzmann superposition of the responses to these two temperature steps yields
310 the time dependent enthalpy $H(t)$:

$$311 \quad H(t) = H_0 + \sum_i \Delta H_i [1 - \phi(t - t_i)], \quad (19)$$

$$312 \quad = H_1 + (H_0 - H_1)\phi(t - t_1) + (H_2 - H_1)[1 - \phi(t - t_2)], \quad (20)$$

$$313 \quad = H_1 + (H_0 - H_1)\phi[(t_2 - t_1) + (t - t_2)] + (H_2 - H_1)[1 - \phi(t - t_2)], \quad (21)$$

314 where $\{H_i\}$ are the equilibrium enthalpies at temperatures $\{T_i\}$ and $\{\Delta H_i\}$ are the enthalpy
 315 changes corresponding to the temperature steps at times $\{t_i\}$. If $\phi(t)$ is exponential and the
 316 retardation times at $\{T_i\}$ are $\{\tau_i\}$ then

$$317 \quad H(t) = H_0 + \sum_i \Delta H_i [1 - \phi(t - t_i)],$$

$$= H_0 + (H_0 - H_1) \exp\left[-\frac{(t_2 - t_1)}{\tau_1} - \frac{(t - t_2)}{\tau_2}\right] + (H_2 - H_1) \left\{1 - \exp\left[-\frac{(t - t_2)}{\tau_2}\right]\right\}, \quad (22)$$

$$318 \quad = H_2 + \left\{(H_0 - H_1) \exp\left[-\frac{(t_2 - t_1)}{\tau_1}\right] - (H_2 - H_1)\right\} \exp\left[-\frac{(t - t_2)}{\tau_2}\right]. \quad (23)$$

319 The expression in braces in eq. (23) is independent of time so that $H(t)$ decays exponentially
 320 from its value at $t - t_2$ with a retardation time τ_2 appropriate for the temperature T_2 . Thus if an
 321 observer's clock started at $t = t_2$ there would be nothing in the subsequent behavior to indicate
 322 how the starting value was reached, i.e., the system would retain no 'memory' of the earlier
 323 temperature step at $t = t_1$. This occurs only when $\phi(t)$ is exponential because the
 324 transformation from eq. (22) to (23) depends on the relation

$$325 \quad \phi[(t_2 - t_1) + (t - t_2)] = \phi(t_2 - t_1)\phi(t - t_2), \quad (24)$$

326 which is unique to the exponential function.

327 Another history that demonstrates the memory effect is exemplified in the 'crossover'
 328 experiment of Spinner and Napolitano [33]. A sample was equilibrated near T_g , taken to a lower
 329 temperature, and annealed until the refractive index reached an arbitrary value equal to that of a
 330 sample equilibrated at temperature T_x . The annealed sample was then placed in a furnace at
 331 temperature T_x and the refractive index monitored as a function of time. It was observed to pass
 332 through a minimum, corresponding to a maximum in the volume. Thus although the
 333 nonequilibrium annealed sample had a refractive index equal to a sample equilibrated at T_x the
 334 subsequent time dependence indicated that the nonequilibrium and equilibrated glasses had
 335 different structures.

336 The memory effect can also be described in terms of the components of a distribution of
 337 retardation times. Although each component decays exponentially and exhibits no memory effect
 338 the overall departure from equilibrium at any time can be partitioned between the components in
 339 several ways, depending on the path by which the nonequilibrium state was reached, and these
 340 different partitionings will produce different relaxation behavior.

341 The memory effect is seen only if the response to the first temperature step still has a
 342 significant time dependence after the second step. This condition is not fulfilled for the two
 343 limiting cases of very small and very large values of $(t_2 - t_1) / \langle \tau_1 \rangle$. If $(t_2 - t_1)$ is very long and/or
 344 $\langle \tau_1 \rangle$ is very short then $\phi(t - t_1) \approx \phi(t - t_2) \approx 0$ and the response to the first temperature jump will
 345 have decayed to zero. On the other hand if $(t_2 - t_1)$ is very short and/or $\langle \tau_1 \rangle$ is very long then
 346 $\phi(t - t_1) \approx \phi(t - t_2)$ and no term containing t_1 will appear in eqs. (19) - (21). In both cases the
 347 effects of thermal history for $t < t_2$ on subsequent relaxation is small.

348 The memory effect occurs in any nonexponentially relaxing system regardless of
 349 (although modified by) any possible nonlinearity in the system, described next.

350

351 1.2.3 Nonlinearity

352 In 1936 Lillie [34] reported a time dependent zero frequency viscosity $\eta_0(t)$ in
 353 inorganic glasses. Since the viscosity is proportional to the average stress relaxation time
 354 $\eta_0 = G_U \langle \tau_{rel} \rangle$ (25)
 355 where G_U is the (essentially time invariant) limiting high frequency modulus, Lillie's
 356 observation is equivalent to a viscosity- and time- dependent $\langle \tau_{rel} \rangle$ so that glassy relaxation is
 357 nonlinear. Viscosity is usually associated with structural relaxation in inorganic glasses (their
 358 activation energies are often the same), implying that structural relaxation is also nonlinear.
 359 Nonlinearity was confirmed in 1955 by Hara and Suetoshi [35] who found, for an equilibrated
 360 soda-lime-silicate glass subjected to temperature jumps of opposite sign and magnitude ≥ 2 K,
 361 that the form of the volume relaxation function depended on the sign of the temperature step:
 362 the approaches to equilibrium from above and below occurred at different rates. A similar
 363 asymmetric approach to volumetric equilibrium was observed in poly(vinyl acetate) (PVAc) by
 364 Kovacs [36]. These observations are independent of the memory effect and nonexponentiality
 365 because relaxation occurred from the equilibrium state. The dependence of $\phi(t)$ on the departure
 366 from equilibrium is equivalent to the structural relaxation kinetics depending on the time
 367 dependent structure of the relaxing system, so that in order to quantify nonlinearity it is
 368 necessary to specify the structural state mathematically. Two equivalent methods are in general
 369 use.

370 One measure of structure is the fictive temperature T_f introduced into the literature by
 371 Tool and Eichlin in 1931 [37] and Tool in 1946 [38] but presented orally in 1924 [39]. Thus
 372 nonlinearity was recognized more than 30 years before the memory effect was observed by
 373 Ritland [28] and Kovacs [29], and some 45 years before nonlinearity and nonexponentiality
 374 were first combined in a consistent way by Narayanaswamy [40,41]. This very early
 375 introduction of T_f indicates the considerable practical importance of nonlinearity to annealing
 376 behavior. Excellent discussions of the definition and use of T_f have been given by
 377 Narayanaswamy [41], Moynihan et al. [42] and Scherer [9]. The definition of T_f for enthalpy is

$$378 \quad H(T) = H_e(T_f) - \int_T^{T_f} C_{pg}(T') dT' \quad (26)$$

379 where $H_e(T_f)$ is the equilibrium value of H at temperature T_f and $C_{pg}(T)$ is the nonstructural,
 380 unrelaxed, glassy state heat capacity. The equilibrium state is defined by the condition $T_f = T$ in
 381 addition to the general requirement of time invariance $dT_f/dt = 0$. The value of T_f defined by
 382 eq. (26) corresponds to the temperature of intersection of the equilibrium $H_e - T$ curve with a
 383 line drawn parallel to the glassy $H_g - T$ curve and passing through the (H, T) point of interest.
 384 This construction is shown in Fig. 2, which also illustrates how T_f is the relaxational part of the
 385 enthalpy expressed in temperature units. The structural contribution to the heat capacity is
 386 obtained by differentiating eq. (26):

$$387 \quad \frac{dT_f}{dT} = \frac{(C_p - C_{pg})|_T}{(C_{pe} - C_{pg})|_{T_f}} = \frac{(C_p - C_{pg})|_T}{C_p(T_f)|_{T_f}} \quad (27)$$

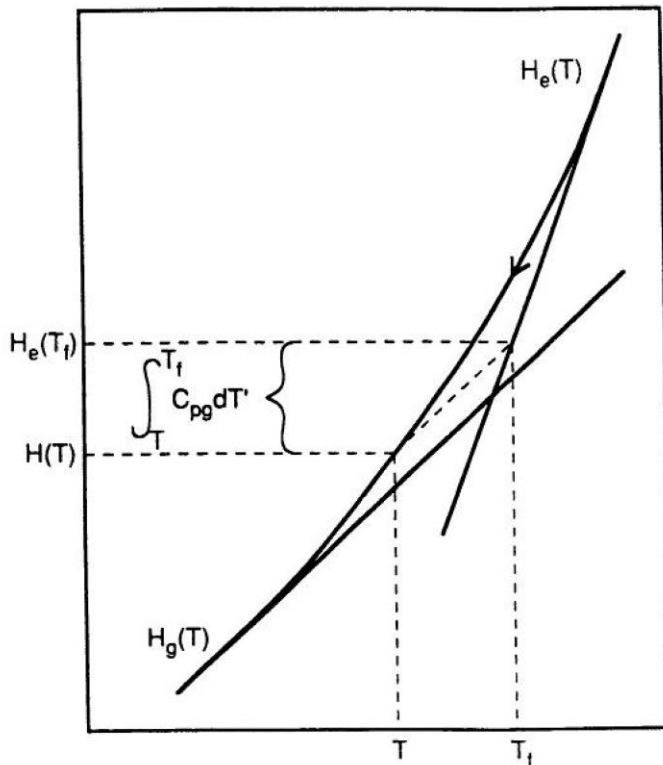
$$388 \quad \approx \frac{(C_p - C_{pg})|_T}{C_p(T_f)|_T} \equiv C_p^N \quad (28)$$

389 where C_{pe} is the equilibrium liquid or rubber heat capacity, C_p is the observed heat capacity,
 390 and C_p^N is the normalized heat capacity. Both C_{pe} and C_{pg} are generally temperature dependent
 391 and must be obtained by extrapolation into the relaxation temperature range. It is often assumed
 392 (although rarely stated explicitly) that ΔC_p in the denominator of eq. (27), specified at the
 393 fictive temperature T_f , is the same as that at temperature T so that dT_f/dT equals C_p^N . The
 394 accuracy of this approximation is demonstrated by noting that $|T_f - T|$ rarely exceeds 10 K or so
 395 during scanning through the relaxation region, so that for the representative hyperbolic relation
 396 $\Delta C_p \sim 1/T$ (eq. (55) below) the error is about 3% for $T_g = 373$ K. The glassy value of T_f ,
 397 denoted by T_f' , is obtained by integration of the normalized heat capacity measured during
 398 heating:

$$399 \quad T_f' = T_{\max} - \int_{T_{\min}}^{T_{\max}} \left(\frac{dT_f}{dT} \right) dT \approx T_{\max} - \int_{T_{\min}}^{T_{\max}} C_p^N dT \quad (29)$$

400 where $T_{\min} \ll T_g \ll T_{\max}$.

401 Since T_f' is defined in terms of the integrated normalized heat capacity measured during heating
 402 its value for annealed glasses can be affected by possible relaxation during cooling from the
 403 annealing temperature to the starting temperature for heating. For glasses equilibrated at $T_a \approx T_g$
 404 such relaxation results in values of T_f' that are less than T_a . The numerical value of T_f'
 405 provides a definition of T_g that is preferred over those given in terms of the heat capacity curve
 406 measured during heating, either as the onset or midpoint temperatures [11,43-45].
 407



408
 409 Fig. 2. Definition of fictive temperature from experimental enthalpy versus temperature data
 410 (eq. (26)).
 411

412
 413 The relative values of T_f' and these definitions of T_g are unambiguous for unannealed glasses
 414 but for annealed glasses the two definitions give T_g values that move in opposite directions as
 415 the amount of annealing increases: T_f' decreases but the heat capacity curve measured during
 416 heating moves to higher temperatures. The definition of T_g from the Deborah condition
 417 $d\tau/dt \approx 1$ (eq. (1)) has been shown by Cooper and Gupta [8] to be approximately equivalent to
 418 $dT_f/dT \approx 1$ during cooling: $d\tau/dt \approx 2.0$ and $dT_f/dT \approx 0.4$ when $T = T_g$

419 The fictive temperature concept becomes more complex when the memory effect
 420 associated with nonexponential relaxation functions is considered. In these cases the structure of
 421 a material must be formally defined by more than one fictive temperature and the global fictive
 422 temperature for one property may not equal that for another. Thus the fictive temperature is
 423 usually subscripted with the property being considered, e.g., $T_{f,H}$ for enthalpy and $T_{f,V}$ for
 424 volume. In this review however we deal almost exclusively with the enthalpic fictive
 425 temperature and the subscript is omitted for convenience. An example of different values of T_f
 426 for different properties was described by Ritland [28] who observed that two glasses with the
 427 same refractive index arrived at by different paths (rate cooling and annealing) had different
 428 electrical conductivities. Thus at least one of these glasses was characterized by different fictive

429 temperatures for refractive index and electrical conductivity. Ritland concluded that a single
 430 fictive temperature gives an inadequate description of a nonequilibrium glass and this is
 431 supported by the thermodynamic analysis of Davies and Jones [46]. Another example of a
 432 different path to the same T_f is a rapid quench compared with a slow cool under pressure
 433 followed by pressure release (see Section 5.1.3.2). In this case the glasses have different
 434 densities and their structures are clearly different. The temptation to equate T_f with a definite
 435 molecular structure should therefore be avoided and too much physical significance should not
 436 be attached to the numerical value of what is essentially a phenomenological convenience.

437 A second method for specifying the structural state pioneered by Kovacs and coworkers
 438 [36,47,48] is to define the departure from equilibrium in terms of a quantity δ_H defined for
 439 enthalpy as

$$440 \quad \delta(T) = H(T) - H(\infty) \quad (30)$$

$$441 \quad \approx \Delta C_p [T_{f,H} - T], \quad (31)$$

442 where $H(\infty)$ is the limiting long time (equilibrium) value of $H(T)$. As with the fictive
 443 temperature we dispense with the enthalpic subscript here. The use of δ is discussed further in
 444 Section 3.2.2 when the KAHR equation is introduced.

445 It is often more convenient to describe the excess enthalpy of a glass using T_f rather
 446 than δ because T_f is a direct measure of excess enthalpy whereas δ differs for the same excess
 447 enthalpy depending on the thermodynamic temperature.

448 Nonlinearity is handled by making the average retardation time a function of both T and
 449 T_f (or δ). The application of this method to nonexponential relaxations is intricate because the
 450 memory effect can generate different relaxation behavior from systems that have the same
 451 instantaneous values of T and T_f . This problem was first solved by Gardon and
 452 Narayanaswamy [40] and Narayanaswamy [41] using the Tool fictive temperature and the
 453 resulting phenomenology is best described as the Tool-Narayanaswamy (TN) formalism. A key
 454 concept introduced by Gardon and Narayanaswamy is the reduced time ξ defined as

$$455 \quad \xi(t) = \int_{-\infty}^t \frac{dt'}{\tau(t')} = \int_{-\infty}^t \frac{dt'}{\tau[T(t'), T_f(t')]} \quad (32)$$

456 The integral is path dependent because it includes the time dependence of both T and T_f .

457 Generally speaking $T(t')$ is specified experimentally by the thermal history and $T_f(t')$ is the
 458 observed response to that history, although in some cases nonthermal perturbations can change
 459 T_f directly (Section 4.7). The reduced time linearizes the kinetics and the methods of linear
 460 response theory can be applied by replacing the time t with ξ . In particular Boltzmann
 461 superposition of responses to all past perturbations can be employed using a generalized form of
 462 thermorheological simplicity in which the shape of $\phi(t)$ or $g(\ln \tau)$ is invariant with respect to
 463 both T and T_f . Thermorheological simplicity has been derived for glasses from the principle of
 464 equivalency between time and temperature (both thermodynamic and fictive) [49]. Thermo-

465 rheological complexity, in which the shape of $\phi(t)$ or $g(\ln \tau)$ changes with T or T_f , has been
 466 introduced into the TN phenomenology by Mazurin and Startsev [50] and others but is rarely
 467 used. Further details of how the TN formalism is implemented are given in Section 3.2.

468 Spurious relaxation parameters can result if nonlinearity is incorrectly incorporated into
 469 the reduced time. An example of such an incorrect analysis has been discussed by Hodge and
 470 O'Reilly [51] using unpublished observations of Scherer [52]. For short annealing times $\tau(t)$
 471 can be approximated as

$$472 \quad \tau(t) = A \tau_0 t^\mu \quad (33)$$

473 where A is a constant with the dimension of (time) $^{-\mu}$ and $\mu \equiv d \ln \tau / d \ln t_a$ is the shift factor
 474 introduced by Struik [6]. Equation (33) has the important consequence that the nonlinear
 475 stretched exponential retains its functional form with an exponent and retardation time modified
 476 by the shift factor μ :

$$477 \quad \phi = \exp(-\xi^\beta) = \exp\left[-\left(\int_0^t \frac{dt'}{\tau_0 t'^\mu}\right)^\beta\right] = \exp\left\{-\left[\frac{t^{1-\mu}}{\tau_0(1-\mu)}\right]^\beta\right\} = \exp\left[-\left(\frac{t}{\tau'}\right)^{\beta'}\right] \quad (34)$$

478 where

$$479 \quad \beta' = (1-\mu)\beta \quad (35)$$

480 and

$$481 \quad \tau' = \tau_0 (1-\mu)^{1/(1-\mu)}. \quad (36)$$

482 Equations (33) - (36) will be referred to here as the Scherer relations. They imply that if a
 483 nonlinear stretched exponential is treated as a linear function a good fit may still be obtained but
 484 with β' and τ' parameters that are determined in part by the nonlinearity parameter μ .

485 Equation (33) is often a reasonably good approximation so that these results may be fairly
 486 general. In any event the Scherer relations provide an excellent illustration of the pitfalls of
 487 neglecting or incorrectly incorporating nonlinearity in the analysis of enthalpy relaxation data.
 488 Analyses based on decay functions that omit or incorrectly incorporate nonlinearity [53-60]
 489 must be considered unreliable. For example it is clearly inconsistent to estimate a nonlinearity
 490 parameter from τ' data obtained from linear fits to the stretched exponential.

491 In recent years another formalism for handling nonlinearity has been introduced by Ngai
 492 and Rendell. This approach differs most significantly from that of Tool-Narayanaswamy in that
 493 the time variable is not simply replaced by ξ and that nonlinearity and nonexponentiality are
 494 less easily separated. It is discussed in Section 4.3.

495

496 1.3 Thermodynamic Aspects of the Glass Transition

497 1.3.1 The Thermodynamic Case

498 The kinetics of the glass transition have a thermodynamic foundation and enthalpy
 499 relaxation therefore has a thermodynamic dimension. This dimension is discussed here.

500 The isobaric heat capacity of a supercooled liquid or rubber exceeds that of the crystal at
 501 the same temperature so that the excess entropy of a liquid or rubber over that of the crystal
 502 decreases with decreasing temperature. Extrapolations for many materials imply that the excess
 503 entropy would vanish at a temperature well above absolute zero. At this temperature the entropy

504 of the supercooled liquid equals that of the crystal and if the same trend were to extend down to
 505 absolute zero the entropy of the liquid would be less than that of the crystal, in conflict with the
 506 third law of thermodynamics. This difficulty was first recognized by Kauzmann [61] and the
 507 extrapolated temperature at which the supercooled liquid and crystal entropies become equal is
 508 known as the Kauzmann temperature T_K . The problem is often referred to as the Kauzmann
 509 paradox because it seems paradoxical that the intervention of a kinetic event, the observed glass
 510 transition, averts rather than resolves a thermodynamic impossibility. The value of T_K is
 511 calculated by equating the excess entropy of the liquid relative to the crystal to the entropy of
 512 melting ΔS_m :

$$513 \quad \Delta S_m = \int_{T_K}^{T_m} \frac{\Delta C_p(T)}{T} dT, \quad (37)$$

514 where T_m is the melting temperature and $\Delta C_p(T)$ is now the difference in isobaric heat
 515 capacity of the liquid or rubber and that of the crystal (equal to that of the glass within 5 - 10%).
 516 Because $\Delta C_p(T)$ must be obtained by extrapolation from T_m or T_g down to T_K the value of T_K
 517 can be very uncertain. For polymers this difficulty is compounded by the need to correct for
 518 tacticity and partial crystallinity. Further, as noted already, Goldstein [25,26] has argued that
 519 $\Delta C_p(T)$ is not entirely configurational and may contain significant contributions from
 520 vibrational and secondary relaxation sources. He estimated that between 20 and 80% of ΔC_p
 521 could originate from nonconfigurational sources and noted that this renders even more uncertain
 522 the extrapolations required to assess T_K . Calculated values of T_K are always found to be less
 523 than T_g although in some cases the difference can be as small as 20 K [62-65]. The value of T_K
 524 is often close to T_0 of the VTF equation [65], suggesting that the kinetic and thermodynamic
 525 aspects of the glass transition are related. The link between thermodynamics and kinetics is an
 526 important aspect of the glass transition phenomenon and is discussed below in more detail.

527 Three resolutions of the thermodynamic difficulties imposed by $T_K > 0$ have been
 528 proposed. One is that the extrapolation of excess entropy to low temperatures is not well defined
 529 and has no firm theoretical basis so that the prediction $T_K > 0$ is a spurious result of incorrect
 530 extrapolation [66,67]. As noted already however the extrapolation is only 20 K or so for some
 531 materials and a nonzero T_K seems inescapable in these cases. A second resolution, suggested by
 532 Kauzmann himself [61], is that the extrapolation is irrelevant because the thermodynamic
 533 driving force for crystallization would always intervene before the entropy problem manifested
 534 itself. However this intervention has been shown to be extremely unlikely in some systems [68]
 535 and it may actually be impossible in two rather bizarre systems ($\text{CrO}_3\text{-H}_2\text{O}$ [69] and $\text{RbAc-H}_2\text{O}$
 536 [70]) in which T_g (and possibly T_K) exceeds the eutectic temperature (the Kauzmann analysis
 537 can be applied to eutectic mixtures [68]). The third resolution is that a thermodynamic second
 538 order transition occurs at T_K at which ΔC_p falls rapidly to zero in a manner similar to that
 539 which is observed kinetically at T_g . Thus T_K is interpreted as a second order thermodynamic
 540 transition temperature (in the Ehrenfest sense, see below) but is unobservable because of kinetic
 541 factors. It seems difficult to refute this hypothesis other than to dismiss it as an artifact of

542 extrapolation but, as has just been noted, this objection is itself weakened by the fact that very
 543 short extrapolations are needed in some cases. Further, an entropically based second order
 544 transition at T_K has been derived for polymers by Gibbs and DiMarzio [71]. Although this
 545 theory has been criticized [72] its predictions agree well with experimental observations near
 546 T_g , including recent ones on the effect of molecular weight on T_g for polymeric rings [73,74].
 547 The case for a thermodynamic foundation for the glass transition is therefore quite strong and it
 548 is appropriate to summarize here some of the properties of thermodynamic second order
 549 transitions.

550

551 1.3.2 Ehrenfest Relations

552 Ehrenfest [75] classified thermodynamic transitions according to the smallest order of
 553 the derivative of the free energy that exhibits a discontinuity at the transition temperature. Thus
 554 discontinuities in second derivative quantities such as the heat capacity, compressibility and
 555 expansivity are classified as second order transitions. Several thermodynamic relations can be
 556 derived for second order transitions of which only those for the pressure dependence of the
 557 transition temperature will be considered here. The purpose of these derivations is to introduce
 558 expressions that are relevant to treatments of pressure dependent kinetics to be discussed later,
 559 and that can be compared with experimental data to identify the most important thermodynamic
 560 variables controlling the glass transition and annealing phenomena. The relations are derived by
 561 setting the differences between the liquid and glassy values of the various first derivatives of the
 562 free energy equal to zero. For volume,

$$563 \quad 0 = d(\Delta V) = \left(\frac{\partial \Delta V}{\partial T} \right)_P dT + \left(\frac{\partial \Delta V}{\partial P} \right)_T dP \quad (38)$$

$$564 \quad = V\Delta\alpha dT - V\Delta\kappa dP, \quad (39)$$

565 where $\Delta\alpha$ and $\Delta\kappa$ are the changes in expansivity and compressibility at T_g , respectively. Thus

$$566 \quad \left(\frac{\partial T}{\partial P} \right)_H = \left(\frac{-(\partial \Delta V / \partial P)_T}{(\partial \Delta V / \partial T)_P} \right) \quad (40)$$

$$567 \quad = \Delta\kappa / \Delta\alpha. \quad (41)$$

568 For entropy

$$569 \quad 0 = d(\Delta S) = \left(\frac{\partial \Delta S}{\partial T} \right)_P dT + \left(\frac{\partial \Delta S}{\partial P} \right)_T dP \quad (42)$$

$$570 \quad = \left(\frac{\partial \Delta S}{\partial T} \right)_P dT - \left(\frac{\partial \Delta V}{\partial T} \right)_P dP \quad (43)$$

$$571 \quad = T^{-1}\Delta C_p dT - V\Delta\alpha dP \quad (44)$$

572 and

$$573 \quad \left(\frac{\partial T}{\partial P} \right)_S = VT(\Delta\alpha / \Delta C_p). \quad (45)$$

574 For enthalpy

$$575 \quad 0 = d(\Delta H) = \left(\frac{\partial \Delta H}{\partial T} \right)_P dT + \left(\frac{\partial \Delta H}{\partial P} \right)_T dP, \quad (46)$$

$$576 \quad = C_p dT + V \left(\Delta V - T \left(\frac{\partial \Delta V}{\partial T} \right)_p \right) dP, \quad (47)$$

$$577 \quad = C_p dT - TV \left(\frac{\partial \Delta V}{\partial T} \right)_p dP, \quad (48)$$

578 where $\Delta V = 0$ because the transition is second order. Thus

$$579 \quad \left(\frac{\partial T}{\partial P} \right)_H = VT \left(\Delta \alpha / \Delta C_p \right). \quad (49)$$

580 Equations (45) and (49) are identical so that entropy and enthalpy cannot be distinguished as
581 controlling variables. Goldstein (cited in ref. [76]) has derived an expression from the condition
582 that TS_c is constant:

$$583 \quad \left(\frac{\partial T}{\partial P} \right)_{TS_c} = VT \frac{\Delta \alpha}{S_c + \Delta C_p} \quad (50)$$

584 where S_c the configurational entropy.

585

586 1.3.3 Prigogine-Defay Ratio

587 Experimental values of dT_g / dP generally agree with eqs. (45) and (49) [76,77] and are
588 smaller than those given by eq. (41) [76], suggesting that enthalpy or entropy and not volume
589 determines T_g . However O'Reilly [77] has pointed out that $\Delta \kappa$ is strongly pressure dependent
590 and that reasonable values of $\Delta \kappa$ can be found that satisfy eq. (41). McKenna [78] has also
591 suggested that the usually quoted values of $\Delta \alpha$, ΔC_p , and $\Delta \kappa$ are not obtained under the
592 proper conditions and that if they were eqs. (41) and (45) would both be satisfied. However
593 enthalpy or entropy **or volume** alone cannot determine T_g . Davies and Jones [46] showed from
594 considerations of thermodynamic stability that are independent of any assumption about a
595 second order transition that more than one thermodynamic variable must determine T_2 if the
596 Prigogine-Defay ratio Π (eq. (51)) is greater than unity:

$$597 \quad \Pi \equiv \frac{\Delta C_p \Delta \kappa}{TV \Delta \alpha^2} = \frac{(\partial T / \partial P)_V}{(\partial T / \partial P)_S} \geq 1. \quad (51)$$

598 Experimental values of Π generally do exceed unity [42,79]. If it is assumed for simplicity that
599 one variable is dominant however it is evidently better to use enthalpy or entropy rather than
600 volume. The superiority of enthalpy or entropy over volume can be rationalized by noting that
601 the isobaric heat capacity has contributions from internal energy sources (the isochoric heat
602 capacity) as well as from volume changes (the term $\alpha^2 TV / \kappa$). Gupta [80] has argued that a
603 fictive pressure P_f in addition to T_f is all that is needed to account for $\Pi > 1$.

604

605 1.3.4 Heat Capacity Change at T_g

606 Heat capacity is an extensive **property** and the appropriate mass unit for configurational
607 heat capacity has been a subject of debate. A frequently used unit is the 'bead' introduced by
608 Wunderlich and Jones [81]. The bead is defined for organic high polymers as a main chain or
609 side chain segment or functional group. Wunderlich observed that ΔC_p per bead is
610 approximately constant for polymers. A review by Mathot [82] summarizes the number of beads

611 per repeat unit and values of ΔC_p per bead for several polymers. Another method for dealing
 612 with mass is to normalize ΔC_p (or C_{pe}) by C_{pg} . Values of $\Delta C_p/C_{pg}$ vary greatly from about
 613 zero for silica to about 2.0 for some hydrogen-bonded liquids [62].

614 The value of $\Delta C_p(T_g)$ often decreases with increasing T_g . For polymers this can be
 615 rationalized in terms of the Gibbs-DiMarzio theory of the glass transition [71] that predicts an
 616 increase in T_g with chain stiffness (amongst other factors). Since stiffness can reasonably be
 617 supposed to decrease the mean square fluctuations in configurational entropy $\langle S_c^2 \rangle$ it follows
 618 from the statistical mechanical relation

$$619 \quad k_B C_p = \langle S^2 \rangle \quad (52)$$

620 that ΔC_p should also decrease (k_B is Boltzmann's constant). A similar argument can be
 621 invoked to rationalize the decrease in ΔC_p with increasing crosslink density in polymers. The
 622 value of $\Delta C_p(T_g)$ has been discussed by Angell [5,20,21,62] in terms of the breakdown in
 623 structure with temperature. Materials whose structures break down rapidly with temperature
 624 have large values of $\Delta C_p(T_g)$ (hydrogen bonded liquids for example) and are termed 'fragile'.
 625 Materials whose structure is resistant to breakdown have correspondingly small values of
 626 $\Delta C_p(T_g)$ (silicates, for example) and are termed 'strong'. The variability in $\Delta C_p(T_g)$ contrasts
 627 with the approximate constancy of the excess entropy at T_g for which there is abundant
 628 evidence, so it can be anticipated that small values of ΔC_p correspond to large ratios of T_g/T_K
 629 [76]. This observation will enter into later discussions of the physical origin of nonlinearity. The
 630 value of ΔC_p also generally decreases with increasing thermodynamic temperature. An

631 illuminating discussion of $\Delta C_p(T_g)$ has been given by Alba et al. [83]. Empirically ΔC_p is
 632 often fitted to the linear equation

$$633 \quad \Delta C_p = a_0 - a_1 T. \quad (53)$$

634 Analysis of the data in ref. [82] reveals that for most polymers the values of a_1/a_0 are such that
 635 ΔC_p has a temperature dependence lying between

$$636 \quad \Delta C_p = C = \text{constant} \quad (54)$$

637 and the hyperbolic form

$$638 \quad \Delta C_p = C' T_g / T = C T_2 / T, \quad (55)$$

639 where C' is the value of ΔC_p at T_g and C is the value at T_2 . The intermediate behavior of
 640 polymers supports the speculation by Angell [5] that the temperature dependence of ΔC_p
 641 should be weaker than hyperbolic for larger molecules. For some materials such as bisphenol A
 642 polycarbonate (BPAPC, often referred to simply as 'polycarbonate'), eq. (53) parameters predict
 643 that ΔC_p would be zero near the melting temperature, an unlikely result. For other materials
 644 ΔC_p is predicted to be negative some 100-200 K above T_g . Negative values are unphysical and
 645 serve to emphasize the empiricism of eq. (53). On the other hand the hyperbolic form of eq. (55)

646 is accurate for many nonpolymeric materials [83-85] and never becomes negative. It should be
 647 noted however that eqs. (53) and (55) are approximately equivalent for $T \approx T_g$ provided

648 $a_1 / a_0 \approx 1 / (2T_g) < 10^{-3} \text{ K}^{-1}$:

649
$$\Delta C_p(T) = \frac{CT_2}{T} = \frac{CT_2}{T_g(1+\Delta)} \approx \frac{CT_2(1-\Delta)}{T_g} = \frac{2CT_2}{T_g} - \frac{CT_2}{T_g^2}T = a - bT \quad (56)$$

650 where $\Delta \equiv T/T_g - 1 \ll 1$.

651

652 2 Experimental Techniques

653 2.1 Scanning Calorimetry

654 The most frequently used technique for studying enthalpy relaxation is differential
 655 scanning calorimetry (DSC). Indeed, the introduction of commercial DSC instruments
 656 essentially made the field of enthalpy relaxation possible. In this technique the difference in
 657 electrical power needed to heat a sample and a reference material to the same temperature is
 658 assessed, produced and measured (hence the term differential). The reference (usually alumina)
 659 is heated at a controlled, known and uniform heating rate (thus the term scanning). The
 660 differential current is proportional to the heat capacity difference between the sample and
 661 reference and is a direct measure of the sample heat capacity if the reference exhibits no
 662 transitions and is thermally stable. Quantitative heat capacities can be obtained if the heat
 663 capacity of the reference is known as a function of temperature. These data are necessary only if
 664 the approximate equality between C_p^N and dT_f/dT (eq. (28)) breaks down, however, and even
 665 in this case only heat capacity values in excess of $C_{pg}(T)$ are needed. As noted already
 666 however eq. (28) is sufficiently accurate in most cases that absolute heat capacities are not
 667 needed. Thus the measurement of absolute heat capacities will not be described here.

668 Experimental heat capacity data must be normalized in order to compare them with
 669 calculated curves. As noted in Section 1.2.3 both $C_{pg}(T)$ and $C_{pe}(T)$ must be extrapolated
 670 through and beyond the glass transition temperature range and this places a premium on
 671 experimental precision. One potential cause of poor reproducibility in $C_p^N(T)$ is a baseline shift
 672 between scans that changes the absolute values of $C_{pg}(T)$ and $C_{pe}(T)$ but not their difference.
 673 Thus it is advisable to compute C_p^N using $C_{pg}(T)$ and $C_{pe}(T)$ data from the same scan, rather
 674 than averaged values for several scans (desirable for the most accurate absolute heat capacities).
 675 The liquid (rubber) heat capacity, being an equilibrium property, is not sensitive to thermal
 676 history (apart from the real possibilities of chemical decomposition or crystallization). The
 677 glassy heat capacity is more problematic because relaxation effects can affect it to quite low
 678 temperatures so that $C_{pg}(T)$ should be determined at temperatures as far below the glass
 679 transition range as possible.

680 It is important that good thermal contact be made between the sample and sample pan,
 681 and between the pan and the instrument cup. Good sample-to-pan contact is readily achieved by
 682 forming samples into thin disks that fit snugly into the pan. Thermal contact between the sample
 683 pan and instrument cup can be improved by applying silicone grease between the pan and the
 684 cup. Thermal contacts can be important in determining the dynamic response of measurements
 685 and thermal transfer corrections are a constant source of uncertainty in all enthalpy recovery

686 experiments. Some researchers insist that corrections should always be applied before any data
 687 analyses are attempted, while others have restricted their analyses to low overshoot data
 688 obtained at relatively slow heating rates (Section 4.6). Thermal transfer is probably a more
 689 important issue for polymers than for inorganics because polymers have lower thermal
 690 conductivities and their glass transitions usually occur over a smaller temperature range. Two
 691 aspects of thermal transfer will be addressed here. The first is the time constant for heat transfer
 692 to the sample arising from the heat capacity of the sample plus pan, and the total thermal
 693 resistance between the instrument cup and sample. The effects of this time constant on the
 694 scanned heat capacity have been estimated by Gray [87]:

$$695 \quad C_p^*(t) = C_p(t) + \tau_{th} \left(dC_p / dt \right) \quad (57)$$

$$696 \quad C_p^*(t) = C_p(t) + \tau_{th} \left(dC_p / dT \right) (dT / dt) \quad (58)$$

$$697 \quad C_p^*(t) = C_p(t) + \tau_{th} \left(dC_p / dT \right) Q_h \quad (59)$$

$$698 \quad C_p^*(t) = C_p(t) + R_0 M C_p \left(dC_p / dT \right) Q_h \quad (60)$$

700 where $C_p(t)$ and $C_p^*(t)$ are the observed and true heat capacities per unit mass respectively, τ_{th}
 701 is the thermal time constant, M is the sample mass, and R_0 is the total thermal resistance
 702 between instrument cup and sample. A predicted baseline shift due to sample mass has been
 703 omitted. Equations (57) - (60) quantify the intuitive notions that large thermal resistance, large
 704 sample mass, fast heating rates and rapidly changing heat capacity will all adversely affect
 705 transient data. The thermal resistance R_0 can be estimated from melting endotherms, which are
 706 predicted to rise linearly with slope $dC_p / dT = 1 / R_0 Q_h$ and to decrease exponentially with time
 707 constant τ_{th} . For good thermal conductors such as indium R_0 obtained in this way is dominated
 708 by the contact resistance between the pan and cup and this dominance can also be expected for
 709 poorer conductors such as polymers and inorganic glasses. Contact resistance is affected by the
 710 flatness of the sample pan bottom, which can be distorted by small misadjustments of sample
 711 preparation devices such as crimping presses. The application of silicone grease to the interface
 712 between the cup and sample pan, mentioned above, reduces this problem by decreasing R_0 .

713 **[section deleted]**

714 Equations (57) - (60) have not yet been applied to enthalpy relaxation analyses although
 715 Hutchinson and co-workers [90,91] used a similar procedure (see below).

716 The thermal resistance of the sample also produces a temperature gradient across the
 717 sample. The first measurement of this appeared in the thesis of DeBolt [88] in which
 718 temperature differences of up to 1 K across ~1 mm thick samples of Vycor glass were reported.
 719 These data were obtained by placing slivers of indium at the bottom and top of the sample and
 720 measuring the two melting temperatures. O'Reilly and Hodge [89] applied the same technique
 721 to polystyrene and observed temperature differences across a 0.5 mm sample ranging from 0.3
 722 K at a heating rate of 1.25 K min⁻¹ to 1.3 K at 20 K min⁻¹. These differences increased linearly
 723 with heating rate for both 0.15 and 0.5 mm thick samples but the variation with sample
 724 thickness depended on heating rate (qualitatively consistent with eq. (60)). Since high
 725 overshoots can have a 'full width at half height' of just a few K (using $C_p^N = 1$ as a 'baseline')
 726 such gradients can be expected to be significant. Hutchinson and coworkers [90,91] proposed

727 that transfer effects be assessed by assuming the heat capacities are exactly described by the
 728 KAHR (and TN [92]) models (Section 3.2.2) and to ascribe all deviations to thermal transfer
 729 effects. The KAHR and TN models predict that for a constant ratio of cooling to heating rate the
 730 heat capacity measured during heating shifts along the temperature axis with changes in heating
 731 rate, but does not change shape. This approach depends on the KAHR or TN formalisms being
 732 correct which is a reasonable assumption for the simple rate cool and reheat histories that the
 733 method uses.

734 Thermal transfer effects have also been discussed by Lagasse [93], Mraw [94],
 735 Richardson and Burrington [95] and Hutchinson [96]. Richardson and Burrington determined a
 736 temperature difference between the temperature sensor and the bottom of a sapphire sample of
 737 about 4 K at a heating rate of 30 K min^{-1} , that decreased linearly with decreasing heating rate
 738 and passed through the origin. Sample mass has been reported to affect the temperature
 739 difference between the sample and temperature sensor [95] as well as the normalized heat
 740 capacity overshoot [97], consistent with eq. (60). Lagasse [93] described a technique for
 741 overcoming thermal transfer in the measurement of enthalpy loss during annealing. It exploits
 742 the transients induced by starting and stopping scans and is similar to the technique used by
 743 Richardson [98] and Gray [99] for measuring the enthalpy of melting of crystalline polymers.

744 2.2 AC Calorimetry

746 This recent technique has been applied to the glass transition by Birge and Nagel
 747 [100,101], Menon et al. [102], and Birge [103]. It is an extension of techniques used to measure
 748 static heat capacities of organic liquids (see refs. [7-9] in ref. [102]) and is an important
 749 development because it measures enthalpy relaxation in the linear region of small temperature
 750 changes, thus avoiding the intricate nonlinear phenomenology and data analysis needed in
 751 scanning calorimetry. The experiments are tedious and demanding however and to date only a
 752 few materials have been characterized.

753 Birge [103] has given an excellent discussion of the frequency dependent heat capacity.
 754 The heat capacity is proportional to the mean square fluctuations in entropy (eq. (52)), and since
 755 these fluctuations have an associated spectral density it follows from the fluctuation-dissipation
 756 theorem that the frequency dependent heat capacity $C_p^*(i\omega)$ is complex. The imaginary
 757 component of a complex response function is normally associated with the absorption of energy
 758 from the applied field but in ac calorimetry there is no net exchange of energy between the
 759 sample and its surroundings. However there is a change in the entropy of the surroundings that
 760 is proportional to C_p'' and the second law of thermodynamics ensures that $C_p'' \geq 0$. The
 761 experimental technique is to drive a sinusoidal current $I(t)$ through a thin heater made from a
 762 material with a large temperature coefficient of electrical resistance (usually nickel). The
 763 magnitude of the temperature oscillations depends on thermal diffusion from the heater into the
 764 sample and is a function of the heat capacity, thermal conductivity and geometry of the sample.
 765 Information on $C_p^*(i\omega)$ is obtained from the magnitude of the temperature oscillations. The
 766 electrical power $P(t)$ is proportional to the square of the current so that the temperature $T(t)$
 767 has a dc component and a phase shifted oscillation at twice the current frequency:

$$768 \quad I(t) = I_0 \cos(\omega t / 2), \quad (61)$$

$$769 \quad P(t) = (I_0^2 R / 2) [1 + \cos(\omega t)], \quad (62)$$

$$770 \quad T(t) = T_{dc} + T_{\omega} \cos(\omega t - \phi). \quad (63)$$

771 The oscillating temperature produces an oscillating heater resistance $R(t)$ which with the
772 current at frequency $\omega/2$ produces a voltage $V(t)$ across the heater with a component at
773 frequency $3\omega/2$:

$$774 \quad R(t) = R_{dc} + R_{\omega} \cos(\omega t - \phi), \quad (64)$$

$$775 \quad R_{\omega} = \alpha R_{dc} T(\omega), \quad (65)$$

$$776 \quad V(t) = I(t)R(t) = V_{\omega/2} \cos(\omega t / 2 - \phi') + V_{3\omega/2} \cos(3\omega t / 2 - \phi), \quad (66)$$

$$777 \quad V_{3\omega/2} = I_0 R_{\omega} / 2, \quad (67)$$

778 where α in eq. (65) is the temperature coefficient of resistance of the heater. Accurate
779 measurement of the third harmonic signal requires considerable care. An important element of
780 the technique is the use of a Wheatstone bridge to cancel the fundamental component of the
781 signal which is much stronger than the third harmonic. An out of phase component at the
782 fundamental (eq. (66)) is not cancelled by the bridge but does not present a problem to any good
783 lock-in amplifier. If the bridge is purely resistive over the frequency range of interest any third
784 harmonic distortion in the source signal is also nulled. The frequency range is 10^{-2} to 6×10^3
785 Hz. For most boundary conditions the product $C_p \kappa$ is obtained from T_{ω} rather than C_p alone
786 (where κ is the thermal conductivity).

787

788 3 Phenomenological Expressions

789 A minimum of four parameters is needed to describe enthalpy relaxation. An effective
790 activation energy is required to specify the cooling rate dependence of T_f' , a pre-exponential
791 factor fixes the absolute value of T_f' , and a minimum of one parameter each is needed to
792 specify nonexponentiality and nonlinearity. In this section we summarize the mathematical
793 expressions used to express these different aspects of relaxation behavior. Activation energies
794 are discussed with nonlinearity because the nonlinearity parameters define the activation
795 energies above and below T_g .

796

797 3.1 Nonexponentiality

798 Many empirical functional forms for nonexponentiality have been suggested. A widely
799 used, versatile, convenient and generally accurate decay function is the stretched exponential

$$800 \quad \phi(t) = \exp\left[-(t/\tau_0)^{\beta}\right] \quad (1 \geq \beta \geq 0). \quad (68)$$

801 This is referred to as the Kohlrausch [104,105], Williams-Watt [106,107] or Kohlrausch-
802 Williams-Watt (KWW) function, and statisticians will find it (and its derivative) familiar as the
803 Weibull distribution (albeit with $\beta > 1$). It has been said with considerable justification [9] that
804 eq. (68) has been in use for so long and in so many different applications that it seems
805 inappropriate to attach individual names to it. We adopt this position here and refer to eq. (68)
806 as the stretched exponential. The average retardation times are

$$807 \quad \langle \tau^n \rangle = \left\{ \tau_0^n / [\beta \Gamma(n)] \right\} \Gamma(n/\beta), \quad (69)$$

$$808 \quad = \left[\tau_0^n / \Gamma(n+1) \right] \Gamma(1+n/\beta), \quad (70)$$

809 and the ratio of retardation to relaxation times is (cf. eq. (18))

$$810 \quad \frac{\tau_{ret}}{\tau_{relax}} = \frac{\langle \tau_{relax}^2 \rangle}{\langle \tau_{relax} \rangle^2} = \frac{\beta \Gamma(2/\beta)}{[\Gamma(1/\beta)]^2}. \quad (71)$$

811 Neither $g(\ln \tau)$ nor $R^*(i\omega\tau)$ is expressible in terms of named functions except for $\beta = 0.5$:

$$812 \quad g(\tau) = \frac{\exp[-\tau/4\tau_0]}{2(\pi\tau\tau_0)^{1/2}} \quad (72)$$

813 and

$$814 \quad R^*(i\omega\tau) - R_U = \frac{(R_R - R_U)}{2} \left(\frac{\pi}{\tau_0} \right)^{1/2} \frac{1}{(i\omega)^{1/2}} \exp\left(\frac{k^2}{i\omega}\right) \operatorname{erfc}\left(\frac{k}{(i\omega)^{1/2}}\right) \quad (73)$$

$$815 \quad = (R_R - R_U) \pi^{1/2} \left(\frac{\pi}{\tau_0} \right)^{1/2} \left(\frac{1-i}{\rho} \right) \exp(-z^2) \operatorname{erfc}(-iz), \quad (74)$$

816 where $2k = (\tau_0)^{-1/2}$, $\rho = (8\omega\tau_0)^{1/2}$ and $z = [(1+i)/\rho]$. Tables of $\exp(-z^2)\operatorname{erfc}(-iz)$ are
 817 available [108] and are included as library functions in some software products. Tables of both
 818 $g(\tau)$ and $R^*(i\omega\tau)$ for $0.3 \leq \beta \leq 1.0$ have been prepared by expressing eq. (68) as a sum of
 819 exponentials [109,110]. The value of β can be obtained from the full width at half height of the
 820 loss component $R''(\omega\tau)$ Δ expressed in decades of $\omega\tau$ [111]:

$$821 \quad \beta^{-1} = -.08984 + 0.96479\Delta - 0.004604\Delta^2 \quad (0.3 \leq \beta \leq 1.0; 1.14 \leq \Delta \leq 3.6), \quad (75)$$

822 which gives β to within ± 0.001 for $\beta \leq 0.7$ and within ± 0.002 for $0.7 \leq \beta \leq 0.95$. The
 823 stretched exponential has also been applied to enthalpy relaxation in a truncated form in which
 824 the short time components of $g(\tau)$ are suppressed [112,113].

825 An empirical function often used in dielectric relaxation spectroscopy is the Davidson-
 826 Cole function [114]. It is characterized by a nearly single relaxation time (Debye) low frequency
 827 response and an extended high frequency tail in the loss. This function is unusual in having
 828 simple forms in the frequency, retardation time and real time domains. In the frequency domain

$$829 \quad R^*(i\omega\tau) - R_U = \frac{(R_R - R_U)}{(1+i\omega\tau_0)^\gamma} \quad 0 \leq \gamma \leq 1 \quad (76)$$

830 from which

$$831 \quad R'(\omega\tau) - R_U = (R_R - R_U)(\cos \phi)^\gamma \cos(\gamma\phi) \quad (77)$$

832 and

$$833 \quad R''(\omega\tau) = (R_R - R_U)(\cos \phi)^\gamma \sin(\gamma\phi), \quad (78)$$

834 where $\tan \phi = \omega\tau_0$. The distribution function is

$$\begin{aligned}
 835 \quad g(\ln \tau / \tau_0) &= \frac{\sin \gamma \pi}{\pi} \left(\frac{\tau}{\tau_0 - \tau} \right)^\gamma & (\tau \leq \tau_0) \\
 &= 0 & (\tau > \tau_0)
 \end{aligned} \tag{79}$$

836 and the decay function is

$$837 \quad \phi(t) = 1 - G(\gamma, t / \tau_0) \tag{80}$$

838 where

$$839 \quad G(\gamma, t / \tau_0) \equiv \frac{1}{\Gamma(\gamma)} \int_0^{t/\tau_0} \exp(-x) x^{\gamma-1} dx \tag{81}$$

840 is the incomplete gamma function [108]. Equation (80) has not been very useful in the past
 841 because of the inaccessibility of $G(\gamma, t / \tau_0)$ but this function is now increasingly available in
 842 Fortran mathematical libraries. A numerical approximation to $\phi(t)$ can be made by discretizing
 843 $g(\tau)$ and expressing $\phi(t)$ as a discretized version of eqs. (8) and (9) and such discretized
 844 functions have been applied to enthalpy relaxation [112,113]. The parameter γ can also be
 845 expressed in terms of the full width at half height of the loss peak $R''(\omega\tau)$ [111]:

$$846 \quad \gamma^{-1} = -1.2067 + 1.6715\Delta + 0.222569\Delta^2 \quad (0.15 \leq \gamma \leq 1.0; 1.14 \leq \Delta \leq 3.3), \tag{82}$$

847 which gives γ to within ± 0.002 for $\gamma \leq 0.9$. Maximum values of $R''(\omega\tau)$ are given by eq. (78)
 848 for $\phi_{\max} = \pi / [2(1 + \gamma)]$. Lindsey and Patterson [110] have given a detailed comparison of the
 849 Davidson-Cole and stretched exponential functions. They found that the two decay functions are
 850 surprisingly similar given the quite different distribution functions.

851 A logarithmic Gaussian distribution for $g(\ln \tau)$ has been fitted to enthalpy relaxation
 852 data [112,113]:

$$853 \quad g(\ln \tau) = \left(\frac{b}{\pi^{1/2}} \right) \exp \left\{ - \left[b^2 \ln^2 (\tau / \tau_0) \right] \right\}. \tag{83}$$

854 It is derived from the reasonable assumption of a Gaussian distribution of activation energies.
 855 The latter implies that $g(\ln \tau)$ changes with temperature and/or fictive temperature although
 856 neither of these possibilities is usually incorporated into enthalpy relaxation calculations.

857 Box and wedge distribution functions have also been applied to enthalpy relaxation. As
 858 introduced by Tobolsky [115] the single box distribution is

$$\begin{aligned}
 859 \quad g(\ln \tau) &= 1 / \ln(\tau_2 / \tau_1) & \tau_2 \geq \tau \geq \tau_1 \\
 &= 0 & \tau_2 < \tau < \tau_1.
 \end{aligned} \tag{84}$$

860 Expressions for $R''(\omega\tau)$ corresponding to the box distribution have been given by Frohlich
 861 [116]. The wedge distribution is

$$\begin{aligned}
 862 \quad g(\ln \tau) &= \frac{1}{\tau^{1/2}} \frac{\tau_1^{1/2} \tau_2^{1/2}}{\tau_2^{1/2} - \tau_1^{1/2}} & \tau_2 \geq \tau \geq \tau_1 \\
 &= 0 & \tau_2 < \tau < \tau_1.
 \end{aligned} \tag{85}$$

863 The double box distribution

$$\begin{aligned}
g(\ln \tau) &= \frac{A}{\ln(\tau_2 / \tau_1)} & \tau_2 \geq \tau \geq \tau_1 \\
864 \quad &= \frac{(1-A)}{\ln(\tau_3 / \tau_2)} & \tau_3 < \tau < \tau_2 \\
&= 0 & \tau_3 < \tau < \tau_1
\end{aligned} \tag{86}$$

865 has been used in the analysis and parameterization of enthalpy relaxation data by Kovacs,
866 Hutchinson and coworkers [47]. The decay functions corresponding to certain double box
867 distributions are remarkably similar to the stretched exponential function for $\beta = 0.5$.

868 Other functions, used principally in the frequency domain of dielectric relaxation,
869 include the Cole-Cole [117], Havriliak-Negami [118] and Glarum [119] functions. However
870 these are inconvenient to use in the time domain and have not yet been applied to enthalpy
871 relaxation.

872

873 3.2 Nonlinearity

874 3.2.1 Narayanaswamy-Moynihan Equation

875 Narayanaswamy [41] introduced a generalized version of the Arrhenius equation of the
876 form

$$877 \quad \tau_0 = A \exp\left(\frac{H_g}{RT} + \frac{H_s}{RT_f}\right), \tag{87}$$

878 where A , H_g and H_s are constant parameters and R is the ideal gas constant [120]. In the
879 equilibrium state above T_g where $T_f = T$ eq. (87) transforms to the familiar Arrhenius form
880 with an activation energy $H_g + H_s$. Moynihan et al. [12] rewrote this equation as

$$881 \quad \tau_0 = A \exp\left[\frac{x\Delta H^*}{RT} + \frac{(1-x)\Delta H^*}{RT_f}\right], \tag{88}$$

882 where x is a partitioning parameter that defines the degree of nonlinearity, and this is the form in
883 which the equation is now used. We refer to eq. (88) as the Narayanaswamy-Moynihan (NM)
884 equation. It has been recognized since its introduction that eq. (88) is only approximately true
885 near T_g because it predicts an Arrhenius temperature dependence in the equilibrium state above
886 T_g that is inconsistent with the VTF equation. However the range in T and T_f over which the
887 glass transition occurs is sufficiently small that the effective VTF activation energy (eq. (5)) is
888 almost constant. In some cases the equilibrium temperature dependence just above T_g reverts to
889 the Arrhenius form rather than continuing a VTF dependence, and eq. (88) is not inconsistent.
890 Such a return to Arrhenius behavior just above T_g is observed for the viscosity of B_2O_3 [121],
891 Ca/KNO_3 [122] and some simple organic compounds [123], and is discussed below (Section
892 6.3).
893

894 3.2.2 The KAHR Equation

895 Kovacs, Aklonis, Hutchinson and Ramos (KAHR) [47] introduced the expression

896
$$\ln \tau_0(T, \delta) - \ln \tau_0(T_r, \delta) = -\theta(T - T_r) - (1-x)\theta\delta / \Delta C_p \quad (89)$$

897 where δ is given by eqs. (30) and (31), T_r is a reference temperature close to T_g , θ is a form of898 activation energy and x is a parameter that partitions T and δ . As noted in the Introduction θ

899 lies in the range 0.1 - 1 K for a wide variety of materials. Equation (89) is referred to as the

900 KAHR equation. The relation between θ and the NM parameter Δh^* is derived by equating the901 temperature derivatives of τ_0 in the equilibrium state ($T = T_f, \delta = 0$) and making the902 approximation $T \approx T_f \approx T_g$:

903
$$\theta \approx \frac{\Delta h^*}{RT^2} \approx \frac{\Delta h^*}{RT_f^2} \approx \frac{\Delta h^*}{RT_g^2}. \quad (90)$$

904 Within the same approximation the x parameters of eqs. (88) and (89) are equivalent:

905
$$-\theta T - (1-x)\theta(T_f - T) \approx \frac{\Delta h^*}{RT} + \frac{\Delta h^*(1-x)}{RT_f} - \frac{\Delta h^*(1-x)}{RT} = \frac{x\Delta h^*}{RT} + \frac{(1-x)\Delta h^*}{RT}. \quad (91)$$

906 Dimensionless and normalized parameters and variables have been defined for the KAHR

907 equation. The dimensionless temperature \mathcal{T} is

908
$$\mathcal{T} = \theta T = \frac{\Delta h^* T}{RT_g^2} \quad (92)$$

909 and the normalized heating or cooling rate \mathcal{D} is

910
$$\mathcal{D} = \theta Q = \frac{\Delta h^*}{RT_g^2} Q. \quad (93)$$

911 The dimensionless amount of annealing \mathcal{D}_H is

912
$$\mathcal{D}_H = \frac{\theta \Delta \delta}{\Delta C_p} = \frac{\Delta h^* \Delta T_f}{RT_g^2}, \quad (94)$$

913 where $\Delta \delta$ and ΔT_f denote changes during annealing. An effective retardation time τ_{eff} is often

914 associated with the KAHR phenomenology:

915
$$\frac{1}{\tau_{eff}} = \frac{1}{\delta} \left(\frac{d\delta}{dt} \right). \quad (95)$$

916 The value of τ_{eff} equals the retardation time for an exponential decay but for a nonexponential917 decay function such as the stretched exponential function with a constant retardation time τ_0 it

918 is time dependent:

919
$$\frac{1}{\tau_{eff}} = \beta \left(\frac{t^{\beta-1}}{\tau_0^\beta} \right). \quad (96)$$

920 Thus its use complicates the treatment of nonlinearity in which τ_0 is also time dependent.

921

922 3.2.3 Adam-Gibbs Equation

923 The Adam-Gibbs theory for linear relaxations [16] is based on transition state theory and
 924 predicts that configurational entropy determines the average relaxation time. It gives rise to
 925 equations that are almost indistinguishable from the VTF equation, and for the hyperbolic form
 926 of $\Delta C_p(T)$ (eq. (55)) it reproduces the VTF equation exactly. The ease with which this
 927 equation can be extended through the glass transition to the glassy state was quickly recognized
 928 by Macedo and Napolitano [121], Goldstein [124], Kovacs et al. [125], Plazek and Magill [126],
 929 Magill [127] and Howell et al. [128], but was not used explicitly for enthalpy relaxation until
 930 the pioneering work of Scherer [129] and in later studies by Hodge [130]. Because it invokes
 931 general concepts that have had an important influence on thinking about the cooperative nature
 932 of molecular motions in the glass transition region, a derivation of the equation is given here.

933 The central assumption is that relaxation involves the cooperative rearrangement of
 934 many ‘particles’ (defined below). The transition state activation energy E_a is expressed as

$$935 E_a = z\Delta\mu \quad (97)$$

936 where $\Delta\mu$ is the elementary excitation energy per particle and z is the number of particles that
 937 cooperatively rearrange. It can be shown mathematically that only the minimum value of z , z^* ,
 938 significantly contributes to the relaxation time. The value of z^* is determined by equating two
 939 expressions for the configurational entropy per particle

$$940 \frac{S_c(T)}{N_A} = \frac{s_c^*}{z^*(T)}, \quad (98)$$

941 where $S_c(T)$ is the macroscopic configurational entropy (defined below), N_A is Avogadro’s
 942 number and s_c^* is the configurational entropy of the smallest number of particles capable of
 943 rearranging. Thus

$$944 \tau_0 = A \exp(E_a / RT) \quad (99)$$

$$945 = A \exp\left(\frac{z^* \Delta\mu}{k_B T}\right) \quad (100)$$

$$946 = A \exp\left(\frac{N_A s_c^* \Delta\mu}{S_c(T) k_B T}\right), \quad (101)$$

947 where a pre-exponential factor $[1 - \exp(-\Delta\mu / k_B T)]^{-1}$ has been suppressed because of its weak
 948 temperature dependence relative to the exponential term. There must be at least two
 949 configurations available to the smallest rearranging group (those before and after
 950 rearrangement) so that

$$951 s_c^* = k_B \ln W^* \geq k_B \ln 2, \quad (102)$$

952 where W^* is the minimum number of configurations needed for rearrangement. The value of S_c
 953 is given by

$$954 S_c = \int_{T_2}^T (\Delta C_p / T) dT \quad (103)$$

955 where T_2 is the temperature at which S_c is zero, i.e., the Kauzmann temperature. As noted in

956 the Introduction we refer to it here as T_2 rather than T_K to emphasize that it is an adjustable
 957 parameter connected with the nonlinear kinetics of the glass transition. Assessment of $\Delta C_p(T)$
 958 requires care. It is common to equate it with the difference between the liquid or rubber and
 959 glass heat capacities on the assumption that this difference is totally configurational but, as
 960 noted already, this assumption has been challenged by Goldstein [25,26]. Moreover the
 961 temperature dependence of ΔC_p must be obtained from extrapolated data and these
 962 extrapolations are uncertain. For example C_{pg} must be obtained at temperatures well below T_g
 963 to ensure that relaxation effects are not included in its temperature dependence. These low
 964 temperature data require lengthy extrapolations that place high demands on experimental
 965 precision. In addition C_{pg} must be measured over a significant temperature range in order that its
 966 temperature dependence be accurately determined. Huang and Gupta [131] evaluated
 967 expressions for $C_{pg}(T)$ suitable for extrapolation into and above the glass transition
 968 temperature range for a soda lime silicate glass.

969 The functional form for $\tau_0(T)$ depends on the temperature dependence of ΔC_p (see
 970 Section 1.3.4). For $\Delta C_p = C = \text{constant}$ (eq. (54))

$$971 \quad \tau_0 = A \exp\left[Q/T \ln(T/T_2)\right] \quad (104)$$

972 where

$$973 \quad Q = \left(\frac{N_A S_c^* \Delta \mu}{k_B C} \right). \quad (105)$$

974 Equation (104) is almost indistinguishable from the VTF equation and in fact retaining only the
 975 first term in the expansion of the logarithmic term reproduces the VTF form. For the hyperbolic
 976 form of eq. (55)

$$977 \quad S_c = C(1 - T_2/T) \quad (106)$$

978 and the VTF form is reproduced exactly [76,132]:

$$979 \quad \tau_0 = A \exp\left\{ \left[\frac{Q}{T(1 - T_2/T)} \right] \right\} = A \exp\left(\frac{Q}{T - T_2} \right). \quad (107)$$

980 As noted already (Section 1.3.4) the hyperbolic eq. (55) has a somewhat stronger temperature
 981 dependence than that observed for most polymers, according to plots of the data compiled in
 982 Ref. [82] and thus should be regarded only as a mathematically convenient approximation for
 983 polymers.

984 Equations (98) and (106) imply that z^* is proportional to $(1 - T_2/T)^{-1}$. Thus z^* and the
 985 barrier height $z^* \Delta \mu$ diverge as $T \rightarrow T_2$ and this divergence can be expected to prevent T_g
 986 approaching T_2 [130,133,134]. Since z^* is conceivably associated with some form of correlation
 987 length it is of interest that the correlation length computed from a random field Ising model also
 988 diverges, albeit as $(1 - T_c/T)^{-\nu}$ [135]. However no evidence for a structural correlation length
 989 was observed in a viscosity study of glycerol by Dixon et al. [136], nor in a molecular dynamics
 990 simulation by Ernst et al. [137]. On the other hand if z^* is interpreted in dynamic terms, for
 991 example as the minimum number of particles needed for the ensemble averaged time correlation
 992 function to be independent of size, it would not necessarily be seen structurally. It is also

993 possible that z^* corresponds in some way to the ‘dynamic characteristic length’ defined by the
 994 ratio of the frequency of the Raman ‘boson’ peak to the speed of sound [138,139]. Adam-Gibbs
 995 behavior has been observed in a spin facilitated kinetic Ising model developed by Frederickson
 996 [140].

997 As noted above the AG equation has been extended through the glass transition to the
 998 glassy state by several investigators by replacing T with T_f in the expression for S_c . In applying
 999 this extension to enthalpy relaxation it must be assumed that the entropic T_f is the same as the
 1000 enthalpic T_f that enters into the nonlinear forms of $\tau_0(T, T_f)$. This equality is a good
 1001 approximation however because the temperature factor relating enthalpy and entropy does not
 1002 vary by more than about 20 K over the glass transition temperature range of integration. Scherer
 1003 [129] inserted the empirical eq. (53) form of $\Delta C_p(T)$ into eqs. (101) and (103) using
 1004 experimental values of the coefficients a_0 and a_1 and obtained good agreement with the
 1005 enthalpy relaxation data for NBS-710 glass reported by Sasabe et al. [141]. Satisfactory fits
 1006 (within experimental uncertainty) were also obtained for published viscosity data [142]. For
 1007 $\Delta C_p = C$ the nonlinear form of eq. (104) is

$$1008 \quad \tau_0 = A \exp \left[\frac{Q}{T} \ln \left(\frac{T_f}{T_2} \right) \right]. \quad (108)$$

1009 For $\Delta C_p = CT_2/T$

$$1010 \quad \tau_0 = A \exp \left\{ \left[\frac{Q}{T(1-T_2/T_f)} \right] \right\}. \quad (109)$$

1011 Equation (108) has been termed AGL [130] (L denoting the logarithmic term) and eq. (109) has
 1012 been referred to as AGF (‘Adam-Gibbs-Fulcher’) [130]. Approximate relations between the
 1013 Narayanaswamy and Adam-Gibbs parameters are derived from the temperature derivatives of
 1014 τ_0 in the equilibrium ($T_f = T$) and glassy ($T_f = T_f'$) states. For eq. (108)

$$1015 \quad \left(\frac{d \ln \tau_0}{d(1/T)} \right) = \left(\frac{\Delta h^*}{RT} \right) \approx Q(L^{-1} + L^{-2}) \approx \left(\frac{Q(1-x)}{x^2} \right) \quad (110)$$

1016 (see eq. (113) below) and

$$1017 \quad \left(\frac{\partial \ln \tau_0}{\partial (1/T)} \right)_{T_f} = \left(\frac{x \Delta h^*}{RT} \right) \approx QL^{-1}, \quad (111)$$

1018 where

$$1019 \quad L \equiv \ln \left(\frac{T_f'}{T_2} \right) \quad (112)$$

1020 and the approximation $T \approx T_f'$ has been used. Thus

$$1021 \quad x \approx L / (1 + L). \quad (113)$$

1022 Equations (110) and (111) were first obtained, using a different notation, by Plazek and Magill
 1023 [126]. For eq. (109)

$$1024 \quad \left(\frac{\Delta h^*}{R} \right) = \frac{Q}{(1-T_2/T)^2} \approx \frac{Q}{(1-T_2/T_f')^2} \approx \left(\frac{Q}{x^2} \right) \quad (114)$$

1025 (see eq. (116) below),

$$1026 \quad \left(\frac{x\Delta h^*}{R} \right) = \frac{Q}{(1-T_2/T)}, \quad (115)$$

1027 and

$$1028 \quad x \approx 1 - T_2/T_f'. \quad (116)$$

1029 Equations (114) and (115) were first obtained by Macedo and Napolitano [121], albeit using a
 1030 different route. They considered the ratio of glassy and liquid state activation energies and
 1031 inferred the eq. (106) form for S_c by equating the VTF and entropic AG equations. They did not
 1032 invoke the hyperbolic form of $\Delta C_p(T)$, first applied to enthalpy relaxation by Hodge [130] but
 1033 having much earlier roots [76,132]. Equations (110) - (116) are special cases of the general
 1034 expressions first derived by Howell et al. [128]:

$$1035 \quad \left(\frac{\Delta h^*}{R} \right) \approx \frac{E}{S_c(T)} + \frac{ET}{S_c^2} \left(\frac{dS_c}{dT} \right) \quad (117)$$

1036 and

$$1037 \quad x\Delta h^*/R \approx E/S_c(T_f'), \quad (118)$$

1038 where $E = \Delta\mu s_c^*$. Thus the general expression for x is, in the approximation $T \approx T_f'$,

$$1039 \quad x \approx \left[1 + \frac{T}{S_c(T_f')} \left(\frac{dS_c}{dT} \right)_{T=T_f'} \right]^{-1}. \quad (119)$$

1040 The difference in T_f'/T_2 evaluated from eqs. (113) and (116) depends on the value of x . For
 1041 small x the difference is small but for large x it can be substantial. For $x = 0.15$ $T_f'/T_2 = 1.19$ and
 1042 1.18 from eqs. (113) and (116) respectively, whereas for $x = 0.70$ values of 10.3 and 3.33 are
 1043 obtained.

1044

1045 3.2.4 Free Volume Equations

1046 Free volume theories are less easily generalized to the nonlinear domain because
 1047 although a fictive temperature can be associated with the free volume it is not clear how a
 1048 sufficiently strong temperature factor can be introduced. This deficiency was first emphasized
 1049 by Goldstein and Nakonecznyi [143] in their analysis of the volume relaxation data for PVAc
 1050 reported by Kovacs [36] and has also been discussed by Macedo and Napolitano [121]. The
 1051 close-packed or occupied volume V_0 that is subtracted from the observed volume to give the free
 1052 volume is temperature dependent [18], but this temperature dependence arises from the
 1053 anharmonicity of vibrational modes and as Ferry [18] has pointed out "...its magnitude and
 1054 thermal expansion coefficient α_0 ... remain a matter of conjecture and can be estimated only
 1055 indirectly".

1056 Free volume theories have been derived that introduce an explicit temperature term but
 1057 the resulting equations contain undesirable extra adjustable parameters. These (and other)
 1058 equations have been discussed by Scherer [129] and Hodge [130]. Macedo and Litovitz [144]
 1059 derived a hybrid equation by modifying the Doolittle equation [145] (rationalized by Cohen and
 1060 Turnbull [146])

$$1061 \quad \tau = A \exp(b/f), \quad (120)$$

1062 where b is a constant of order unity and f is the free volume fraction defined as

$$1063 \quad f = \left(\frac{V - V_0}{V_\infty} \right) = \left(\frac{V_\infty - V_0}{V_\infty} \right) + \left(\frac{V - V_\infty}{V_\infty} \right) = f_T + \delta_v, \quad (121)$$

1064 where V_∞ and V_0 are the equilibrium (limiting long time) and 'occupied' volumes respectively.
 1065 The quantity δ_v has been discussed above in the context of the KAHR phenomenology and can
 1066 be identified here with the recoverable part of the fractional free volume. Macedo and Litovitz
 1067 suggested that an activation energy be added to the free volume term to account for the thermal
 1068 activation needed for a particle to move from one pocket of free volume to another:

$$1069 \quad \tau = A' \left(\frac{b}{V_f} + \frac{E}{RT} \right). \quad (122)$$

1070 If V_f is assumed to vary as $T_f - T_2$ eq. (122) becomes

$$1071 \quad \tau = A' \exp \left(\frac{B'}{T_f - T_2} + \frac{E}{RT} \right), \quad (123)$$

1072 whose linear form ($T_f = T$) was first proposed by Dienes [147]. The Dienes equation was
 1073 reported by Macedo and Litovitz to give a good fit to viscosity data for B_2O_3 , SiO_2 , alkali
 1074 silicates, alcohols and poly(isobutylene).

1075 Mazurin et al. [148] proposed the equation

$$1076 \quad \tau = A'' \exp \left[\frac{B''}{R(T_f - T_2)} + \frac{Q}{R} \left(\frac{1}{T} - \frac{1}{T_f} \right) \right] \quad (124)$$

1077 which becomes the VTF equation above T_g where $T_f = T$ and is Arrhenius in the glassy state.

1078 This equation is not attractive however because it contains an additional adjustable parameter.

1079 Free volume concepts have been applied through and below T_g by Kovacs et al. [125].

1080 They wrote the equilibrium fractional free volume f_T (eq. (121)) as

$$1081 \quad f_T = f_g + \alpha_f (T - T_g) \quad (125)$$

1082 where α_f is the coefficient of fractional free volume thermal expansivity and f_g is the fractional
 1083 free volume of the glassy state. Thus

$$1084 \quad \tau(T, \delta) = \tau_g \exp \left(\frac{b\delta / f_T}{f_T + \delta} \right) \exp \left[\frac{b / f_g (T - T_g)}{f_g / \alpha_f + T - T_g} \right]. \quad (126)$$

1085 Comparing eq. (126) with the KAHR equation (eq. (89)) yields

$$1086 \quad \theta = b\alpha_f / f_g^2 \quad (127)$$

1087 and

$$1088 \quad (1-x)\theta = b\Delta\alpha / f_T^2, \quad (128)$$

1089 where $\Delta\alpha$ is the change in free volume expansivity at T_g . For $T \approx T_g$

$$1090 \quad x \approx (\alpha_f - \Delta\alpha) / \alpha_f. \quad (129)$$

1091 A free volume expression can also be formulated using Adam-Gibbs concepts by
 1092 defining z^* in terms of the free volume per particle rather than the entropy per particle. This

1093 approach is straightforward but does not appear to have been described before. Equation (98) is
1094 replaced by

$$1095 \quad V_f(T) / N_A = v^* / z^*(T) \quad (130)$$

1096 so that

$$1097 \quad z^*(T) = \frac{N_A v^*}{V_f(T)}, \quad (131)$$

1098 where v^* is the minimum volume needed for rearrangement. The nonlinear free volume version
1099 of the Adam-Gibbs equation then becomes

$$1100 \quad \tau_0(T, T_f) = A \exp \left[\frac{N_A v^* \Delta \mu}{k_B T V_f(T_{f,v})} \right]. \quad (132)$$

1101 It seems natural to interpret v^* as the activation volume for the pressure dependence of τ_0 . For
1102 polystyrene this is about $300 \pm 100 \text{ cm}^3$ per mol of monomer [149].

1103

1104 3.3 Pre-exponential Factor

1105 This is determined by T_f' and the TN and KAHR activation energies Δh^* and θ :

$$1106 \quad \ln A = -\frac{\Delta h^*}{RT_f'} + \ln \tau(T_f') = -\frac{\Delta h_{eff}}{RT_f'} + 4.6 \left[\tau(T_f') \approx 100 \text{ s} \right] \quad (133)$$

$$1107 \quad = \theta T_g + 4.6. \quad (134)$$

1108 For thermal histories without annealing changing $\ln A$ moves the T_f vs. T curve along the $T_f = T$
1109 equilibrium line, and the dT_f / dT vs. T curve along the T axis by an amount

$$1110 \quad \Delta T = (RT_g^2 / \Delta h^*) \Delta \ln A \approx \Delta \ln A / \theta. \quad (135)$$

1111 Changes in $\ln A$ affect annealing behavior because the difference between T_f' and T_a determines
1112 in part the rate of annealing.

1113

1114 4 Calculation Procedures

1115 4.1 The KAHR Method

1116 Kovacs, Aklonis, Hutchinson and Ramos [47] described a procedure for solving the set
1117 of coupled nonlinear differential equations that arises in the KAHR phenomenology. The
1118 nonexponential decay function is written as a finite series of exponentials where the retardation
1119 times $\{\tau_i\}$ are defined by the KAHR equation (89):

$$1120 \quad \phi(t) = \sum_i g_i \exp[-t / \tau_i(T, \delta)]. \quad (136)$$

1121 The coefficients g_i also define the weighting factors dividing the total departure from
1122 equilibrium δ of eqs. (30) and (31) into components δ_i that correspond to each τ_i .

1123 Thermorheological simplicity is enforced by keeping the $\{g_i\}$ constant. The differential
1124 equations are those defining the exponential function:

$$1125 \quad \frac{d\tau_i}{dt} = \frac{-\delta_i}{\tau_i(T, \delta)} \quad (137)$$

1126 where

$$1127 \quad \delta = \sum_i g_i \delta_i; \quad \sum_i g_i = 1. \quad (138)$$

1128 Equation (137) is the same as that used in the pioneering work of Tool [38]. However Tool used
 1129 the equation to define the complete decay function whereas in the KAHR phenomenology it
 1130 defines only one component of a nonexponential decay function. Equations (136) and (137) are
 1131 coupled because the τ_i are defined in terms of the global value of δ rather than the components
 1132 δ_i . The numerical solution of these coupled nonlinear differential equations is computationally
 1133 expensive, in part because the time increments must be very small in the equilibrium state above
 1134 T_g where the retardation times are short. Thus considerable time is spent on calculating the
 1135 equilibrium heat capacity before the departures from equilibrium that are of interest are
 1136 **computed** during cooling. This formalism was the first to be applied to rate cooling and heating
 1137 histories with intervening annealing and gave the first prediction and explanation of sub- T_g
 1138 endotherms in scans of annealed glasses [47], but it has been used to fit only a limited number
 1139 of experimental heat capacity data.

1140

1141 4.2 The Tool-Narayanaswamy (TN) Method

1142 The TN method is based on Boltzmann superposition of responses that have been
 1143 linearized using the reduced time method of Gardon and Narayanaswamy [40] (Section 1.2.3). It
 1144 was used to describe annealing effects by Narayanaswamy [40,41] and others [150] but was first
 1145 applied to thermal histories that included rate cooling and heating in 1975 by Mazurin et al.
 1146 [151] and Moynihan et al. [150]. The TN method has since been used by many groups. The
 1147 method is computationally more efficient and more easily implemented than the KAHR method
 1148 and has been extensively used to extract enthalpy relaxation parameters from experimental data.
 1149 Both the Boltzmann and reduced time integrals must be evaluated numerically. Numerical
 1150 evaluation of the Boltzmann integral is accomplished by expressing the thermal history $T(t)$ as a
 1151 series of temperature steps ΔT_k that are small enough to ensure a linear response (generally 1 K
 1152 but see below). For uniform cooling and heating without intervening annealing $T_f(t)$ is given
 1153 by

$$1154 \quad T_{f,n} = T_0 + \sum_{j=1}^n \Delta T_j \left[1 - \phi(\xi_{j,n}) \right] \quad (139)$$

$$1155 \quad = T_0 + \sum_{j=1}^n \Delta T_j \left[1 - \phi \left(\sum_{k=j}^n \Delta T_k / Q_k \tau_{0,k} \right) \right], \quad (140)$$

1156 where T_0 ($\gg T_g$) is the temperature from which cooling starts, Q_k is the cooling or heating rate

1157 (negative for cooling), $\tau_{0,k}$ is a function of $T_{f,k}$, and $T_k = T_0 + \sum_{j=1}^k \Delta T_j$. During annealing the

1158 upper index of the Boltzmann summation is fixed at n_A and the reduced time summation
 1159 becomes [152]

$$1160 \quad \xi_{j,n} = \sum_{k=n_A}^{n_A+n} \frac{\Delta t_k}{\tau_{0,k}} \quad (n=1, n_B), \quad (141)$$

1161 where Δt_k are subintervals of the annealing time t_a such that

$$1162 \quad t_a = \sum_{k=n_A}^{n_A+n_B} \Delta t_k. \quad (142)$$

1163 To ensure linearity the intervals Δt_k must be small enough that T_f decays by less than about 1
 1164 K. Dividing the annealing time into five logarithmically even increments per decade is usually
 1165 satisfactory so that $n_B = 5 \log_{10} t_a$ (s). However time increments of 0.2 decades can be too large
 1166 to ensure linearity during initial relaxation in some rapidly relaxing systems such as those
 1167 formed by extremely rapid cooling rates, or for the last stages of relaxation after very long
 1168 annealing times. These cases draw attention to themselves by changes in T_f that exceed ~ 1 K
 1169 per time subinterval and can be corrected by using shorter time increments.

1170 For the commonly computed combination of a stretched exponential for $\phi(t)$ and the
 1171 NM expression for τ_0 the explicit expression for $T_{f,n}$ for rate cooling and heating is

$$1172 \quad T_{f,n} = T_0 + \sum_{j=1}^n \Delta T_j \left\{ 1 - \exp \left[- \left(\sum_{k=j}^n \Delta T_k / Q_k \tau_{0,k} \right)^\beta \right] \right\}, \quad (143)$$

$$1173 \quad \tau_{0,k} = A \exp \left[\frac{x \Delta h^*}{RT_n} + \frac{(1-x) \Delta h^*}{RT_{f,n-1}} \right]. \quad (144)$$

1174 There is no requirement that ΔT_k or Q_k be constant although they are usually made so for
 1175 convenience. The value of dT_f / dT is discretized as

$$1176 \quad \frac{dT_f}{dT} \approx \frac{T_{f,n} - T_{f,n-1}}{T_n - T_{n-1}}. \quad (145)$$

1177 The maximum values of dT_f / dT can be very large for annealed glasses and in these cases a
 1178 temperature step of 1 K in eq. (143) is too large. Hodge [130] corrected this problem by making
 1179 ΔT_k an inverse function of $\left(dT_f / dT \right)_{k-1}$ for the previous step:

$$1180 \quad \Delta T_k \rightarrow \Delta T_k \begin{cases} \left(\frac{dT_f}{dT} \right)_{k-1} = \frac{T_{k-1} - T_{k-2}}{T_{f,k-1} - T_{f,k-2}} & \left(\frac{dT_f}{dT} > 1 \right) \\ = 1 & \left(\frac{dT_f}{dT} \leq 1 \right). \end{cases} \quad (146)$$

1181 This procedure broke down when the rate of change of dT_f / dT was too large (**more than 6 or**
 1182 **so**). Prest et al. [153] used a self-consistency test for each calculation of $T_{f,n}$ in which the
 1183 magnitude of each temperature step was changed until the computed value of $\tau_{0,k}$ became
 1184 independent of ΔT_k to within a specified error amount. The maximum number of iterations was
 1185 usually two or three and the computation time did not increase substantially.

1186 Integration of eq. (143) is considerably faster than solving the KAHR differential
 1187 equations but it is still CPU intensive because the double exponentiation needed to evaluate the
 1188 stretched exponential function occurs in the innermost of two nested DO loops (corresponding
 1189 to the reduced time and Boltzmann summations). Scherer [154] and Rekhson [155] have

1190 reported (and the present writer can confirm) that a considerable saving in computing time is
 1191 gained if the decay function $\phi(\xi)$ is expressed as a weighted sum of exponentials. This
 1192 procedure is computationally more efficient because the memory effect is absent for each
 1193 exponential component. Each term for each component of the distribution is obtained by
 1194 multiplying the value at the beginning of a time step by $\exp(-\Delta\xi_i)$, where i indexes the
 1195 component of the decay function. This is much faster than the addition of $\Delta\xi$ to the argument
 1196 of the stretched exponential followed by exponentiation to the power β and computation of the
 1197 exponential function. In the program used by Hodge [130] a two dimensional array of $g_i(\beta)$
 1198 values is specified in a DATA statement for values of β differing by 0.05, with intermediate
 1199 values of $g_i(\beta)$ obtained by linear interpolation. Alternatively $g_i(\beta)$ can be obtained by a
 1200 subroutine that least square fits $\sum_i g_i(\beta)\exp(-t/\tau_i)$ to $\exp[-(t/\tau)^\beta]$ for each iteration.

1201 The stretched exponential expression for $\phi(t)$ was first incorporated into the TN
 1202 formalism by Rekhson et al. [156]. However it should be clear from the exposition just given
 1203 that any form for $\phi(t)$ can be used and the box, wedge, Davidson-Cole, truncated stretched
 1204 exponential, and log Gaussian forms for $g(\tau)$ have all been applied to enthalpy relaxation
 1205 [112,113,157]. The stretched exponential has been used with the TN formalism more often than
 1206 these other expressions only because of its convenience and general accuracy and not because
 1207 the phenomenology demands it.

1208 1209 4.3 The Ngai-Rendell (NR) Theory

1210 This theory [158] derives the stretched exponential decay function from basic principles
 1211 and thus attaches a fundamental significance to its functional form. The relaxation time τ_0 in
 1212 eq. (68) is a function of β :

$$1213 \quad \tau_0 = (\beta \omega_c^{1-\beta} \tau_0^0)^{1/\beta} \quad (147)$$

1214 where ω_c , τ_0^0 and β may depend on T_f (or δ). If only τ_0^0 or ω_c depends on T_f nonlinearity in
 1215 the TN sense is produced. The theory identifies the relaxation rate as the relevant variable and
 1216 the rate equation for the isothermal decay function $\phi(t)$ is

$$1217 \quad \frac{d \ln \phi}{dt} = \frac{-1}{\tau_0^0} (\omega_c t)^{\beta-1} = \frac{-\beta t^{\beta-1}}{\tau_0^\beta}, \quad (148)$$

1218 where β and ω_c have been assumed to be independent of time. In the linear case where τ_0 and
 1219 τ_0^0 are also independent of time integration of eq. (148) yields the stretched exponential
 1220 function. The nonlinear decay function is obtained by inserting the isothermal time dependence
 1221 of τ_0 into eq. (148) and integrating:

$$1222 \quad \phi(t) = \exp \left\{ \frac{-\beta \int_0^t dt' (\omega_c t')^{\beta-1}}{[\tau_0(t')]^\beta} \right\}. \quad (149)$$

1223 This differs from the TN nonlinear form

$$1224 \quad \phi(t) = \exp \left\{ - \left[\int_0^t dt' / \tau_0(t') \right]^\beta \right\} \quad (150)$$

1225 whose differential

$$1226 \quad \frac{d \ln \phi}{dt} = -\beta \left| \int_0^t \frac{dt'}{\tau_0(t')} \right|^{\beta-1} \frac{d}{dt} \left| \int_0^t \frac{dt'}{\tau_0(t')} \right| \quad (151)$$

$$1227 \quad = -\frac{\beta}{\tau_0(t)} \left[\int_0^t \frac{dt'}{\tau_0(t')} \right]^{\beta-1} \quad (152)$$

1228 is not the same as eq. (148) when $d\tau_0/dt = d\tau_0[T_f(t)]/dt \neq 0$.

1229 There is recent evidence that eq. (149) is inconsistent with Boltzmann superposition
 1230 [111,159] even for the linear case where $d\tau_0/dT_f = 0$. For a simple thermal history of two
 1231 opposite temperature steps between which the temperature is so low that no significant
 1232 relaxation can occur, eq. (149) predicts a relaxation function that depends on the time between
 1233 temperature steps which is inconsistent with experimental observation. Consider a special case
 1234 of the history leading to eqs. (19) - (21) in which $T_2 = T_0$ is sufficiently above T_g that
 1235 equilibrium prevails [159]. The fictive temperature is given by an appropriately modified
 1236 version of eq. (19):

$$1237 \quad T_f(t) = T_0 - \Delta T [1 - \phi(t, t_1)] + \Delta T [1 - \phi(t, t_2)] \quad (153)$$

1238 where $\Delta T = T_0 - T_1 = T_2 - T_1$. Insertion of the NR expression for $\phi(t)$ (eq. (149)) into eq. (153)
 1239 yields

$$1240 \quad T_f(t) = T_0 - \Delta T \left\{ 1 - \exp \left[\int_{t_1}^t \frac{\beta(t'-t_1)^{\beta-1}}{\tau^\beta} dt' \right] \right\} + \Delta T \left\{ 1 - \exp \left[\int_{t_2}^t \frac{\beta(t'-t_2)^{\beta-1}}{\tau^\beta} dt' \right] \right\}. \quad (154)$$

1241 The first integral of eq. (154) may be written as

$$1242 \quad \int_{t_1}^t \frac{\beta(t'-t_1)^{\beta-1}}{\tau^\beta} dt' = \int_{t_1}^{t_2} \frac{\beta(t'-t_1)^{\beta-1}}{\tau_1^\beta} dt' + \int_{t_2}^t \frac{\beta(t'-t_1)^{\beta-1}}{\tau_2^\beta} dt'. \quad (155)$$

1243 If T_1 is sufficiently low that no relaxation occurs in the time interval $t_2 - t_1$ the first term on the
 1244 right-hand side of eq. (155) is zero and eq. (154) becomes

$$1245 \quad T_f(t) = T_0 + \Delta T \left\{ 1 - \exp \left[\int_{t_2}^t \frac{\beta (t' - t_1)^{\beta-1}}{\tau_2^\beta} dt' \right] \right\} - \Delta T \left\{ 1 - \exp \left[\int_{t_2}^t \frac{\beta (t' - t_2)^{\beta-1}}{\tau_2^\beta} dt' \right] \right\}. \quad (156)$$

1246 The two integrals in eq. (156) are not the same for $t_1 \neq t_2$ so that a time dependence of T_f is
 1247 incorrectly predicted for $t > t_2$. Thus the NR formalism predicts a memory effect even when the
 1248 response to the first temperature step has a negligible time dependence (Section 1.2.2). The TN
 1249 result for the same history is

$$1250 \quad T_f = T_0 + \Delta T \exp \left[- \left(\int_{t_2}^t \frac{dt'}{\tau_2} \right)^\beta \right] - \Delta T \exp \left[- \left(\int_{t_2}^t \frac{dt'}{\tau_2} \right)^\beta \right] = T_0, \quad (157)$$

1251 in accord with experiment. The Boltzmann superposition problem for NR is seen from eq. (156)
 1252 to reside in the choice of a correct zero for time that seems inherent in the selection of the time
 1253 dependent relaxation rate as the physically relevant variable.

1254 If $\phi(t)$ is expressed as a sum of exponentials the integrated version of eq. (148) can be
 1255 expressed as [113]

$$1256 \quad \phi(t) = 1 - \sum_i \int_0^t \left[\frac{1}{\tau_i} \left(\frac{d\tau}{dt'} \right) \exp(-t'/\tau_i) \right] dt'. \quad (158)$$

1257 However if the $\{\tau_i\}$ are isothermally time dependent this expression does not go to zero in the
 1258 limit of long time [159]. This particular difficulty appears to arise from integrating the partial
 1259 derivative of $\phi(t)$ rather than the full derivative. It can be shown [11] for the simplified form of

$$1260 \quad \tau(t) \\
 1261 \quad \tau(t) = \tau_1 + (\tau_2 - \tau_1)(t/t_m) \quad (0 \leq t < t_m) \\
 \quad \quad = \tau_2 \quad (t_m \leq t < \infty) \quad (159)$$

1262 that

$$1263 \quad \phi(t) = 1 - \sum_i \int_0^t \left[\frac{1}{\tau_i} - \frac{t'}{\tau_i^2} \frac{d\tau_i}{dt'} \right] \exp(-t'/\tau_i) dt' \quad (160)$$

1264 gives the correct physical limit $\phi(t \rightarrow \infty) = 0$. This difficulty is a separate issue from the
 1265 Boltzmann superposition problem.

1266 It must be emphasized that these difficulties with the NR approach are the subject of
 1267 ongoing research and may yet be resolved. They serve to emphasize once again, however, the
 1268 need for special care when dealing with relaxations that are both nonlinear and nonexponential.

1269

1270 4.4 Evaluation of Parameters from Experimental Data

1271 4.4.1 Activation Energy

1272 Values of Δh^* or θ are best evaluated from the cooling rate dependence of T_f'

1273 determined before any annealing has occurred:

$$1274 \quad \theta = T_f'^2 = h^*/R \approx -\frac{d \ln Q_c}{d(1/T_f')} \quad (161)$$

1275 Equation (161) is valid over a larger range of cooling rates than that expected from the
 1276 approximations used in its derivation. Scherer [9] has discussed this and associated issues
 1277 related to the temperature dependence of τ_0 . The theoretical consistency between eq. (161) and
 1278 the TN formalism has been demonstrated by Moynihan and coworkers [12,160] and for the
 1279 KAHR formalism by Kovacs et al. [47]. Equation (161) generally gives Δh^* to within 2%
 1280 although larger errors of the order of 10% occur when x and β are very small [111]. As noted
 1281 by Richardson and Savill [43], DeBolt et al. [160] and Hodge [130,161], the evaluation of Δh^*
 1282 or θ from eq. (161) has three experimental advantages over other methods. (i) Thermal transfer
 1283 effects are largely integrated out. (ii) Temperature calibration is simplified because T_f' is
 1284 determined from data measured at a single heating rate. In fact temperature calibration is not
 1285 required at all provided any temperature discrepancy is constant over the temperature range of
 1286 integration and does not drift with time. The need for temperature calibration is vitiated because
 1287 differentiation with respect to $T_f' + \delta T$ rather than T_f' produces errors of the order $\delta T / T_f'$ or a
 1288 few percent for $T_f' \leq 5$ K and experimental uncertainties in the derivative in eq. (161) are
 1289 usually larger than this. (iii) The usable range of cooling rates is wider than that for heating rates
 1290 because no instrumental sensitivity limits are met at low cooling rates. A large range in cooling
 1291 rates is needed for accurate determinations of high values of Δh^* because the uncertainties in
 1292 T_f' are fairly large (typically ± 0.5 K for polymers, smaller for inorganics).

1293 A second method for determining Δh^* is to determine the heating rate dependence of
 1294 T_g (defined either as the midpoint or the onset value) for glasses heated at the same rate as the
 1295 cooling rate used to form them [90,160]. This method does not require integration of the heat
 1296 capacity curves but has some disadvantages. These include the need for temperature calibration
 1297 at several heating rates and a possible shift in T_g resulting from thermal transfer effects at high
 1298 heating rates (Section 2.1).

1299 Values of Δh^* can also be obtained in principle from least squares fits of the normalized
 1300 heat capacity but this method has its own special set of problems (Section 4.5). Values of Δh^*
 1301 obtained by curve fitting are often less than those obtained from eq. (161).

1302 There are conflicting claims about whether accurate values of Δh^* can be obtained from
 1303 the heating rate dependence of T_g of glasses formed at a constant cooling rate. Tribone et al.
 1304 [162] reported that this method gave values for Δh^* that agreed with those obtained by keeping
 1305 $Q_c = Q_h$ but Hodge [130] challenged this by asserting that calculations using known input
 1306 values of Δh^* yielded constant Q_c activation energies that were substantially less than the input
 1307 Δh^* .

1308

1309 4.4.2 Pre-exponential Factor

1310 The pre-exponential parameter A is fixed by Δh^* and T_f' . It is given to a first
 1311 approximation by eq. (133) but best values are obtained by matching calculated values of T_f'
 1312 with experimental values for whatever history is being parameterized (including those with
 1313 annealing). As has been emphasized by Moynihan and coworkers [42,160] it is very important
 1314 that the experimental and calculated values of T_f' be matched to ensure a self-consistent set of
 1315 parameters (Section 4.5).

1316

1317 4.4.3 Nonexponentiality

1318 By far the most frequently used method for obtaining nonexponentiality parameters from
 1319 experimental data is the curve fitting method described below. Because of the intricacy of the
 1320 phenomenology, and the possibility of systematic experimental error it is probably asking too
 1321 much at the present level of development to determine the components of $g(\tau)$ from
 1322 experimental data. To date a specific functional form for $g(\tau)$ or $\phi(t)$ has always been used
 1323 (most often the stretched exponential function) and best fit estimates obtained for a single shape
 1324 parameter (e.g. β). The assumption of a specific functional form for $g(\tau)$ or $\phi(t)$ is not ideal
 1325 but seems inescapable at the present time. Hutchinson and Ruddy [163] suggested that, given
 1326 values of x and θ , a nonexponentiality parameter can be estimated from the value of $C_{p,\max}^N$ as a
 1327 function of Q_c / Q_h . This method is attractive because it uses the same histories as those needed
 1328 to determine θ or Δh^* . It has been used by Hutchinson [96] to determine the stretched
 1329 exponential parameter for poly(vinylchloride) (PVC), polystyrene (PS) and three Ag-Te-MoO₄
 1330 glasses.

1331

1332 4.4.4 Nonlinearity

1333 Several methods have been proposed for determining the KAHR and NM nonlinearity
 1334 parameter x from heat capacity data obtained for different thermal histories. Some of the
 1335 proposed methods are incorrect and others have particular difficulties or a restricted range of
 1336 validity.

1337

1338 4.4.4.1 Annealing Method.

1339 Moynihan et al. [164] used a method that exploited thermal histories for which the decay
 1340 function could be approximated as an exponential. As with some of the other methods described
 1341 here this has so far only been applied to one material. In this case however the value of x agreed
 1342 with that found by curve fitting under conditions in which the curve fitting method was believed
 1343 to be valid. The annealing method is based on the expansion of a nonexponential decay function
 1344 as a weighted sum of exponentials. For short annealing times only the shortest retardation time
 1345 component τ_1 contributes to the relaxation and the decay is approximately exponential. The
 1346 weighting factor for this component g_1 is the same as that for the component of T_f , T_{f1} , that
 1347 relaxes with time constant τ_1 and is estimated from the fraction of relaxation that occurs after
 1348 long annealing times:

$$1349 \quad g_1 \approx \frac{T_f(0) - T_f(t_a)}{T_f(0) - T_a}. \quad (162)$$

1350 The time dependence of $T_f(t)$ is then given by

$$1351 \quad T_f(t) = T_a + g_1 [T_{f1}(0) - T_a] \exp \left[- \int_0^t \frac{dt'}{\tau_1(t')} \right] + \sum_{i=2}^n g_i [T_{fi}(0) - T_a] \quad (163)$$

1352 where $\tau_1(t)$ is given by

$$1353 \quad \tau_1(t) = A_i \exp \left[\frac{x \Delta h^*}{RT_a} + \frac{(1-x) \Delta h^*}{RT_{f1}(t)} \right]. \quad (164)$$

1354 For the material being studied (a ZBLA glass) the value of Δh^* obtained from eq. (161) was
1355 sufficiently large that differences in τ_i gave rise to relatively small changes in T_{fi} compared

1356 with $T_f(0) - T_f(t_a)$. Thus

$$1357 \quad T_{fi} \approx T_f \quad (\text{for all } i) \quad (165)$$

1358 and eq. (163) simplified to

$$1359 \quad T_f(t) = g_1 T_a + (1 - g_1) T_f(0) + g_1 [T_f(0)] + g_1 [T_f(0) - T_a] \exp \left[- \int_0^t \frac{dt'}{\tau_1(t')} \right]. \quad (166)$$

1360 The parameters x and A_i are now the only unknowns and can be obtained by fitting eqs. (164)

1361 and (166) to experimental values of $T_f(t)$. Note that eqs. (162) and (166) are consistent because

1362 for long annealing times the exponential decay falls to zero and

$$1363 \quad \begin{aligned} T_f(t \rightarrow 0) &= g_1 T_a + (1 - g_1) T_f(0) \\ &= T_f(0) - g_1 [T_f(0) - T_a], \end{aligned} \quad (167)$$

1364 so that a fraction g_1 of the maximum possible change in T_f has occurred. Some judgment must

1365 be made as to how short the annealing time needs to be for eq. (163) to be valid. In principle

1366 different values for t_a could be chosen to establish a range in x but this has not yet been

1367 attempted.

1368

1369 4.4.4.2 Method of Curve Shifting.

1370 Hutchinson and Ruddy [91] determined x by exploiting two theoretical results. Both the

1371 KAHR and TN phenomenologies predict that for scans of unannealed glasses for which the ratio

1372 of cooling to heating rates is constant the normalized heat capacity curves shift to higher

1373 temperatures with increasing heating rate but do not change shape. Deviations from this

1374 prediction are attributed to thermal transfer effects. After corrections for these effects have been

1375 applied x is obtained from a second theoretical result, that a unique function $F(x)$ describes the

1376 shift in peak temperature T_p with respect to Q_c , Q_h , T_a and the enthalpy lost during annealing

1377 [90,162,165-167]:

$$1378 \quad F(x) = -\frac{\theta \partial T_p}{\partial \ln |Q_c|} = \frac{\theta \partial T_p}{\partial \ln Q_h} - 1 = \Delta C_p \left(\frac{\partial T_p}{\partial \bar{\delta}} \right), \quad (168)$$

$$1379 \quad \partial T_p / \partial T_a = 0, \quad (169)$$

1380 where $\bar{\delta}$ (eq. (30)) is the enthalpy lost during annealing between times t_1 and t_2 :

$$1381 \quad \bar{\delta} = \frac{\Delta H_a}{\Delta C_p} = H(t_1) - H(t_2). \quad (170)$$

1382 The partial derivatives are by definition evaluated by holding all other variables constant and
 1383 this can be done with experimental ease only for the derivatives with respect to $\bar{\delta}$ and Q_h , or
 1384 with respect to Q_c if no annealing occurs between cooling and reheating. The Q_h derivative is
 1385 subject to all the disadvantages associated with heating rate methods (see above) but the
 1386 derivative with respect to Q_c can be obtained from the same experiments needed to determine
 1387 Δh^* or θ (eq. (161)). The derivative with respect to $\bar{\delta}$ has only the minor disadvantage, shared
 1388 by most of the methods described here, that time consuming long anneals are needed to ensure
 1389 (a) the shift in T_p is large enough for an accurate determination of the derivative, and (b) the
 1390 peak is due to annealing. Under these conditions the peak heights can be very large and
 1391 corrections for thermal transfer become important. Analysis of the published plot of $F(x)$ [91]
 1392 reveals that it can be approximated as

$$1393 \quad F(x) \approx K \left[(1/x) - 1 \right]. \quad (171)$$

1394 The value of K is a weak function of the distribution of retardation times, decreasing from 0.87
 1395 for an exponential decay to 0.75 for a stretched exponential with $\beta = 0.456$. Most values of β
 1396 exceed 0.46 (Table 1) so the approximation that $F(x)$ is independent of $g(\ln \tau)$ is a good one.

1397 Moreover the variation that **occurs does** so in a region where $F(x)$ changes rapidly with x so that
 1398 estimates of x are insensitive to uncertainties in $F(x)$. An approximate mathematical analysis
 1399 predicts $K=1$ [91,168]. Hutchinson and Ruddy [91,163] applied this method to polystyrene and
 1400 obtained a value of 0.48 for x that is in excellent agreement with values obtained by other
 1401 researchers, mostly by curve fitting (Section 4.5).

1402

1403 4.4.4.3 Temperature Step Method

1404 This method was proposed by Lagasse et al. [169] for the analysis of volume recovery
 1405 data. It has not yet been applied to experimental volume or enthalpy relaxation data and has
 1406 been criticized by Hutchinson and Kovacs [170], but is included here for the sake of
 1407 completeness. The method was originally described in terms of the KAHR phenomenology
 1408 which we augment here with the equivalent TN expressions. The method uses two temperature
 1409 steps of different magnitudes but same sign, $T_1 \rightarrow T_2$ at $t=0$ and $T_2 \rightarrow T_3$ at $t=t_a$ ($T_1 > T_2 > T_3$)

1410 and extracts x from the limiting ratios $\left(\frac{T_f(t_a) - T_3}{T_f(t_a) - T_2} \right) \Big|_{t_a \rightarrow 0}$ and $\left(\frac{\tau(T_2)}{\tau(T_3)} \right) \Big|_{t_a \rightarrow 0}$ for different

1411 magnitudes of the second jump at t_a . The ratio of the relaxation times is given by

$$1412 \quad \left(\frac{\tau(T_2)}{\tau(T_3)} \right) \Big|_{t_a \rightarrow 0} = \exp(-x\theta\Delta T_2) = \exp \left[\left(\frac{x\Delta h^*}{R} \right) \left(\frac{1}{T_2} - \frac{1}{T_3} \right) \right]. \quad (172)$$

1413

1414 4.4.4.4 Heating Rate Dependence of T_g

1415 This method [171,172] has been criticized by Crichton and Moynihan [173], Hutchinson
 1416 and Ruddy [174] and Hutchinson [175], but is included here to illustrate some of the pitfalls in
 1417 analyzing nonexponential and nonlinear enthalpy relaxations. The principal criticism is that the
 1418 method does not properly account for the memory effect associated with nonexponentiality. The
 1419 method centers around an equation derived from the simplification that T_f remains unchanged
 1420 during scanning until $T \approx T_f \approx T_f'$ is reached, but this approximation is valid only for
 1421 unannealed glasses formed at very slow cooling rates that are difficult or impractical to achieve.
 1422 Using calculated dT_f / dT data Crichton and Moynihan [173] obtained values of x using this
 1423 method that differed greatly from the input values. For $\{\Delta h^*/R = 5 \times 10^4 \text{ K}, \beta = x = 0.5\}$ values
 1424 of x evaluated by this method ranged between 0.63 and 0.97, depending on history. If T_g was
 1425 defined as the inflection point of the heat capacity rise, slow cooled and annealed glasses
 1426 produced values for x of 0.63 - 0.65, consistent with each other but again different from the
 1427 input value. Crichton and Moynihan observed that these estimated values of x would seem very
 1428 reasonable to someone who did not know the correct input values. Hutchinson and Ruddy [174]
 1429 showed that this method, using slow cooling rates, was equivalent to their peak shift method
 1430 [91] using annealing (Section 4.4.4.2). Both methods depend on the glass being close to
 1431 equilibrium ($T_f \approx T_a$) but Hutchinson and Ruddy noted that this condition is difficult to achieve
 1432 without annealing. This objection is consistent with the criticism of Crichton and Moynihan
 1433 because glasses that are close to equilibrium have almost erased the effects of their thermal
 1434 history and therefore do not exhibit strong memory effects.

1435

1436 4.4.4.5 Adam-Gibbs T_2

1437 Good estimates of T_2 can be made if T_g and the NM parameters are known using eqs.
 1438 (113) and (116). The accuracy of these equations has been demonstrated by several researchers
 1439 [86,113,130,133,154,157]. Values of T_2 can also be obtained by the curve fitting methods
 1440 described next.

1441

1442 4.5 Curve Fitting Techniques

1443 Enthalpy relaxation parameters can be obtained from experimental heat capacity data
 1444 using computer assisted visual fitting [160], or nonlinear regression optimization methods
 1445 [86,161]. The simplest technique is to compare experimental and calculated heat capacity curves
 1446 with trial and error changes in parameters. This method was used in the early work of the
 1447 Moynihan school and produced estimated uncertainties in x and β of ± 0.05 . In the past few
 1448 years it has become increasingly common to use the multidimensional Marquardt [176]
 1449 optimization algorithm, first applied to enthalpy relaxation by Hodge and Huvad [177]. This
 1450 optimization technique changes continuously from the method of steepest descents when the fit
 1451 is far from optimum to the Newton-Raphson method when the optimum is approached. A user
 1452 specified objective function Φ is minimized in a multi-parameter search space that is bounded
 1453 by user specified parameter limits. A FORTRAN algorithm has been published [178]. To date
 1454 Φ has always been specified by the residual sum of squared differences between

1455 experimentally observed and calculated normalized heat capacities:

$$1456 \quad \Phi = \sum_{i=1}^n [C_{pi}^N(\text{obs}) - C_{pi}^N(\text{calc})]^2. \quad (173)$$

1457 This objective function places most weight on the largest values of C_p^N that occur in the
 1458 overshoot region, which is not entirely satisfactory because thermal transfer problems are most
 1459 significant for high overshoot heat capacity data. A better expression for Φ that would not
 1460 introduce other problems, for example sensitivity to the choice of $C_{pg}(T)$ for small values of
 1461 C_p^N , is not evident although defining Φ as the logarithm of the sum of squared residuals is an
 1462 interesting possibility (set to zero for sums less than unity, so that an appropriate scaling factor
 1463 would be needed). Sales [86] applied an optimization algorithm due to Bevington [179]. The
 1464 Marquardt and Bevington algorithms are hard pressed to optimize all four parameters of the
 1465 standard TN formalism because the parameters are strongly correlated [130,161]. Reliable and
 1466 history invariant values of β can usually be obtained from four parameter optimizations but the
 1467 parameters x and Δh^* often vary with thermal history. A better procedure is to use a three
 1468 parameter optimization by fixing one of the parameters, preferably Δh^* obtained from eq. (161).
 1469 When Δh^* is fixed the value of $\ln A$ is tightly constrained because variations in it shift the heat
 1470 capacity curve along the temperature axis, and even small shifts produce large changes in Φ
 1471 because of the steepness of the heat capacity curves near T_g . In addition, $\ln A$ and Δh^* together
 1472 determine T_f' which should be matched to the experimental value to ensure consistency. The
 1473 parameter search space is then two dimensional and x and β can be obtained quickly. If desired
 1474 the fourth parameter can be estimated from the minimum in Φ although this is often quite broad
 1475 and its position can shift with thermal history. In these cases it is commonly found that β is
 1476 fairly constant across the minimum but that β changes systematically with Δh^* to produce
 1477 values of $x\Delta h^*$ that are almost constant.

1478 Hodge and Huvad [177] found that the best fit value of Δh^* for PS obtained from the
 1479 minimum in Φ was the same as that found from the cooling rate dependence of T_f' . Hodge
 1480 [161] also observed consistent values obtained by the two methods. Others have reported that
 1481 values of Δh^* obtained by curve fitting are less than those determined from eq. (161).
 1482 Substantially smaller values were reported by Prest et al. [153] for PS. They found that Δh^*
 1483 obtained by several methods of analysis of the cooling rate and heating rate dependences of T_f'
 1484 were self-consistent but were about a factor of 2 larger than those found by curve fitting. The
 1485 only significant difference between the data sets of Hodge and Huvad and of Prest et al. is the
 1486 ratio of heat to coding rates (0.25 and 1 respectively), so it seems that thermal transfer effects
 1487 may be significant.

1488 Adam-Gibbs parameters can also be obtained using Marquardt or similar optimizations
 1489 [86,113,130,133,154,157] but, as with the NM equation, four parameter optimizations are not
 1490 practical. For three parameter optimizations it is not clear whether Q or T_2 should be fixed
 1491 because both Q and T_2 determine x and Δh^* . Hodge [130] reported that three parameter
 1492 Marquardt optimizations performed by fixing T_2 were less dependent on starting estimates of
 1493 the parameters and less likely to become caught in local minima than optimizations in which Q

1494 was fixed. Sales [86] also fixed T_2 in his optimizations using the Bevington algorithm and
 1495 obtained a best fit T_2 from the minimum in Φ .

1496

1497 4.6 Thermal Transfer Effects and High Overshoot Data

1498 The experimental sources for these effects were discussed in Section 2.1.3. They are
 1499 most severe for the highest overshoot data although as noted earlier Hutchinson and coworkers
 1500 have raised questions about the validity of applying curve fitting methods to all experimental
 1501 data. These investigators found that heat transfer effects shift T_{\max} to higher temperatures for
 1502 heating rates greater than about 20 K min^{-1} (in addition to the well-recognized effect of heating
 1503 rate on temperature calibration), and calculations by the present writer using eqs. (57) - (60)
 1504 confirm this shift [111]. Thermal transfer effects were also recognized by Hodge [130,161] who
 1505 averaged parameters from low overshoot data obtained at 10 K min^{-1} and assessed predictions of
 1506 long aging time behavior by comparing experimental and calculated values of T_f' . O'Reilly and
 1507 Hodge [89] observed that x and β for PS varied strongly with thermal history and that these
 1508 variations occurred using a heating rate (1.25 K min^{-1} , with signal averaging) at which heat
 1509 transfer effects were negligible. They concluded that the phenomenology was deficient and
 1510 suggested that the methods for describing nonlinearity were incorrect. Moynihan et al. [113]
 1511 also concluded that the treatment of nonlinearity is imperfect (See Section 7).

1512 High overshoot data also provide challenges to the approximations inherent in numerical
 1513 integrations, and other simplifications. These include the following:

1514 (1) Selection of a suitably small time subinterval during long anneals. In some cases 0.2 decades
 1515 is too long (Section 4.2).

1516 (2) Temperature steps used for Boltzmann summations must be sufficiently small. The need for
 1517 small temperature steps is especially important in the overshoot region (see eq. (146) for
 1518 example) but, in some circumstances, temperature steps of 1 K can also be too large during
 1519 cooling, or heating below the main transition temperature range.

1520 (3) The approximate equivalence between dT_f / dT and C_p^N may break down. However it is
 1521 unlikely that any difference is more than a few percent (Section 1.2.3).

1522 The relative importance of experimental and computational difficulties in handling high
 1523 overshoot data is not known with any confidence. Thermal transfer effects may be smaller for
 1524 inorganics than for polymers because their glass transitions occur over a wider temperature
 1525 range [113] and their thermal conductivities are higher. However there is increasing agreement
 1526 that the thermal history dependence of model parameters is due to a real deficiency in the
 1527 current phenomenologies rather than thermal transfer effects. Nevertheless a better quantitative
 1528 assessment of thermal transfer effects is desirable before the accuracy of alternative
 1529 phenomenologies can be properly assessed.

1530

1531 4.7 Nonthermal Histories

1532 4.7.1 Hydrostatic Pressure

1533 Hodge and Berens [180] used a simplified method for introducing hydrostatic pressure P
 1534 that was adequate for their purposes but is not rigorous enough to be regarded as a general
 1535 method. They noted that P lengthens the enthalpic retardation time and suggested three ways for
 1536 introducing this. The logarithm of the pre-exponential factor $\ln A$ or the NM activation energy
 1537 Δh^* can be increased in direct proportion to P , or a shift in T_f can be used. In the last case the

1538 equilibrium condition is redefined as $T_f = T - KP$ where K is a positive constant so that the
 1539 usual equilibrium condition $T_f = T$ only holds for $P = 0$. It was assumed that the nonlinearity
 1540 parameter x and the stretched exponential parameter β were independent of P . The shift in τ_0
 1541 with P was estimated from the enthalpic Ehrenfest relation eq. (49), repeated here in a modified
 1542 form for convenience:

$$1543 \left(\frac{\partial T_g}{\partial P} \right)_H \approx V_g T_g (\Delta\alpha / \Delta C_p) \quad (174)$$

1544 where V_g is the volume at T_g . The constancy of H in eq. (174) corresponds to fixed T_f and in
 1545 the approximation $T \approx T_f \approx T_g$ one has

$$1546 \left(\frac{\partial T_g}{\partial P} \right)_H \approx \left(\frac{\partial T_g}{\partial P} \right)_{\ln \tau_0} = \frac{-(\partial \ln \tau_0 / \partial P)_T}{(\partial \ln \tau_0 / \partial T)_P}. \quad (175)$$

1547 Partial differentiation of the NM equation under these conditions yields

$$1548 d \ln \tau_0|_{T_f} = \frac{-x \Delta h^*}{RT^2} dT \approx \frac{x \Delta h^* V_g \Delta \alpha}{RT_g \Delta C_p} dP. \quad (176)$$

1549 The corresponding changes in $\ln A$, Δh^* and T_f are

$$1550 d \ln A \approx \frac{x \Delta h^* V_g \Delta \alpha}{RT_g \Delta C_p} dP, \quad (177)$$

$$1551 d \Delta h^* \approx \frac{x \Delta h^* V_g \Delta \alpha}{\Delta C_p} dP, \quad (178)$$

1552 and

$$1553 d T_f \approx \left(\frac{-x}{1-x} \right) \frac{T_g V_g \Delta \alpha}{\Delta C_p} dP. \quad (179)$$

1554 For $T = T_a < T_f \approx T_g$ the right-hand sides of eqs. (176) - (179) are multiplied by a factor of order
 1555 $(T_2/T_a)^2$ [180] obtained by replacing T^2 with T_a^2 in eq. (176) and retaining T_g in eq. (174). None
 1556 of these equations are readily generalized to arbitrary temperature and pressure histories,
 1557 although pressure scans at constant temperature could presumably be approximated by ramping
 1558 $\ln A$.

1559 Ramos et al. [181] adopted a more rigorous method for introducing pressure into the
 1560 KAHF formalism. They wrote

$$1561 d\delta = -\delta \Delta \alpha dT + \delta \Delta \kappa dP + \sum_{i=1}^N \left(\frac{\partial \delta}{\partial \xi_i} \right)_{T;P;\xi_{j \neq i}} d\xi_i - \sum_{i=1}^N \Delta \alpha_i dT + \sum_{i=1}^N \Delta \kappa_i dP \quad (180)$$

1562 where ξ is an order parameter (not the reduced time), and then neglected the first two terms for
 1563 small δ . The time dependence of the components δ_i is given by

$$1564 \frac{d\delta_i}{dt} = -\Delta \alpha_i \frac{dT}{dt} + \Delta \kappa_i \frac{dP}{dt} + \frac{\delta_i}{\tau_i} \quad (1 \leq i \leq N), \quad (181)$$

1565 where the exponential decay of each δ_i has been introduced. For changes in both T and P the
 1566 shift factor a_δ is given by

$$a_\delta = \exp \left[-(1-x)\theta_T \frac{\delta}{\Delta\alpha} + (1-x)\theta_P \frac{\delta}{\Delta\kappa(P)} \right], \quad (182)$$

$$\theta_P = (b\kappa_f / f_g^2)P, \quad (183)$$

1569 where b is a constant and κ_f is the pressure coefficient of the free volume $f_{T,P}$. Gupta [80]
 1570 introduced pressure into structural relaxation phenomenology by considering a fictive pressure
 1571 in addition to the fictive temperature.

1572

1573 4.7.2 Mechanical Stress and Vapor Induced Swelling

1574 The only attempt to introduce these perturbations into enthalpy relaxation
 1575 phenomenology was made by Hodge and Berens [180]. They considered annealing of
 1576 poly(vinyl chloride) (PVC) that had been exposed to mechanical stress (near or above the yield
 1577 stress), or to swelling induced by solvent vapor absorption followed by rapid desorption.
 1578 Annealing took place after the release of these nonthermal perturbations. It was assumed that the
 1579 treatments increased T_f instantaneously (a reasonable assumption given the rapid application
 1580 and release of stress or solvent vapor) by an amount ΔT_f that decayed with reduced time during
 1581 subsequent annealing and reheating. This decay was assumed to be described by the same
 1582 relaxation parameters as the thermal history and was superimposed on the response to the purely
 1583 thermal history. Good agreement with experimental data was obtained using values of ΔT_f that
 1584 increased linearly with the applied perturbation (stress or solvent vapor pressure). In particular
 1585 the calculations reproduced the experimental result that only the sub- T_g endotherm peak heights
 1586 and not the peak temperatures were affected by the applied perturbations.

1587

1588 5 Experimental Results

1589 In this section we restrict our attention to qualitative experimental results and defer a
 1590 discussion of relaxation parameters to Section 6.

1591

1592 5.1 Scanning Calorimetry

1593 5.1.1 Enthalpy Recovery Near T_g

1594 Simple cooling and reheating histories produce heat capacity curves during heating that
 1595 exhibit an increase in C_p over the glass transition range followed by a maximum and a decrease
 1596 to the equilibrium liquid or rubber value. Exceptions to this are seen in glasses with high values
 1597 of T_f' produced by very fast cooling rates, such as in splat quenching, vapor deposition or
 1598 quenching of fine fibers. Slow scans of these glasses exhibit exothermic dips in the heat
 1599 capacity just before the increase in C_p at T_g . These exotherms occur because the relatively high
 1600 value of T_f' produced by a fast quench greatly shortens the average retardation time and during
 1601 the slow reheat T_f has time to relax towards the equilibrium state defined by $T_f = T$ from
 1602 values $T_f > T$. This relaxation produces negative values of dT_f / dT and an exothermic
 1603 excursion below the glassy heat capacity. The phenomenon is illustrated in Fig. 1(B). The
 1604 exotherm can be suppressed by decreasing the high initial values of T_f' by annealing below T_g .

1605 For the more common simple overshoot the equilibrium condition $T_f = T$ is reached before any
1606 relaxation can occur and dT_f / dT remains positive as T_f approaches the equilibrium $T_f = T$
1607 line from values $T_f < T$ (Fig. 1(A)).

1608

1609 5.1.2 Isothermal Annealing

1610 Enthalpy lost during annealing is usually (but not always) recovered near T_g during
1611 reheating, producing the familiar high overshoot in annealed glasses. Pioneering studies of this
1612 phenomenon were made by Volkenstein and Sharonov [182], Foltz and McKinney [183] and
1613 Petrie [184], all of whom demonstrated that the magnitude of the overshoot was a quantitative
1614 measure of the enthalpy relaxation that had occurred during annealing. Other quantitative
1615 studies were reported by Straff and Uhlmann [185], O'Reilly [186], Ali and Sheldon [187] and
1616 Ophir et al. [188]. The number of papers containing qualitative statements about annealing
1617 peaks near T_g , either as the primary area of study or as part of a larger investigation, is immense
1618 and no useful purpose would be served by citing them all. Every study of which this writer is
1619 aware reveals that enthalpy recovery near T_g responds to changes in annealing conditions the
1620 same as enthalpy recovery in the glassy state, discussed in the next section. Thus we discuss
1621 here only those studies of enthalpy recovery near T_g that are of special interest or novelty, or
1622 illustrate the variety of materials studied. The selection is inevitably subjective.

1623 Ten Brinke and coworkers [189,190] applied results from enthalpy relaxation
1624 phenomenology to blends of PVC/poly(isopropyl methacrylate) (PVC/P(iPr)MA),
1625 PVC/poly(methyl methacrylate) (PVC/PMMA), and PS/poly(2-vinyl pyridine) (PS/PVP), and
1626 showed that the miscibility or immiscibility of components with closely similar T_g could be
1627 established if appropriate annealing histories were used. For the PS/PVP blends [190] for which
1628 the T_g of the PS and PVP used were 106 and 100°C respectively, annealing at 91°C for longer
1629 than 6 h produced two heat capacity maxima that became increasingly better resolved as
1630 annealing times increased to a month or so, demonstrating that PS and PVP are immiscible. The
1631 better resolution at longer annealing times occurred because PVP reached its equilibrium state
1632 after only relatively short annealing times at 9°C below its T_g , producing an annealing peak that
1633 did not shift with further annealing, whereas the annealing peak for PS continued to move to
1634 higher temperatures even after long annealing times at 15°C below its T_g . For the PVC blends
1635 [189] a separate PVC phase could easily be identified because annealing of PVC produced sub-
1636 T_g peaks that were easily distinguished from the more usual overshoots for PMMA and
1637 P(iPr)MA. Quan et al. [191] used enthalpy relaxation to experimentally characterize the
1638 interfacial regions of a styrene-hydrogenated butadiene-styrene triblock copolymer. Ten Brinke
1639 [192] showed that Quan's results could be reproduced by the TN formalism but noted some
1640 complications associated with estimating the amount of interfacial material. Cowie and
1641 Ferguson [57] investigated annealing in blends of PS and poly(vinyl methyl ether) (PVME).
1642 They observed heat capacity maxima in the middle of the glass transition and reported that the
1643 PVME component annealed independently of the PS component. Mijovic and coworkers
1644 [193,194] investigated blends of PMMA and SAN (styrene-co-acrylonitrile). The annealing
1645 rates for SAN rich blends were slightly faster for anneals 20 and 35°C below T_g but at 50°C

1646 below T_g the rates were independent of composition. The response to different annealing
1647 temperatures also changed with blend composition. Gomez-Ribelles et al. [55] studied enthalpy
1648 relaxation in PVC plasticized with dioctyl phthalate (DOP). They reported that only some of the
1649 polymer was plasticized (i.e. showed a decrease in T_g with increasing DOP content), with the
1650 remainder showing a concentration-independent T_g (albeit very weakly with $\Delta C_p(T_g) \approx 0.01 \text{ J}$
1651 g^{-1}). Their plots also exhibited the extremely broad melting endotherms just above T_g associated
1652 with the crystallinity of this material [195]. The breadth of the melting endotherm is due to the
1653 extremely small average size, but not unusual size distribution, of crystallites that are subject to
1654 large surface contributions to the crystal free energy. (The small amount of crystallinity is
1655 responsible for the toughness of PVC and crystallinity is not reduced by plasticization of the
1656 predominant amorphous phase).

1657 Johari and Mayer and coworkers [196 - 198] annealed vapor deposited water and
1658 hyperquenched aqueous solutions just below their T_g to remove the large exotherm resulting
1659 from the high initial T_f' . This enabled the observation of glass transitions in the presence of
1660 large ice crystallization exotherms just above T_g . Gupta and Huang [199] investigated enthalpy
1661 relaxation and recovery in slowly cooled bulk samples and rapidly cooled fibers (8-12 μm
1662 diameter) of a soda-lime-silicate glass. They observed the usual exotherm below T_g for the
1663 rapidly quenched and slowly reheated fibers but were unable to fit the TN model to these
1664 histories. Warner [200] observed enthalpy relaxation in some thermotropic anthraquinone
1665 polymers, and Hedmark et al. [201] reported annealing endotherms in a liquid crystalline
1666 polyester copolymer. Petrie [202] reported enthalpy relaxation effects in nonpolymeric
1667 mesogens. These observations are consistent with other parallels between the glass transition
1668 and thermotropic transitions in liquid crystals [20]. Stephens [203] described annealing
1669 endotherms in amorphous Se as a function of annealing time and temperature. The enthalpy loss
1670 on annealing increased linearly with $\log t_a$ in the usual manner (see next section), and a plot of
1671 data taken from the published figure exhibits the usual approximately linear increase with T_a
1672 (also see next section). Ma et al. [204] observed annealing endotherms and shifts in T_g with
1673 annealing time in a series of chalcogenide glasses containing Te as a common component.
1674 Changes in T_g , the breadth of the glass transition, and in annealing behavior were observed as a
1675 function of average coordination number (defined by composition). Tatsumisago et al. [205]
1676 observed a minimum in the enthalpic activation energy as a function of average coordination
1677 number in a series of Ge-As-Se glasses. Koebrugge et al. [206] observed annealing endotherms
1678 in a metallic glass of composition $\text{Pd}_{40}\text{Ni}_{40}\text{P}_{20}$ that increased in magnitude with annealing time.
1679 Sommer et al. [207] studied the enthalpy lost during annealing of amorphous alloys of
1680 composition $\text{Cu}_{67}\text{Ti}_{33}$, $\text{Cu}_{50}\text{Ti}_{50}$, $\text{Cu}_{34}\text{Ti}_{66}$, $\text{Ni}_{33}\text{Zr}_{67}$ and $\text{Pd}_{26}\text{Zr}_{74}$ as a function of annealing time.
1681 The lost enthalpy increased linearly with $\log t_a$ at short annealing times and reached constant
1682 values at long times, consistent with the annealed glasses reaching the equilibrium state at long
1683 times.
1684

1685 5.1.3 Sub- T_g Endotherms

1686 5.1.3.1 Thermal Histories

1687 The occurrence of heat capacity peaks well below T_g , defined for present purposes as
 1688 the midpoint of the glass transition for unannealed glasses (Fig. 1(A)), was first reported (for
 1689 PVC) by Illers in 1969 [208]. Gray and Gilbert [209] also observed sub- T_g heat capacity peaks
 1690 in annealed PVC. Chen and Wang [210] reported a well developed shoulder just below T_g in PS
 1691 annealed for 260 h at 320 K (50 K below T_g). Hutchinson and Ruddy [166] observed sub- T_g
 1692 peaks in PS, as did Ruddy and Hutchinson [211] in rapidly quenched PS that had been annealed
 1693 at 333 K for more than about 48 h. Wysgoski [212] observed sub- T_g endotherms in annealed
 1694 ABS (acrylonitrile-butadiene-styrene) and SAN (styrene-acrylonitrile) copolymers and found
 1695 that they became more intense and moved to higher temperatures with increased annealing
 1696 temperature, until at $T_a \approx T_g - 20$ K the endotherms merged with the familiar T_g overshoot.
 1697 Berens and Hodge [213] observed similar behavior in rapidly quenched and annealed PVC and
 1698 reported an increase in both peak height and peak temperature with increasing annealing time.
 1699 Qualitatively similar but smaller sub- T_g peaks have been observed in B_2O_3 [214], and sub- T_g
 1700 shoulders have also been reported in zirconium fluoride based glasses [112,164]. Hodge
 1701 [130,161] observed a well-developed sub- T_g heat capacity peak and a shoulder just below T_g
 1702 for two annealing histories in atactic PMMA, as did Ribelles and coworkers [215,216]. Ribas
 1703 [217] observed sub- T_g peaks in epoxy resins. Hofer et al. [218] observed sub- T_g peaks in
 1704 annealed hydrogel glasses of aqueous lithium chloride and ethylene glycol solutions imbibed in
 1705 poly(2-hydroxy-ethyl methacrylate). The bulk solutions exhibited the more common overshoots
 1706 in the glass transition range. Senapati and Angell [219] observed sub- T_g endotherms in mixed
 1707 anion glasses in the system $60AgI-(40 - y)Ag_2SO_4-yAg_2WO_4$ for y values near 20, after
 1708 annealing well below T_g . For y values near 0 and 40 annealing produced overshoots above T_g .
 1709 McGowan et al. [220] observed sub- T_g peaks in some main chain nematic polymers. Altounian
 1710 et al. [221] observed endothermic peaks in annealed Fe-B metallic glasses, and Chen [222]
 1711 observed annealing induced sub- T_g shoulders in an amorphous metal alloy (composition
 1712 $Pd_{48}Ni_{32}P_{20}$). Sub- T_g endothermic peaks with exothermic minima between them and the glass
 1713 transition have been observed in several metallic glasses. The exotherm results from the
 1714 nonequilibrium glass approaching the equilibrium $T_f = T$ line from above, commonly observed
 1715 in rapidly quenched glasses heated at relatively slow heating rates (Fig. 1(B) and Section 5.1.1).
 1716 The annealing endotherm is superimposed on, and thus attenuated by, this exotherm.
 1717 Representative examples of these effects have been reported in a series of papers by Inoue,
 1718 Chen and Masumoto for $(Pd_{0.86}Ni_{0.14})_{83.5}Si_{16.5}$, a series of $(Fe, Co, Ni)_{75}Si_{10}B_{15}$ alloys [224],
 1719 several Zr-Cu-Fe and Zr-Cu-Ni compositions [225] and in $(Fe_{0.5}Ni_{0.5})_{83}P_{17}$ and $(Fe_{0.5}Ni_{0.5})_{83}B_{17}$
 1720 [226].

1721 These observations testify to the occurrence of sub- T_g endotherms in a wide variety of
 1722 glasses. Such behavior was first explained in terms of enthalpy relaxation and recovery by
 1723 Kovacs et al. [47]. Quantitative fits of the TN phenomenology to experimental data were first
 1724 given by Hodge and Berens [152], who found that the endotherms were most easily produced in

1725 materials with the most extreme nonexponentiality (broadest distribution of retardation times).
 1726 These authors, as well as others [48], suggested that the phenomenon was a manifestation of the
 1727 memory effect. Sufficient data have been published to establish some clear experimental trends
 1728 [130,161]:

1729 (1) The sub- T_g peak temperature T_{\max} , the decrease in T_f during annealing ΔT_f , and the peak
 1730 height $C_{p,\max}^N$ all increase approximately linearly with $\log t_a$ at constant T_a and short t_a . At long
 1731 t_a these quantities approach limiting values as the annealed glass approaches the equilibrium
 1732 state and the sub- T_g peaks evolve into overshoots.

1733 (2) The quantities T_{\max} , ΔT_f and $C_{p,\max}^N$ increase linearly with T_a at constant t_a when $T_a \ll T_g$.
 1734 At $T_a \approx T_g - 20\text{K}$, ΔT_f and $C_{p,\max}^N$ pass through a maximum. These maxima occur because at
 1735 higher T_a the annealed glasses reach the equilibrium state ($T_f = T_a$) and the difference between
 1736 T_f and T_a decreases to zero as T_a approaches T_g .

1737 (3) Faster cooling rates before annealing increase $C_{p,\max}^N$ but have little effect on T_{\max} .

1738 Nonthermal perturbations applied and released before annealing produce similar behavior (see
 1739 next section).

1740 Sub- T_g endotherms are superimposed on the glass transition heat capacity ‘background’
 1741 observed at the same cooling and heating rates but without intervening annealing. This
 1742 superposition is clearly seen in published heat capacity curves such as those for PS [210],
 1743 zirconium fluoride based glasses [112,164], and PVC [213, 227]. It is also evident in calculated
 1744 curves [32,152]. This phenomenon is surprising at first glance since it might be expected that
 1745 the nonlinear kinetics would couple the glass transition to changes in T_f induced by annealing.
 1746 The apparent absence of coupling can be rationalized by noting that the effective reduced times
 1747 for the annealing and glass transition processes are different. The glass transition and sub- T_g
 1748 peaks are Boltzmann superimposed responses to two separate perturbations: cooling through the
 1749 glass transition and annealing. The long average retardation times associated with low annealing
 1750 temperatures produce short reduced times and these promote sub- T_g peaks. In these
 1751 circumstances only the shorter retardation time components of the distribution relax and partial
 1752 recovery occurs in the glassy state. Thus materials with more nonexponential decay functions,
 1753 corresponding to broader distributions with a greater proportion of very short retardation time
 1754 components show an increased tendency to produce sub- T_g endotherms. At longer reduced
 1755 times produced by longer anneals and/or by higher annealing temperatures, and shorter average
 1756 retardation times, the reduced timescale for annealing lengthens and approaches the
 1757 characteristically long reduced times associated with the glass transition. In these circumstances
 1758 the sub- T_g annealing peak merges with the glass transition and the glass transition begins to be
 1759 affected by annealing, as noted by Hutchinson and Ruddy [91] for example. At still longer
 1760 annealing times enthalpy recovery is manifested as the familiar high overshoot above T_g .

1761 The reproduction of sub- T_g endotherms and their behavior with respect to annealing
 1762 conditions by the KAHR and TN phenomenologies indicates that these endotherms are indeed a
 1763 manifestation of enthalpy relaxation and recovery, and are not due to changes in crystallinity or
 1764 the development of qualitatively different molecular structures. Nor are they the result of

1765 secondary relaxations that are somehow manifested as heat capacity anomalies by annealing,
1766 since the endotherms can be calculated assuming unimodal distributions.

1767

1768 5.1.3.2 Nonthermal Histories.

1769 Sub- T_g endotherms also occur in polymeric glasses that have experienced hydrostatic
1770 pressure perturbations, undergone mechanical deformation, or been exposed to solvent or vapor
1771 treatments. Weitz and Wunderlich [228] observed sub- T_g peaks in PS and PMMA samples that
1772 had been cooled under pressure to form densified glasses and then reheated under atmospheric
1773 pressure. At low pressures a simple reduction in overshoot was observed with the sub- T_g peaks
1774 appearing only at pressures above 200 MPa. At the highest pressures (345 MPa) a broad
1775 exotherm developed between the sub- T_g peak and T_g . Although annealing was not intentionally
1776 introduced in these experiments the samples were stored in a freezer for a day or more between
1777 cooling and heating, or were at or near room temperature for at least the time required to
1778 transfer samples from the pressure vessel to the calorimeter. Modeling calculations suggest [32]
1779 that unusually high fictive temperatures can be attained following pressure release and that
1780 significant relaxation can occur in a few minutes at room temperature, so it seems reasonable to
1781 speculate that some annealing could have occurred during sample transfer. The exotherms
1782 observed for the highest pressure densified glasses are characteristic of rapidly cooled and
1783 slowly reheated glasses and are also consistent with a high fictive temperature being generated
1784 by release of the high pressures applied during cooling. These data are qualitatively similar to
1785 those found in splat quenched and annealed metals, discussed earlier. Nonpolymeric materials
1786 (phenolphthalein, sucrose, $\text{KNO}_3/\text{Ca}(\text{NO}_3)_2$) exhibited only a decrease in overshoot with
1787 increasing pressure, presumably because of the less nonexponential decay functions (narrower
1788 distributions) for these materials. Similar results to those observed by Weitz and Wunderlich for
1789 PS and PMMA were reported for PS by Richardson and Savill [227], Yourtee and Cooper [229],
1790 Dale and Rogers [230] and Brown et al. [231], and for PMMA by Kimmel and Uhlmann [232]
1791 and Price [233]. Wetton and Moneypenny [234] observed sub- T_g peaks in pressure densified
1792 PVC, PMMA, PS, poly(4-methoxystyrene), poly(3-chlorostyrene) and poly(4-chlorostyrene).
1793 Prest and coworkers [235,236] reported sub- T_g endotherms in pressure densified PVC and
1794 observed that they became more asymmetric and moved to slightly lower temperatures with
1795 increasing pressure. Hutchinson et al. [237] observed a sub- T_g endotherm in an annealed sample
1796 of a pressure densified silver iodomolybdate glass.

1797 Sub- T_g endotherms have also been observed in polymers subjected to various mechanical
1798 stresses. Prest and Roberts [235] reported them in mechanically compacted PS, and Berens and
1799 Hodge [238] observed them in PVC samples that had been cold drawn to near or beyond the
1800 yield stress, or subjected to simple powder compaction (thought to generate localized shear
1801 stresses between the powder particles that exceeded the yield stress). Brady and Jabarin [239]
1802 observed sub- T_g endotherms in tensile drawn PVC. Vapor- or solvent- induced swelling stresses
1803 have also been reported to accelerate the development of sub- T_g endotherms in polymers.
1804 Shultz and Young [240] reported such an effect for freeze-dried PS and PMMA and Berens and
1805 Hodge [213] observed that vapor-induced swelling of PVC accelerated the development of sub-
1806 T_g peaks.

1807 Very few data are available on the effects of nonthermal perturbations applied during
 1808 annealing but released before heating. Berens and Hodge [213,238] observed that vapor induced
 1809 swelling, pressure (approximately hydrostatic), and mechanical stress all decreased the rate of
 1810 annealing in PVC when applied during annealing. Chan and Paul [241] found that exposure of
 1811 BPAPC to high CO₂ pressure during annealing reduced the magnitude of the annealing
 1812 endotherm.

1813 The results obtained to date suggest that it is the release of the nonthermal perturbations
 1814 before annealing, rather than the perturbations per se, that increases T_f' [32]. An increase in
 1815 enthalpy following pressure release is known to occur in pressure densified PS [242] and could
 1816 well be a general phenomenon. The reduction in annealing endotherms by some form of stress
 1817 applied after annealing has sometimes been referred to as 'rejuvenation', and it seems likely that
 1818 this rejuvenation is caused by the increase in T_f induced by the application and release of stress
 1819 compensating for the decrease in T_f during annealing. It appears that the application and release
 1820 of nonthermal perturbations, particularly when applied to polymers, can elevate T_f' to higher
 1821 values than those achievable by rapid thermal quenches. Thus the tendency of many materials to
 1822 produce sub- T_g endotherms after long anneals well below T_g may simply be accelerated by the
 1823 application and release of nonthermal stresses, and that nonthermal histories do not produce any
 1824 qualitatively new effects. Modeling results [32] support this hypothesis.

1825

1826 6 Enthalpy Relaxation Parameters

1827 Opalka [112] and Moynihan et al. [113] determined the best functional forms for $\phi(t)$
 1828 and $\tau(T, T_f)$ for several inorganic glasses, including B₂O₃ and a series of ZBLA [243] fluoride
 1829 glasses. They compared the stretched exponential and a truncated stretched exponential form for
 1830 $\phi(t)$, and the Davidson-Cole, log Gaussian, box and wedge distributions. For $\tau(T, T_f)$ they
 1831 compared NM, AGL and AGF. The stretched exponential and AGF gave the best overall fits to
 1832 heat capacity data. When the fits were within or close to probable experimental uncertainty, the
 1833 NM, AGL and AGF forms for $\tau(T, T_f)$ were indistinguishable when combined with the
 1834 stretched exponential form for $\phi(t)$. When the best fits were well outside experimental
 1835 uncertainty, the AGL and AGF forms for $\tau(T, T_f)$ gave better fits than NM. Here we discuss
 1836 the KAHR, NM and AG phenomenologies for nonlinearity. For almost all parameterizations the
 1837 nonlinear stretched exponential decay function has been used.

1838

1839 6.1 KAHR Equation

1840 The activation energy θ and nonlinearity parameter x have been determined for PS by
 1841 Hutchinson and Ruddy [91]. For a monodisperse sample with $M_n = 30.1 \times 10^3$ they found
 1842 $\theta = 0.52 \text{ K}^{-1}$ (corresponding to $\Delta h^*/R = 70 \text{ kK}$) and $x = 0.48$. These x and Δh^* values agree
 1843 within typical experimental uncertainties (about $\pm 10\%$ in Δh^* and ± 0.05 in x) with those
 1844 obtained by others using the NM equation and TN formalism (see below). Prest et al. [153] also
 1845 obtained KAHR parameters for PS and found $\theta = 0.47 \text{ K}^{-1}$ using curve fitting and $\theta = 1.0 \text{ K}^{-1}$
 1846 from the cooling rate dependence of T_f' . As discussed in Section 4.5 the reason for the large
 1847 discrepancy is not known but we note here that the curve fitting value is close to the average

1848 value obtained by other groups. Hutchinson et al. [244] determined θ and x for three glasses in
 1849 the AgI-AgPO₃-Ag₂MoO₄ system. The average value of x was 0.68 and θ increased with AgI
 1850 content from 0.21 K⁻¹ for 0% AgI to 0.31 K⁻¹ for 50% AgI. Ingram et al. [245] reported values
 1851 of θ , Δh^* and x for three AgI/Ag₂MoO₄ glasses. By contrast with the phosphate containing
 1852 glasses the values of θ and Δh^* decreased and x increased with increasing AgI content.

1853

1854 6.2 Narayanaswamy-Moynihan Equation

1855 Simple thermal histories involving only cooling and reheating were the first to be
 1856 parameterized and a large number of results have been published. Many types of material have
 1857 been studied with most classes being represented. A compilation of all published (and some
 1858 previously unpublished) NM parameters, averaged over histories that include only rate cooled
 1859 and heated glasses with small or no amounts of annealing, is given in Table 1. Examples of how
 1860 well the TN phenomenology fits experimental data for B₂O₂ and 5P4E are shown in Fig. 3.

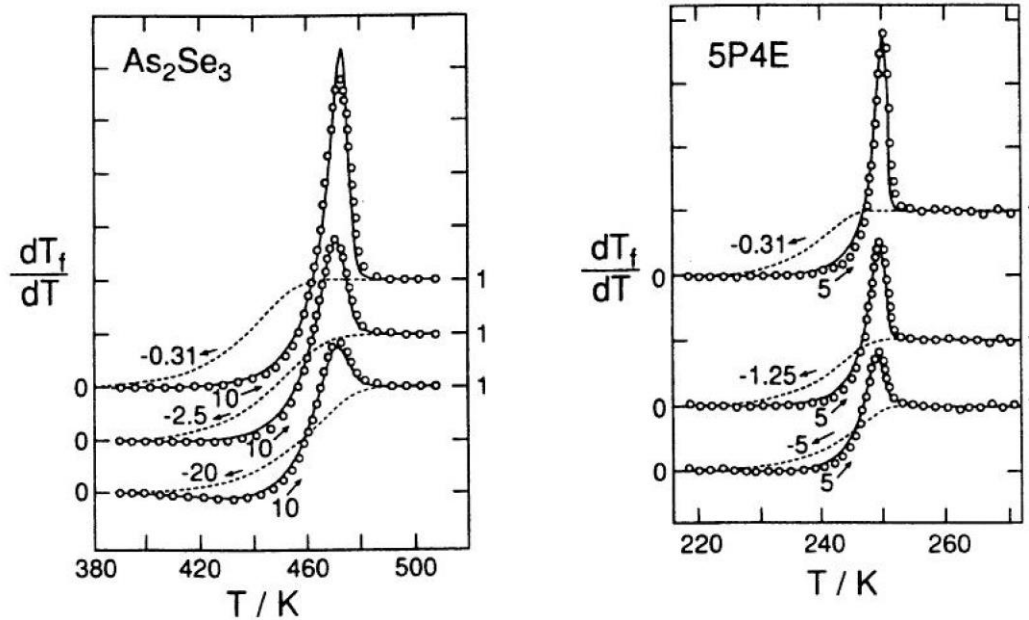
1861 Parameters for PS obtained by different groups are in good agreement for low molecular
 1862 weight monodisperse samples ($M_n \leq 40 \times 10^3$) and polydisperse samples with $M_n \sim 85 \times 10^3$.
 1863 Averages are $\Delta h^*/R = 78 \pm 7$ kK, $x = 0.48 \pm 0.06$ and $\beta = 0.67 \pm 0.08$. The stated uncertainties
 1864 are standard deviations for the eight or nine histories for which only modest departures from
 1865 equilibrium were generated. The spreads in values for $\Delta h^*/R$ and x are comparable with typical
 1866 individual experimental uncertainties but the variability in β is somewhat larger. Values of
 1867 $\Delta h^*/R$ lying outside the range cited above were reported by Privalko et al. [246] for higher
 1868 molecular weights (101 and 110 kK for $M_n = 110 \times 10^3$ and 233×10^3 respectively). The value of
 1869 $\Delta h^*/R$ reported by Stevens and Richardson [247] for a monodisperse sample of $M_n = 36 \times 10^3$ is
 1870 higher still (125 kK) but this result was heavily weighted by a single datum at a very slow
 1871 cooling rate obtained outside the DSC. Although there is no apparent reason for questioning this
 1872 datum the remaining data lie within the DSC cooling rate range of the other experiments and are
 1873 consistent with $\Delta h^*/R = 80$ kK. An increase in $\Delta h^*/R$ with increasing M_n for monodisperse
 1874 samples was observed by Privalko et al. [246] and Aras and Richardson [248] but the absolute
 1875 values observed by the two groups differ, particularly at lower molecular weights. The
 1876 differences are illustrated by the parameters of the equation used by Aras and Richardson to fit
 1877 their data:

$$1878 \quad \Delta h^*/R = A - (B/M_n). \quad (184)$$

1879 For 29 M_n values ranging between 5.16×10^2 and 1.5×10^7 Aras and Richardson obtained
 1880 $A = 103$ kK and $B = 1.05 \times 10^8$. Fitting the Privalko data ($M_n = 9 - 233 \times 10^3$) to the same
 1881 equation yields $A = 106$ kK and $B = 2.88 \times 10^5$. For $M_n = 10^6$ these two sets of parameters give
 1882 $\Delta h^*/R = 130$ kK and 106 kK, respectively, almost the same within experimental uncertainty. For
 1883 $M_n = 10^4$ on the other hand the values are 121 kK and 77 kK, a difference of 60% that is well
 1884 outside experimental uncertainty.

1885

1886

1887
1888

1889 Fig. 3. Fits of TN formalism to experimental data for As_2Se_3 and 5P4E, using eqs. (143) and
1890 (144). After ref. [42].

1891
1892

1893 If the highest M_n data of Privalko and lowest M_n data of Aras and Richardson are discarded,
1894 leaving M_n values in the overlapping range $M_n = 1-17 \times 10^3$, the average value of $\Delta h^*/R$ is $79 \pm$
1895 11 kK. With the high and low M_n values included $\Delta h^*/R = 83 \pm 20$ kK. Fictive temperature data
1896 tabulated by Wunderlich et al. [249] for PS yield a value for $\Delta h^*/R$ of 78 kK, in agreement with
1897 the averages just cited. Hodge and Huvard [177] and Hodge [130,161] found $\{\Delta h^*/R = 80$ kK, x
1898 $= 0.43-0.49$, $\beta = 0.68-0.74\}$ for a polydisperse PS, and Hutchinson [96] reported $(\Delta h^*/R = 70$
1899 kK , $x = 0.46$, $\beta = 0.46\}$ for a monodisperse sample. Prest et al. [153] reported parameters for a
1900 total of 17 thermal histories, the averages being $\Delta h^*/R = 81 \pm 14$ kK, $x = 0.62 \pm 0.09$ and $\beta = 0.81$
1901 ± 0.16 . These last variabilities in $\Delta h^*/R$ and x are comparable with typical experimental
1902 uncertainties but the spread in β values is substantially larger than the typical uncertainty of
1903 ± 0.05 , principally because some of the reported values of β were greater than 1. These all
1904 occurred for the highest overshoots (where thermal transfer effects are greatest and the departure
1905 from equilibrium largest), and if these histories are excluded the average becomes $\beta = 0.74 \pm$
1906 0.09 . The averages and variabilities for the other parameters, after exclusion of the histories for
1907 which $\beta \geq 1$, are $x = 0.58 \pm 0.07$ and $\Delta h^*/R = 66 \pm 8$ kK, both uncertainties being comparable
1908 with typical experimental uncertainty. No systematic trends with thermal history or overshoot
1909 $C_{p,max}^N$ were observed. Tsitsilianis and Mylonas [60] observed that a star PS had similar
1910 parameters to linear PS although their value of β was obtained from a linear decay function and
1911 is therefore unreliable (see discussion of the Scherer relations in Section 1.2.3). The PS
1912 parameters obtained from an analysis [177] of the data of Chen and Wang [210] are inconsistent
1913 with the values cited above. The discrepancy could arise from the relatively low annealing

1914 temperature used in this study although the $\Delta h^*/R$ parameter (175 kK) is still much larger than
 1915 the next largest value reported by Stevens and Richardson [247] (125 kK). It is possible that
 1916 larger values of $\Delta h^*/R$ result in some way from the low values of T_f' induced by long aging
 1917 times [210] or very slow cools [247].

1918 For PVAc there is good agreement between the data of Sasabe and Moynihan [250] and
 1919 Hodge [130,161], which improves if the values of $\Delta h^*/R$ are forced to be equal [130] (the two
 1920 reported values of 71 and 88 kK are statistically indistinguishable at about the 60% confidence
 1921 level for typical standard deviations of $\pm 10\%$). For $\Delta h^*/R = 71$ kK the differences of 0.06 in
 1922 both β (0.57 and 0.51) and x (0.35 and 0.41) are close to experimental uncertainty and can
 1923 reasonably be attributed to sample differences (such as molecular weight distribution). The
 1924 values of β are in good agreement with linear dielectric values when these are extrapolated to
 1925 the same temperature [250]. However the activation energy at $T_g = 304$ K for enthalpy
 1926 relaxation is higher than that for dielectric relaxation by a factor of 1.8.

1927 There is also good agreement between the best fit parameters reported for aPMMA by
 1928 Hodge [130,161] and Ribelles et al. [215] when compared for similar thermal histories. The
 1929 Ribelles group reported a thermal history dependence for their parameters but their best fit
 1930 values for one particular history agreed with the averaged set reported by Hodge that was itself
 1931 heavily weighted by a single thermal history that produced a similarly shaped sub- T_g heat
 1932 capacity peak: Hodge reported [$\Delta h^*/R = 138$ kK, $\ln A(s) = -355.7$, $x = 0.22$, $\beta = 0.37$], and
 1933 Ribelles et al. found ($\Delta h^*/R = 125 - 150$ kK, $x = 0.18 - 0.21$, $\beta = 0.33 - 0.35$). Mijovic and
 1934 coworkers [193,194] reported $\Delta h^*/R = 132$ kK, in agreement with Hodge and Ribelles et al. Ott
 1935 [251] reported a lower value of $\Delta h^*/R = 60.6$ kK for aPMMA. Tribone et al. [162] found $\Delta h^*/R$
 1936 $= 106$ kK, $x = 0.15 - 0.40$ and $\beta = 0.35 - 0.45$ for aPMMA. The difference between the $\Delta h^*/R$
 1937 values of Hodge/Ribelles et al. and Tribone et al. can reasonably be attributed to the different
 1938 methods for determining it. Hodge reported that the parameter set found by him produced a
 1939 value of $\Delta h^*/R$ very similar to that found by Tribone et al. if it was defined in the same way
 1940 (from the heating rate dependence of T_g at fixed Q_c). Avramov et al. [252] reported that the
 1941 activation energies obtained from Q_h at constant Q_c and from Q_c at constant Q_h differed
 1942 substantially, even when determined on the same sample of the same material (a bismuth
 1943 germanate). The activation energy determined from Q_h was smaller than that obtained from Q_c
 1944 by a factor (2.4) that was larger than, but in the same direction as, the discrepancy between the
 1945 Hodge/Ribelles et al. and Tribone et al. activation energies for aPMMA (a factor of 1.3). The
 1946 values of β obtained by Hodge, Ribelles et al. and Tribone et al. are all similar to values
 1947 obtained by linear techniques such as dielectric relaxation spectroscopy. For example $\beta =$
 1948 0.31 ± 0.02 is estimated from the data of Ishida and Yamafuji [253] using eq. (75). By contrast
 1949 with PVAc the average enthalpic activation energies reported by Hodge, Mijovic et al. and
 1950 Ribelles et al. are somewhat smaller than the dielectric value of 155 kK at $T_g = 375$ K (again
 1951 estimated from the data of Ishida and Yamafuji). Tribone et al. also determined the parameters
 1952 for hydrogenated and deuterated isotactic and syndiotactic PMMA. The activation energies for
 1953 these tacticities differed substantially from that of the atactic form (see Table 1) which as
 1954 expected lay between the isotactic and syndiotactic values. No significant differences were
 1955 found between the parameters for hydrogenated and deuterated samples for any of the
 1956 tacticities. A dependence of x on thermal history and an invariance of β were observed for all
 1957 three tacticities.

1958 Parameters for PVC have been reported by Hodge and Berens [152], Hodge [130,161]
 1959 and Pappin et al. [254]. Both groups used material from the same source. The exceptionally low
 1960 values for β obtained by Hodge and collaborators, 0.23-0.27 depending on details of the data
 1961 analysis, were consistent with average values extracted from the extraordinarily broad dielectric
 1962 loss peaks (which were strongly temperature dependent however). It is the lowest value of β
 1963 yet reported for enthalpy relaxation. The extremely low value of β may be caused by the small
 1964 amount of crystallinity in PVC and a corresponding heterogeneous structure giving rise to a
 1965 physically significant distribution of relaxation times in addition to inherent nonexponentiality.
 1966 The value of x obtained by Hodge and Berens, 0.10-0.11, is also extraordinarily small. These x
 1967 and β parameters were determined from the behavior of sub- T_g peaks for different histories and
 1968 did not produce a particularly good fit to the heat capacity in the glass transition region.
 1969 However the experimental uncertainties in the data were rather high, especially for data near the
 1970 minima between the sub- T_g peak and the heat capacity rise at T_g . Uncertainties near these
 1971 minima are determined largely by the extrapolated glassy heat capacity which for the powder
 1972 samples was quite noisy, and the rubbery heat capacity was rendered unusually uncertain by the
 1973 broad melting endotherm that almost overlaps with the glass transition. The cooling rate was
 1974 also estimated rather than controlled. Thus the relatively poor fits to the glass transition were
 1975 less significant than usual although it seems a problem does exist. Pappin et al. [254] reported x
 1976 = 0.27 (almost three times larger than the Hodge and Berens value) and $\Delta h^*/R = 135$ kK (65%
 1977 lower than the value 225 kK found by Hodge and Berens). Ott [251] reported an intermediate
 1978 value of $\Delta h^*/R = 168$ kK for PVC. The origin of the discrepancies, particularly in Δh^* obtained
 1979 from integrated heat capacities, is not known but is conceivably due to experimental
 1980 uncertainties that are larger than claimed by both groups. There are also possible differences in
 1981 sample crystallinities due to different stabilization protocols above T_g before cooling [195], and
 1982 differences in $C_{pe}(T)$ could also have arisen from different assessments of the melting
 1983 endotherm. Crystallinity has been reported to affect the amorphous phase [255,256] and as
 1984 noted above could affect the β parameter. The difference in x cannot be ascribed to the
 1985 different values of Δh^* , however, because the values of $x\Delta h^*/R$ are very different, ~36 kK for
 1986 Pappin et al. [254] and 25 kK for Hodge and Berens [152].

1987 For BPAPC Hodge [130,161] reported $\Delta h^*/R = 150$ kK, $x = 0.19$ and $\beta = 0.46$. Except
 1988 for β these parameters are similar to those reported by the same author for aPMMA. The value
 1989 of β is about 0.10 larger than that of PMMA and this difference probably accounts for the
 1990 infrequent observation of sub- T_g endotherms in BPAPC. Ott [251] reported $\Delta h^*/R = 207$ kK for
 1991 BPAPC.

1992 The values of $\Delta h^*/R$ for inorganic glasses such as B_2O_3 [86,160], As_2Se_3 [257],
 1993 $Ca/K/NO_3$ [258], $NaKSi_3O_7$ [259], NBS 710 (a soda-lime-silicate) [129,141] and lead silicate
 1994 (NBS 711) [260], are generally smaller than those observed for polymers and the values of x and
 1995 β are generally larger (see Table 1). The parameters for the monomeric organic material 5P2E
 1996 [42,261] are similar to those of the inorganics. Three materials stand apart from this trend
 1997 however. The parameters for polystyrene are similar to those observed for many inorganics
 1998 while those for a series of inorganic ZBLA fluoride glasses [243] and lithium acetate (LiAc) are
 1999 similar to those for polymers. The parameters for LiAc are very uncertain however because of
 2000 the inability to obtain an independent value of $\Delta h^*/R$ (the samples crystallized at slow cooling
 2001 rates). For alkali, mixed alkali and lead silicates [259,260] the values of x (0.65-0.70) are much

2002 higher than for any other material but the values for $\Delta h^*/R$ and β are not unusual. Enthalpic
 2003 values of β cannot be compared with dielectric values for many inorganics because of the high
 2004 conductivity of the latter, although Moynihan et al. [42] compared enthalpy, volume, strain and
 2005 stress relaxation parameters for 5P2E, B₂O₃, As₂Se₃ and a mixed alkali silicate. They found that
 2006 the values of β for different relaxation properties were, with a couple of exceptions, within the
 2007 typical uncertainty of ± 0.05 . Activation energies generally agreed to within 10% with the largest
 2008 difference being 20%. There is excellent agreement between the parameters for B₂O₃ obtained
 2009 by Sales [86] and DeBolt et al. [160].

2010 Hofer et al. [218] reported parameters for aqueous solutions of ethylene glycol (22
 2011 mol%) and lithium chloride (16 mol%), both in the bulk and imbibed in poly(hydroxyethyl
 2012 methacrylate) (PHEMA) as a hydrogel. The x parameters changed somewhat with thermal
 2013 history but the values of $\Delta h^*/R$ and averaged x for the bulk and hydrogel materials were the
 2014 same within uncertainties. The values of β changed less with history but their averages were
 2015 substantially smaller for the solutions imbibed in PHEMA than for the bulk: β decreased from
 2016 0.64 to 0.39 for ethylene glycol and from 0.93 to 0.68 for lithium chloride.

2017 As noted in the Introduction the values of $\theta = \Delta h^*/RT_g^2$ are similar for a wide variety of
 2018 materials, generally being of the order of unity for polymers and 0.1 for inorganics. The average
 2019 and standard deviation for all materials listed in Table 1 are 0.57 ± 0.32 .

2020 The enthalpic activation energies for inorganics are for the most part the same as those
 2021 determined from viscosity data above T_g . An exception to this occurs for the ZBLA glasses for
 2022 which the enthalpic activation energy is 40% larger than the average of two viscosity
 2023 measurements [112,113].

2024 Hodge [161] reported correlations between all four TN parameters for all materials
 2025 analyzed up to that time and these correlations have been confirmed in more recent compilations
 2026 [130,133]. Low values of $\Delta h^*/R$ are associated with high values of x and β and high values of
 2027 $\Delta h^*/R$ are found with low values of x and β . They have been rationalized in terms of the Adam-
 2028 Gibbs phenomenology, discussed next.

2029 2030 6.3 Adam-Gibbs-Fulcher (AGF) Equation

2031 This equation has been discussed in Section 2.3.3. It was noted in that section that the
 2032 accuracy of eqs. (110) and (112) - (116) relating the AGF parameters Q and T_2 to the NM
 2033 parameters x and Δh^* has been established by Hodge [130], Opalka [112], Moynihan et al.
 2034 [113], Scherer [129], Sales [86], and Ribelles et al. [215]. Thus the AGF nonlinearity parameters
 2035 for materials subjected only to NM analyses can be estimated with some confidence. This
 2036 confidence is reinforced by the finding that the β parameter is the same within uncertainties for
 2037 both NM and AGF analyses, where these have been performed on the same materials and for the
 2038 same thermal histories. Published AGF parameters are summarized in Table 2 together with
 2039 values of the **parameters** T_K and T_0 where these are known.

2040 In assessing the AGF formalism we consider first the quality of fits relative to NM.
 2041 Following this we discuss the parameter T_2 and its relation to the Kauzmann temperature T_K
 2042 and to the VTF temperature T_0 obtained from linear relaxation data above T_g (most often
 2043 dielectric). Enthalpic activation energies are then compared with values obtained by dielectric

2044 and other linear relaxation techniques, followed by a discussion of the ‘primary’ activation
2045 energy $\Delta\mu$.

2046 The goodness of fits afforded by AGF is comparable with that given by NM although
2047 modest improvements of AGF fits over those of NM have been reported by Hodge for PS [130],
2048 Opalka and coworkers for some ZBLA glasses [112,113], and Ribelles et al. for a-PMMA
2049 [215]. A comparison of the NM, AGL and AGF best fits to atactic PMMA, for a single thermal
2050 history that produces a heat capacity peak in the middle of the glass transition range, is shown in
2051 Fig. 4. Because of the similarity in fits almost none of the fitting problems found for NM are
2052 significantly improved by the AGF formalism. The advantages of AGF are restricted to the
2053 physical significance of its parameters and its ability to rationalize the correlations observed
2054 between the NM and β parameters. The reasons for the similarity in fitting quality of the NM
2055 and AGF equations have been discussed by Moynihan et al. [113]. They observed that the ratio
2056 of nonlinear to linear retardation times at temperature T is approximately proportional to the
2057 departure from equilibrium $(T - T_f)$ for both NM and AGF expressions. For NM

$$2058 \quad \ln\left(\frac{\tau}{\tau_e}\right) \approx \left[\frac{(1-x)\Delta h^*}{RTT_f} \right] (T - T_f) \quad (185)$$

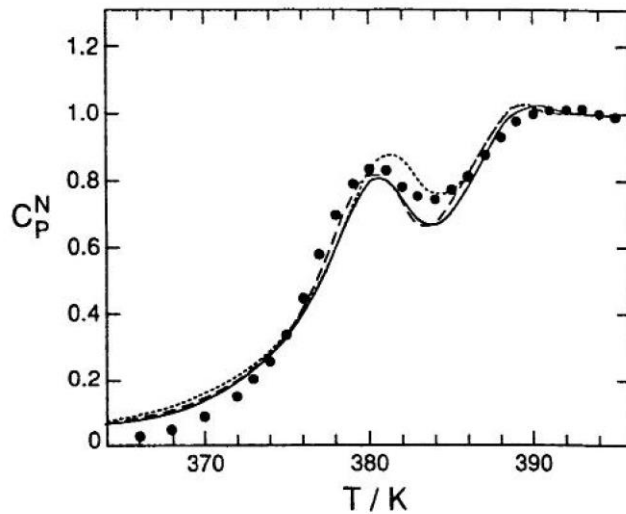
2059 and for AGF

$$2060 \quad \ln\left(\frac{\tau}{\tau_e}\right) \approx \left[\frac{QT_2}{T(T_f - T_2)(T - T_2)} \right] (T - T_f). \quad (186)$$

2061 The AGF derived values of T_2 are within 1 K of T_K for the inorganic materials B_2O_3 and
2062 As_2Se_3 . This agreement is unusually significant both because $\Delta C_p(T)$ for these materials closely
2063 follows the hyperbolic form of eq. (55) from which the AGF equation is derived and because the
2064 values of T_K are particularly reliable. The agreement for B_2O_3 is significant in another regard. It
2065 has been a long standing puzzle why the viscosity of B_2O_3 becomes Arrhenius slightly above
2066 T_g , in contrast with the VTF behavior of enthalpy relaxation indicated by the equality of T_2 and
2067 T_K . Angell [21,262] has argued that the processes responsible for viscosity at temperatures just
2068 above T_g can decouple from the longer time processes probed by enthalpy relaxation. The AGF
2069 enthalpy relaxation parameters for B_2O_3 support this view.

2070 For aPMMA Hodge [130] reported $T_2 = 325$ K. A Kauzmann temperature cannot be
2071 calculated for the uncrystallizable atactic polymer of course but a value of 285 K has been
2072 estimated for isotactic PMMA by O’Reilly et al. [263]. The measured values of $\Delta C_p(T)$ are the
2073 same for isotactic and atactic PMMA [263] so the difference in T_K is the same as the difference
2074 in T_g if the residual entropies at T_g are assumed to be equal. For iPMMA $T_g = 325$ K, $T_K = 285$
2075 K and $T_g - T_2 = 40$ K. Thus, $T_K \approx T_g - 40 \approx 335$ K is estimated for aPMMA. This value for T_K is
2076 equal to the T_2 value reported by Hodge [130] within experimental and computational
2077 uncertainties. For PS Hodge [130] found $T_2 = 210$ K, substantially lower than the values for T_K
2078 obtained by Karasz et al. [264] (280 ± 15 K) and by Miller [265] (260 ± 15 K). This discrepancy
2079 is the best documented failure of the AGF formalism to date both because of the relatively large
2080 number of published enthalpy relaxation parameters for PS and because of the reliable estimates

2081 of T_K . The cause of the discrepancy is unknown. Curiously however the value of $T_2 = 260$ K
 2082 estimated from the anomalous NM parameters obtained from the Chen and Wang data [130]
 2083 agrees very well with T_K . The AGF value of T_2 for BPAPC (325 K) is substantially above T_K
 2084 (220 K) but since this value of T_K is almost 200 K below T_g [85] there is reason to doubt its
 2085 reliability. It is possible that the Kauzmann analysis could be compromised by the parameters
 2086 used to define $\Delta C_p(T)$, which as noted above (Section 1.3.4) predict $\Delta C_p = 0$ near the melting
 2087 point. Moynihan et al. [113] obtained AGF parameters for glycerol and propylene glycol.
 2088



2089
 2090
 2091 Fig. 4. Fits of NM (eq. (88)), AGL (eq. (108)) and AGF (eq. (109)) expressions for $\tau(T, T_f)$ to
 2092 data for atactic poly(methylmethacrylate). After ref. [130].
 2093
 2094

2095 **Their** averaged AGF parameters for glycerol were in excellent agreement with the ac
 2096 calorimetry data of Birge and Nagel [100,101] but the stretched exponential parameters were
 2097 very different. The AGF parameters changed systematically with cooling rate at fixed heating
 2098 rate for simple rate scans without annealing and the authors concluded, as have other
 2099 investigators, that the phenomenology is deficient, probably in the way nonlinearity is handled.
 2100 In cases where T_K is unavailable it is of interest to compare T_2 with the VTF T_0 parameter
 2101 obtained from linear relaxation data above T_g . Part of this interest arises from the possible
 2102 decoupling of enthalpy (and volume) relaxation from viscosity, diffusion, dielectric, viscoelastic
 2103 or other dynamic processes, suggested by Angell [20,21,262] and discussed for B_2O_3 above.

2104 Such decoupling manifests itself as differences in T_0 or T_2 for different processes. For
 2105 PVAc the enthalpic value of $T_2 = 182$ K obtained from the data of Sasabe and Moynihan [250]
 2106 is less than $T_0 = 238$ K obtained dielectrically by the same investigators on the same sample.
 2107

2108
2109

TABLE TWO
Adam-Gibbs-Fulcher Parameters

Material	Q (kK)	T_2 (K)	β	$-\ln A$ (s)	[Ref] ^a AGF	T_K (K) [ref]	T_0 (K) [ref]
PVAc	6.23	225	0.55	66.60	[130]		238[250]
PVC	2.61	320	0.28	59.74	[130]	290[130]	350[266]
BPAPC	7.03	325	0.54	70.30	[130]	(220)[85]	
PS	17.1	210	0.74	100.3	[130]	260[265]	
						280[264]	
aPMMA	3.43	325	0.34	55.45	[130]	335[263]	222[253]
B ₂ O ₃	11.6	321	0.65	25.68	[113,260]	335[65]	402[65]
As ₂ Se ₃	9.82	237	0.67	43.10	[130]	236[203]	
5P2E	6.16	147	0.70	63.00	[130]		
40Ca(NO ₃) ₂ -60KNO ₃	6.73	238	0.46	62.90	[130]		
Na/K silicate	24.0	222	0.66	46.30	[130]		
NBS711 ^b	18.9	248	0.67	34.95	[260]		
NBS710 ^c	8.06	494	0.63	32.83	[260]		
ZBLA	5.96	525	0.50	53.00	[130]		
	12.5	425	0.46	61.38	[113]		
Glycerol ^d	2.18	134	0.51	34.20	[113]	135[64]	132[65]
Glycerol ^e	3.37	120	0.51	43.41	[113]		
LiAc	5.8	335	0.56	-	[133]	370[62]	
yPbO. (1-y)P ₂ O ₅	13-19	150- 350	0.49- 0.77	23.7- 69.2	[86]		
xFe ₂ O ₃ . (1-x)Pb(PO ₃) ₂	19-25	300- 420	0.60- 0.68	53.7- 69.3	[86]		

2110 ^a Parameters obtained directly using the AGF eq. (109) for $\tau_0(T, T_f)$ 2111 ^b Lead silicate.2112 ^c Soda-lime-silicate.2113 ^d $Q_h = 5 \text{ K min}^{-1}$.2114 ^e $Q_c = 20 \text{ K min}^{-1}$

2115

2116

2117 On the other hand the enthalpic T_2 value obtained by Hodge [130] for a different sample of
 2118 PVAc (227 K) agrees well with the dielectric T_0 . Bearing in mind the uncertainties in both T_2
 2119 and T_0 associated with fitting the AGF and VTF equations the two values are probably
 2120 statistically indistinguishable.

2121 For PVC a least squares analysis of the dielectric data of Ishida [266] shown in ref. [267]
 2122 produces a good VTF fit with $B = 290$ K and $T_0 = 351$ K. The value for T_0 is larger than the
 2123 enthalpic value for T_2 of 320 K estimated by Hodge [130], but forcing $T_0 = T_2 = 320$ K
 2124 produces a fit almost as good as the best fit (see discussion of VTF parameter uncertainties in
 2125 Section 1.2.1). Both values far exceed the value for T_2 of 193 K estimated from the NM
 2126 parameters obtained by Pappin et al. [254]. An approximate value of $T_K = 290 \pm 20$ K has been
 2127 reported by Hodge for PVC [130] using the calorimetric data of Gouinlock [268] but requiring
 2128 uncertain corrections for crystallinity and syndiotacticity. This value for T_K agrees with T_2
 2129 within the (considerable) uncertainties in each. For aPMMA analysis of the dielectric data of
 2130 Ishida and Yamafuji [253] yields $T_0 = 222$ K, considerably below both the enthalpic value $T_2 =$
 2131 325 K cited by Hodge and the estimated Kauzmann temperature of 290 K cited above. It is
 2132 possible that this difference reflects a decoupling of the dielectrically active relaxation processes
 2133 from the broader more inclusive enthalpic processes, similar to that proposed for the viscosity of
 2134 B_2O_3 .

2135 Estimates of the ‘primary’ activation energy $\Delta\mu$ have been published for polymers by
 2136 Hodge [130,133]. The numerical factor relating $\Delta\mu$ to the AGF parameter Q contains the
 2137 minimal entropy s_c^* and the heat capacity change at T_g (or T_2), both of which depend on mass.
 2138 Using the Wunderlich bead as the mass unit and putting $s_c^* = k_B \ln 2$ and $s_c^* = k_B \ln 3!$ yields
 2139 values for $\Delta\mu/k_B$ in the range 3.6 - 18 kK (for $s_c^* = k_B \ln 2$) and 1.4-7.0 kK (for $s_c^* = k_B \ln 3!$).
 2140 The values for $s_c^* = k_B \ln 3!$ are comparable with rotational energy barriers. The rationale for
 2141 choosing $s_c^* = k_B \ln 3!$ was that three chain segments are involved in crankshaft motions and
 2142 that these motions are reasonable candidates for the localized rearrangements involving the
 2143 smallest number of chain segments. Thus the AGF Q parameters are consistent with
 2144 intersegmental rotational energy barriers being the primary excitation barrier for cooperative
 2145 motions near T_g for polymers. For inorganic glasses Scherer [129], Opalka [112] and Moynihan
 2146 et al. [164] obtained sensible values of $\Delta\mu$ comparable with bond energies, assuming
 2147 $s_c^* = k_B \ln 2$.

2148 Sales [86] studied a series of lead and iron phosphate glasses in which the number of
 2149 non-bridging oxygens per PO_4 tetrahedron was varied systematically by changing chemical
 2150 composition. The AGF equation was used to analyze structural relaxation in the glass transition
 2151 for histories without annealing. This work is particularly revealing because of the detailed
 2152 correlation it establishes between the AGF parameters and well defined chemical and structural
 2153 changes. As already noted (Section 6.3) Sales found that eq. (114) relating the AGF parameter
 2154 Q and NM parameter $\Delta h^*/R$ was a good approximation for all materials studied. The AGF
 2155 equation could be well justified for these materials because of the approximate equivalency of
 2156 the hyperbolic and linear forms for ΔC_p (Section 1.3.4). The NM activation energy Δh^*
 2157 increased smoothly with the number of non-bridging oxygens (defined as Q by Sales but
 2158 referred to here as R to avoid confusion with the AGF parameter). The increase was due largely
 2159 to changes in the ratio T_2/T_g and was accompanied by an increase in $\Delta C_p(T_g)$, consistent with
 2160 Angell’s ‘fragility’ increasing with R (Section 6.5). The product $\Delta\mu s_c^*$ was independent of
 2161 composition except for the most iron rich glasses. Assuming $\Delta\mu$ to be determined by the P-O

2162 chemical bond energy that is independent of composition (about 100 kcal mol⁻¹) the estimated
 2163 value of W^* that determines s_c^* (eq. (102)) was found to be about 4.6, or 2^{2.2}. Both W^* and
 2164 T_g/T_2 increased with increasing iron content which was interpreted in terms of different
 2165 coordination numbers and geometries for the Fe³⁺ and Pb²⁺ cations. It was suggested that the
 2166 structural constraints imposed by the crystal field stabilized octahedral Fe³⁺ moieties increased
 2167 the values of both $\Delta\mu s_c^*$ and T_g/T_2 compared with the less geometrically constrained Pb²⁺
 2168 species. As discussed below in Section 6.5 with regard to the NM parameter correlations the
 2169 increases in both $\Delta\mu s_c^*$ and T_g/T_2 are consistent with the idea that $\Delta\mu$, and possibly s_c^* ,
 2170 determine the ratio T_g/T_2 . The values of β did not exhibit any significant variation with R .
 2171 Further interesting speculations about the relationship between coordination number and
 2172 geometry, the pre-exponential factor, strong and fragile behavior and viscosity above T_g can be
 2173 found in the original paper [86].

2174

2175 6.4 AC Calorimetry

2176 This experimental technique has been described in Section 2.2 Real and imaginary
 2177 components of the complex heat capacity C_p^* are obtained as a function of temperature and
 2178 frequency, and it is found that the temperature dependences of the fixed frequency real
 2179 component resemble the heat capacity scans during cooling observable with some DSC
 2180 instruments. As with other linear relaxation techniques stretched exponential (or other
 2181 functional) parameters can be obtained from the real and imaginary components (e.g., by
 2182 applying eqs. (75) or (82) to the loss peaks), and VTF parameters can be obtained from the
 2183 temperature dependence of the position of the peak in the imaginary component or of the
 2184 relaxation time obtained from stretched exponential fits. It is of considerable interest and
 2185 importance to compare the linear parameters obtained by ac calorimetry with the nonlinear
 2186 parameters obtained by scanning calorimetry on the same materials. Unfortunately ac
 2187 calorimetry has so far been applied to only three materials: propylene glycol [101], glycerol
 2188 [101,102], and orthoterphenyl/orthophenyl-phenol mixtures [269-271]. The linear relaxation
 2189 parameters for these materials are collected in Table 3. AC calorimetric and nonlinear DSC
 2190 enthalpy relaxation parameters have been directly compared only for glycerol [113] and the
 2191 nonlinear AGF parameters for this material from Table 2 are included in Table 3 for
 2192 convenience. Excellent agreement between the linear VTF and nonlinear AGF parameters is
 2193 observed but the stretched exponential parameter β is significantly different for the two
 2194 techniques. It is curious that the discrepancy lies in the nonexponentiality which is believed to
 2195 be well described, rather than in the description of nonlinear behavior about which doubts are
 2196 mounting. The discrepancy in β could perhaps be caused by a frequency dependent thermal
 2197 conductivity $\kappa(\omega)$ since the stretched exponential was fitted to $C_p(\omega)\kappa(\omega)$ rather than
 2198 $C_p(\omega)$ (Section 2.2). Such a frequency dependence would not have to be very strong to modify
 2199 the shape of the real and imaginary components from which β is found but could be sufficiently
 2200 weak that the peak frequency in C_p'' and the retardation time are not significantly affected,
 2201 therefore accounting for the agreement in VTF parameters. However κ has been found to be
 2202 independent of frequency for o-terphenyl and its mixtures [269].

2203

2204
2205TABLE THREE
AC Calorimetry Parameters

Material	β	$-\log_{10}A$	T_0 (K)	B (K)	Ref.	Comment
Glycerol	0.65 ± 0.03	14.6 ± 0.9	128 ± 5	2500 ± 300	[100,101]	
(Nonlinear AGF)	0.505	18.85	120	3372	[113]	5 K min^{-1}
	0.510	14.85	134	2179	[113]	20 K min^{-1}
Propylene Glycol	0.61 ± 0.04	13.8 ± 0.4	114 ± 7	2020 ± 130	[100]	
OTP _{1-x} -OPP _x	^a					
$x = 0$ (extrap)				184 ± 13	[269]	
$x = 0.09$		18.7 ± 1.3	117 ± 6	3175 ± 320	[269]	
$x = 0.16$		16.9 ± 2.1	186 ± 12	2397 ± 590	[269]	
$x = 0.22$		20.2 ± 2.3	172 ± 13	3436 ± 820	[269]	
$x = 0.33$		22.2 ± 2.8	164 ± 14	4145 ± 900	[269]	

2206 ^a OTP, o-terphenyl; OPP, o-phenylphenol.2207 ^b Temperature dependent: $\beta = -0.81 - 425/T$ (K).2208
2209

2210 For o-terphenyl the ac calorimetric value of T_0 (184 ± 13 K by extrapolation) agrees
 2211 with T_K (200 ± 11 K) [272]. For glycerol the linear ac calorimetric and nonlinear AGF values of
 2212 T_0 (128 ± 5) and T_2 (127 ± 7 K) also agree with T_K (135 ± 3 K) [64]. The stretched exponential
 2213 parameter β is independent of temperature for glycerol and propylene glycol but is strongly
 2214 temperature dependent for o-terphenyl. Extrapolation of the latter trend [269] indicates that β
 2215 would be zero at or near T_K and T_0 . The stretched exponential β parameters for glycerol and
 2216 propylene glycol obtained calorimetrically are smaller by about 0.15 than the dielectric values
 2217 [103].

2218
2219

6.5 Parameter Correlations

2220 Strong correlations between β , x and Δh^* have been reported by Hodge [130,133] and
 2221 were rationalized in terms of the AGF phenomenology. Major conclusions from this work are
 2222 that the correlations can be consistently mapped onto the classification of strong and fragile
 2223 behavior in liquids advocated by Angell [5,20,21,62] (the origins of which can be traced to the
 2224 work of Laughlin and Uhlmann [123]), and that a high degree of nonlinearity is associated with
 2225 fragile liquid behavior. The mapping arises from (i) the link between nonlinearity and the ratio
 2226 T_g/T_2 (eqs. (113) and (116)), (ii) the VTF result that deviations from Arrhenius behavior
 2227 increase with decreasing T_g/T_2 (eq. (114)), and (iii) the fact that the strong and fragile
 2228 classification rests on T_g/T as a scaling variable. If it is hypothesized that $\Delta\mu$ determines the
 2229 ratio T_g/T_2 , i.e. that a high primary activation energy prevents T_g from approaching T_2 , it can
 2230 be shown that $x\Delta h^*$ is approximately constant:

$$2231 \quad Q \approx K_1 \Delta\mu \approx K_2 \left(\frac{T_f'}{T_2} - 1 \right) \approx K_3 \left(1 - \frac{T_2}{T_f'} \right) \approx K_3 x \quad (187)$$

$$2232 \quad \Rightarrow \frac{\Delta h^*}{R} \approx \frac{Q}{x^2} \approx K_2 / x \Rightarrow \frac{xh^*}{R} \approx K_2. \quad (188)$$

2233 Equation (188) is consistent with the experimental observation that $x\Delta h^*$ is relatively constant
 2234 compared with Δh^* alone (see Table 1). **However** it has been noted by Angell [21] that the VTF
 2235 equation implies that Q and $T_g/T_0 = T_g/T_2 = T_g/T_K$ should be linearly related if the pre-
 2236 exponential factor and the relaxation time at T_g are material independent. For hydrogen bonded
 2237 materials Angell found $T_g/T_0 = 1.0 + 0.0255Q/T_0$, consistent with $T_g \rightarrow T_0 = T_2 = T_K$ when
 2238 $Q \rightarrow 0$. On the other hand the assumption that $\Delta\mu$ determines T_g/T_2 could also be regarded as
 2239 being vindicated by the correct prediction that $\tau(T_g)$ is relatively constant for different
 2240 materials. Angell [5,20,21,83] has also argued that the thermodynamic contribution $\Delta C_p(T_g)$ to
 2241 the AG Q parameter as well as the kinetic factor $\Delta\mu$ are both important in determining liquid
 2242 state dynamics. Thus the assumption that $\Delta\mu$ is the dominant factor may only be valid for
 2243 similar classes of material, and this would be consistent with the separate correlations observed
 2244 for different classes of materials discussed below. On the other hand it can also be argued that
 2245 the thermodynamic factor ΔC_p would be more consistently assessed at the thermodynamic
 2246 temperature T_K rather than the kinetically determined T_g , although this would require longer
 2247 extrapolations and introduce additional uncertainties. One analysis [83] has suggested that using
 2248 $\Delta C_p(T_g)$ can generate spurious discrepancies.

2249 If $\Delta C_p(T_g)$ is assumed constant rather than $\Delta C_p(T_2)$ the proportionality constant
 2250 between Q and $\Delta\mu$ and the relation between Q and Δh^* are both modified. Inserting
 2251 $C = C'T_g/T_2$ (eq. (55)) into eq. (105) for Q yields

$$2252 \quad Q = \left[N_A s_c^* \Delta\mu / (k_B C') \right] (T_2 / T_g) \quad (189)$$

$$2253 \quad = Q'(T_2 / T_g) \quad (190)$$

2254 so that

$$2255 \quad Q' = Q(T_g / T_2) \quad (191)$$

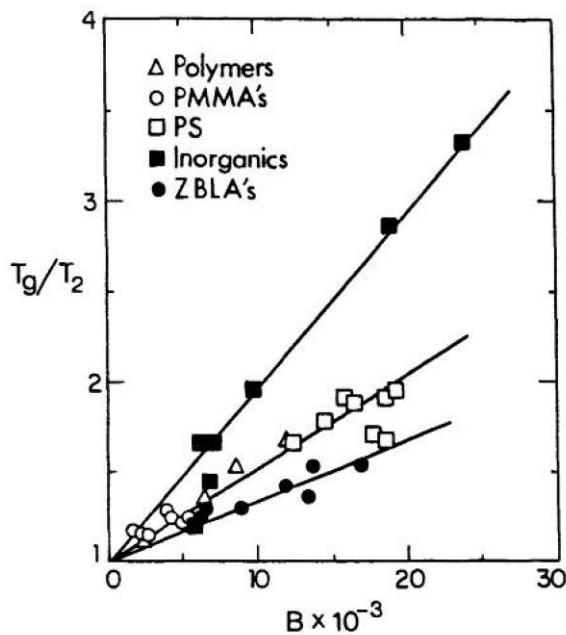
$$2256 \quad = \frac{x^2 \Delta h^*}{R} \left(\frac{T_g}{T_2} \right) \quad (192)$$

$$2257 \quad = \frac{x^2 \Delta h^*}{R(1-x)}. \quad (193)$$

2258 Equation (193) is identical to eq. (110) obtained from $\Delta C_p = C = \text{constant}$.

2259 When $T_f'/T_2 \approx (1-x)^{-1}$ is plotted against $Q \approx x^2 \Delta h^* / R$ [133] linear relations consistent
 2260 with eqs. eq. (187) are observed Separate correlation lines are observed for different classes of
 2261 materials corresponding to different groupings of constant $x\Delta h^*$, suggesting that K_2 of eqs.
 2262 (187) and (188) depends on material type. These correlations are shown in Fig. 5. The separate

2263 correlation lines could be due to the dependence of ΔC_p on the class of material discussed
 2264 above, or to a variable s_c^* as in the iron rich phosphate glasses studied by Sales [86]. These
 2265 separate correlation lines must be regarded as provisional however since the correlations for
 2266 different material types degrade into an uncorrelated broad scatter if T_f'/T_2 is plotted against
 2267 $Q' = x^2 \Delta h^* [R(1-x)]$.



2268
 2269 Fig. 5. Correlation between T_g/T_2 and AGF parameter B (equal to Q of eq. (109)). After ref.
 2270 [133].

2271
 2272 The stretched exponential parameter β also correlates with x and T_g/T_2 . The correlation
 2273 between x and β is shown in Fig. 6. Hodge [133] used the long standing idea, based on the
 2274 Adam-Gibbs concept of increasing size of relaxing groups and increasing cooperativity with
 2275 decreasing temperature, to suggest that β should approach 1.0 in the limit $T_f'/T_2 \rightarrow \infty$ ($x \rightarrow 1.0$)
 2276 and tend to zero as $T_f' \rightarrow T_2$ ($x \rightarrow 0$). A simple functional relation that satisfies these limits and
 2277 which is consistent with the approximately linear correlation observed between x and β is

$$2278 \frac{T_f'}{T_2} \approx \frac{A}{1-x} \approx \frac{B}{1-\beta}. \quad (194)$$

2279 As already noted independent experimental evidence for $\beta \rightarrow 0$ as $T \rightarrow T_2$ exists for o-
 2280 terphenyl and salol [269]. Two objections to eq. (194) have been raised however. First, although
 2281 its equilibrium form $T_f' = T$ is consistent with the strong temperature dependence of β observed
 2282 in many (but not all) materials (the o-terphenyl mixtures observed by Dixon and Nagel [269] for
 2283 example), it is inconsistent with the TN assumption that β is constant. This criticism can be
 2284 countered by appealing to the same reasoning used to explain the success of the generalized

2285 Arrhenius NM equation (Section 3.2.1), namely that the range in thermodynamic and fictive
 2286 temperatures over which relaxation occurs in a DSC scan is sufficiently small that β can be well
 2287 approximated as being constant. A second objection [273] is that eq. (194) is inconsistent for the
 2288 many other materials for which the linear values of β are constant (glycerol and propylene
 2289 glycol, for example [103]). In particular, the generally lower values of x for polymers implies a
 2290 stronger temperature dependence for z^* and therefore of β yet β is generally less temperature
 2291 dependent for polymers than for monomeric glasses. However the temperature dependence of z^*
 2292 from which eq. (194) is derived is weaker for $T \gg T_g$ than for $T \approx T_g$. Also, the range in T_f/T_2
 2293 over which significant changes in enthalpic β values occur ($\sim 1.11 - 2.5$) is much larger than the
 2294 typical ranges in T/T_2 over which linear data are acquired. Independent support for eq. (194)
 2295 has come from recent work by Moynihan and Schoeder [274] who described light scattering
 2296 evidence for nanoscale inhomogeneities in glass forming liquids that relax at different rates.
 2297 They suggested that this could be the source of nonexponentiality. Expressions relating the
 2298 nonlinearity parameters to the size of these regions were derived and the predicted sizes of the
 2299 inhomogeneities were shown to be in excellent agreement with those determined by other
 2300 methods. In this interpretation the physical significance of nonexponentiality lies in the
 2301 distribution of retardation times associated with the inhomogeneities rather than the inherent
 2302 nonexponentiality of cooperative or collective molecular motions. A temperature dependent β is
 2303 predicted that is consistent with β approaching zero as $T \rightarrow T_2$.

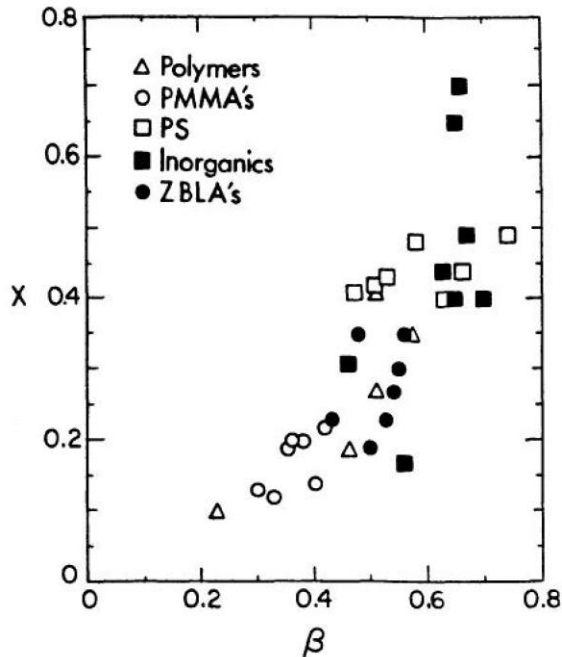
2304 Exceptions to eq. (194) nevertheless occur. For bulk and hydrogel imbibed aqueous
 2305 ethylene glycol (EG) and LiCl solutions [218] the value of β is much smaller for the solutions in
 2306 gel than in the bulk but the corresponding values of x and T_g/T_2 are very similar. The lower
 2307 values of β for the solutions imbibed in gel support the interpretation of a low β as originating
 2308 from a heterogeneous environment in the hydrogels rather than from increased cooperativity, if
 2309 it is assumed that these different environments have similar nonlinear characteristics. Sales [86]
 2310 observed that β was independent of composition in a series of phosphate glasses for which
 2311 T_g/T_2 changed systematically. The silicate glasses are also exceptional in having by far the
 2312 largest values of x and T_g/T_2 for any material, but normal values of β . The large values of
 2313 T_g/T_2 can reasonably be attributed to high values of $\Delta\mu$ associated with the breaking of a
 2314 covalent bond [275], and the relatively normal values of β can be attributed to the fact that, once
 2315 the chemical bond is broken, geometric constraints make further relaxation normally
 2316 cooperative. Thus the unusually tight three dimensional network structure of silicates may be
 2317 the reason for their exceptional enthalpy relaxation parameters.

2318

2319 7 Summary and Future Considerations

2320 The current phenomenologies give good to excellent descriptions of enthalpy relaxation
 2321 near equilibrium. For many (perhaps most) engineering applications, such as those discussed in
 2322 Scherer's book [9], they appear to be adequate. The Adam-Gibbs phenomenology provides
 2323 valuable insights into the physical origin of nonlinearity. It establishes a link between
 2324 nonlinearity and Angell's strong/fragile classification of liquid behavior, between nonlinearity
 2325 and the Kauzmann paradox, and provides a plausible rationalization of the correlations observed
 2326 between the NM parameters. As with the empirical NM and KAHHR equations, however, Adam-
 2327 Gibbs does not provide a satisfactory description of relaxation far from equilibrium. Resolution

2328 of the failure of these formalisms must be counted among the most important goals of future
 2329 research.
 2330



2331
 2332 Fig. 6. Correlation of NM parameter x with nonexponentiality parameter β . After ref. [133].

2333
 2334

2335 Moynihan [276] has attempted to modify the phenomenology in several ways to improve
 2336 the quality of fits, without success. The attempted modifications were as follows:

2337 (1) Make τ_i in $\phi(t) = \sum \exp(-t/\tau_i)$ depend partly on T_{fi} in addition to its dependence on

2338 the global T_f (in KAHR terms making τ_i a function of both δ_i and $\delta = \sum_i g_i \delta_i$:

$$2339 \quad \tau_i = \tau_{0i} \exp \left[\frac{x\Delta h^*}{RT} + \frac{y(1-x)\Delta h^*}{RT_{f(avg)}} + \frac{(1-y)(1-x)\Delta h^*}{RT_{fi}} \right]. \quad (195)$$

2340 No improvement was observed (best fits were obtained with $y = 1$).

2341 (2) Add a tail to the stretched exponential decay function:

$$2342 \quad \ln g(\tau) = \ln g_{KWW}(\tau) + K \ln^2(\tau/C). \quad (196)$$

2343 Best fits were obtained when $K = 0$, i.e. when $g(\tau_i)$ was the stretched exponential distribution.

2344 (3) Abandon thermorheological simplicity by making β depend on T or T_f . The introduction
 2345 of such dependences did not improve the situation, presumably because the range in T and T_f
 2346 over the glass transition is too small to significantly affect β (Section 6.5).

2347 (4) Change the form of the nonlinearity expression to make it more sensitive to $T - T_f$:

$$\tau = \tau_0 \exp \left[\frac{x\Delta h^*}{RT} + \frac{(1-x)\Delta h^*}{RT_f} + K(T_f - T)^3 \right]. \quad (197)$$

2349 No improvement was found.

2350 Ritland [11] also suggested a modification to $\tau(T, T_f)$,

$$dT_f / dt = \pm \left(|T - T_f| + k |T - T_f|^N \right) / \tau, \quad (198)$$

2352 which was evaluated by Scherer [154] for volume relaxation in a Na/Ca/SiO₂ glass. Scherer
 2353 found improved fits at large departures from equilibrium using $k = 1.0 \times 10^{-13}$ and $N = 7$,
 2354 corresponding to a modification of only one part in 10^6 in dT_f / dt for $T_f - T \approx 10$ K. Scherer
 2355 also noted that the stretched exponential parameter β decreased at smaller reduced times but that
 2356 although incorporating this into the calculation improved most of the fits not all of the data
 2357 could be described within uncertainties. Gupta and Huang [199] also noted a failure in the TN
 2358 phenomenology for rapidly quenched silicate fibers that were far from equilibrium, although
 2359 satisfactory fits could be made to slowly cooled bulk and fiber data obtained relatively close to
 2360 equilibrium. Rekhson and Ducroux [277] have described a phenomenology based on the AGF
 2361 equations in which a distribution in (Q_i) is assumed. The fastest time constants in $g(\ln \tau_i)$ are
 2362 characterized by the smallest Q_i . These authors showed that this phenomenology removed the
 2363 inconsistencies observed by Scherer.

2364 Since none of the modifications listed above allow all histories to be fit with a single set
 2365 of parameters it seems that a more fundamental change in the phenomenology is needed.
 2366 However any modification must converge to the present phenomenology in the limit of small
 2367 departures from equilibrium because the current methods for describing nonlinearity are
 2368 consistent with behavior seen near T_g . The search for a new phenomenology is made
 2369 particularly challenging by the fact that a rigorous theoretical derivation of nonlinearity, and of
 2370 the glass transition in general, is not yet in sight. The heuristic Adam-Gibbs approach is
 2371 probably still the best account available.

2372 A more modest short term goal is to parameterize more materials in more detail. The
 2373 validity of the correlations between x , Δh^* and β needs to be tested for many more material
 2374 types. More systematic studies of the type made by Sales [86] for lead and iron phosphate
 2375 glasses need to be made, and the relationship between the AGF T_2 , VTF T_0 , and Kauzmann T_K
 2376 temperatures needs to be better defined. For polymers the effects of crystallinity and
 2377 crosslinking density need further exploration.

2378 A rigorous and fully satisfactory account of experimental thermal transfer effects has not
 2379 yet been given. Although the data of O'Reilly and Hodge [89] at very slow heating rates
 2380 indicate that thermal transfer cannot account for all the observed fitting problems, a standard
 2381 and rigorous procedure for correcting for thermal transfer is needed. To date only Hutchinson
 2382 and coworkers [90,91] have explicitly addressed this issue.

2383 Despite the fact that enthalpy relaxation should now be considered to be a standard
 2384 experimental technique its inherent nonlinearity is too often not fully appreciated, or is
 2385 incorrectly handled, by too many practitioners. There are too many literature reports that contain
 2386 incorrect data analyses. It is to be hoped that this situation will improve and that the field will
 2387 continue to advance in the future.

2388 It is a pleasure to thank J.M. O'Reilly, W.M. Prest Jr. and A.J. Kovacs for valuable and

2389 stimulating discussions, G.W. Scherer and J.M. Hutchinson for their valuable comments and
2390 sharing some of their preprints and unpublished observations, and C.T. Moynihan for valuable
2391 discussions and permission to cite some results in advance of publication.
2392

2393 8. References

- 2394 [1] S.M. Rekhson, *J. Non-Cryst. Solids* 95&96 (1987) 131.
- 2395 [2] P.K. Gupta, *Rev. Solid State Sci.* 3 (1989) 221.
- 2396 [3] G.W. Scherer, *J. Non-Cryst. Solids* 123 (1990) 75.
- 2397 [4] J. Wong and C.A. Angell], *Glass: Structure by Spectroscopy* (Dekker, New York, 1976).
- 2398 [5] C.A. Angell], *Pure Appl. Chem.* 63 (1991) 1387.
- 2399 [6] L.C.E. Struik, *Physical Aging in Amorphous Polymers and Other Materials* (Elsevier, Amsterdam, 1978).
- 2400
- 2401 [7] A.R. Cooper, *Glastech. Ber.* 56K Bd.2 (1983) 1160.
- 2402 [8] A.R. Cooper and P.K. Gupta, *Phys. Chem. Glasses* 23 (1982) 44.
- 2403 [9] G.W. Scherer, *Relaxation in Glass and Composites* (Wiley-Interscience, New York, 1986).
- 2404
- 2405 [10] I.M. Hodge and C.A. Angell, *J. Phys. Chem.* 67 (1977) 1647.
- 2406 [11] H.N. Ritland, *J. Am. Ceram. Soc.* 37 (1954) 370.
- 2407 [12] C.T. Moynihan, A.J. Easteal, M.A. DeBolt and J. Tucker, *J. Am. Ceram. Soc.* 59 (1976) 12.
- 2408
- 2409 [13] G.S. Fulcher, *J. Am. Ceram. Soc.* 77 (1925) 3701.
- 2410 [14] G. Tamman and W. Hesse, *Z. Anorg. Allg. Chem.* 156 (1926)
- 2411 [15] H. Vogel, *Phys. Z.* 22 (1921) 645. The Vogel equation, $\eta(T) = \eta_{\infty}^{\frac{[T-T_1]}{T-T_{\infty}}}$ is
- 2412 superficially different from the Fulcher and Tamman-Hesse equations, but in fact **is**
- 2413 **easily shown to be** equivalent to them with $A = \ln \eta_{\infty}$, $B = \ln \eta_{\infty} (T_{\infty} - T_1)$ and $T_{\infty} = T_0$
- 2414 [G.W. Scherer, *J. Am. Ceram. Soc.* 75 (1992) 1060]. It is common practice to refer to eq.
- 2415 (3) as the Vogel-Tamman-Fulcher (VTF) equation, and with apologies to Hesse we
- 2416 continue this tradition here. A brief history of these equations has been given by Scherer
- 2417 in the paper cited above.
- 2418 [16] G. Adam and J.H. Gibbs, *J. Chem. Phys.* 43 (1965) 139.
- 2419 [17] M.L. Williams, R.F. Landell and J.D. Ferry, *J. Am. Chem. Soc.* 77 (1955) 3701.
- 2420 [18] J.D. Ferry, *Viscoelastic Properties of Polymers*, 3rd Ed. (Wiley, New York, 1980).
- 2421 [19] P.W. Anderson, comment in *Ann. NY Acad. Sci.* 484 (1986) 288.
- 2422 [20] C.A. Angell, *J. Phys. Chem. Solids* 49 (1988) 863.
- 2423 [21] C.A. Angell, *J. Non-Cryst. Solids* 131-133 (1991) 13.
- 2424 [22] Proc. 1st Int. Discussion Meeting on Relaxation in Complex Systems, Crete, June 1990,
- 2425 *J. Non-Cryst. Solids* 131-133 (1991).
- 2426 [23] Glasses can be in a (metastable) equilibrium state near T_g although these are probably
- 2427 better called supercooled liquids.
- 2428 [24] F. Simon, *Ergeb. Exact. Naturw.* 9 (1930) 225; *Anorg. Allgem. Chem.* 203 (1931) 220.
- 2429 [25] M. Goldstein, *Ann. NY Acad. Sci.* 279 (1976) 68.
- 2430 [26] M. Goldstein, *J. Chem. Phys.* 64 (1976) 4767.
- 2431 [27] M. Goldstein, in: *Modern Aspects of the Vitreous State*, ed. J.P. MacKenzie, Vol. 3
- 2432 (Butterworth, London, 1964) p. 90.
- 2433 [28] H.N. Ritland, *J. Am. Ceram. Soc.* 39 (1956) 403.
- 2434 [29] A.J. Kovacs, *J. Polym. Sci.* 30 (1958) 131.
- 2435 [30] K. Hofer, J. Perez, and G.P. Johari, *Philos. Mag. Lett.* 64 (1991) 37.
- 2436 [31] The observed scatter in the enthalpy results, obtained by integration of heat capacity

- 2437 curves, was comparable with that in adiabatic calorimetry [K. Adachi and T. Kotaka,
2438 Polym. J. 12 (1982) 959].
- 2439 [32] I.M. Hodge, in: *Relaxations in Complex Systems*, ed. K.L. Ngai and G.B. Wright
2440 (Office of Naval Research, Arlington, VA, 1984) p. 65.
- 2441 [33] S. Spinner and A. Napolitano, *J. Res. Nat. Bur. Stand.*, 70A (1966) 147.
- 2442 [34] H.R. Lillie, *J. Am. Ceram. Soc.* 19 (1936) 45.
- 2443 [35] M. Hara and S. Suetoshi, *Rep. Res. Lab. Asahi Glass Co.* 5 (1955) 126.
- 2444 [36] A.J. Kovacs, *Fortschr. Hochpolym.-Forsch.* 3 (1963) 394.
- 2445 [37] A.Q. Tool and C.G. Eichlin, *J. Am. Ceram. Soc.* 14 (1931) 275
- 2446 [38] A.Q. Tool, *J. Am. Ceram. Soc.* 29 (1946) 240.
- 2447 [39] A.Q. Tool and C.G. Eichlin, presentation at Am. Ceram. Soc. Meeting, Atlantic City,
2448 1924.
- 2449 [40] R. Gardon and O.S. Narayanaswamy, *J. Am. Ceram. Soc.* 53 (1970) 380.
- 2450 [41] O.S. Narayanaswamy, *J. Am. Ceram. Soc.* 54 (1971) 491.
- 2451 [42] C.T. Moynihan, P.B. Macedo, C.J. Montrose, P.K. Gupta, M.A. DeBolt J.F. Dill, B.E.
2452 Dom, P.W. Drake, A.J. Easteal, P.B. Elterman, R.P. Moeller, H. Sasabe and J.A. Wilder,
2453 *Ann. NY Acad. Sci.* 279 (1976) 15.
- 2454 [43] M.J. Richardson and N.G. Savill, *Polymer* 30 (1975) 2246.
- 2455 [44] J.H. Flynn, *Thermochim. Acta* 8 (1974) 69-
- 2456 [45] Yu.A. Sharonov and M.V. Volkenshtein, in *Structure of Glasses*, Vol. 6, ed. E.A. Porai-
2457 Koshits (Consultants Bureau, New York, 1966).
- 2458 [46] R.O. Davies and G.O. Jones, *Proc. R. Soc. (London)* 217A (1953) 27.
- 2459 [47] A.J. Kovacs, J.J. Aklonis, J.M. Hutchinson and A.R. Ramos, *J. Polym. Sci.* 17 (1979)
2460 1097.
- 2461 [48] J.M. Hutchinson and A.J. Kovacs, *J. Polym. Sci.-Phys.* 14 (1976) 1575.
- 2462 [49] O.S. Narayanaswamy, *J. Am. Ceram. Soc.* 71 (1988) 900.
- 2463 [50] O.V. Mazurin and Yu.K. Startsev, *Sov. J. Glass Phys. Chem. (Eng. Trans)* 7 (1981) 274.
- 2464 [51] I.M. Hodge and J.M. O'Reilly, *Polymer* 33 (1992) 4883. Equation (5) in this paper is
2465 mathematically incorrect but this does not affect the qualitative arguments given there.
2466 The correct expression for τ' is given by eq. (36) of the present paper.
- 2467 [52] G.W. Scherer, personal communication.
- 2468 [53] J.M.G. Cowie and R. Ferguson, *Polym. Commun.* 27 (1986) 258.
- 2469 [54] J.M.G. Cowie, S. Elliot, R. Ferguson and R. Simha, *Polym. Commun.* 28 (1987) 298.
- 2470 [55] J.L. Gomez-Ribelles, R. Diaz-Calleja, R. Ferguson and J.M.G. Cowie, *Polymer* 28
2471 (1987) 2262.
- 2472 [56] J.M.G. Cowie and R. Ferguson, *Macromolecules* 22 (1989) 2307.
- 2473 [57] J.M.G. Cowie and R. Ferguson, *Macromolecules* 22 (1989) 2312.
- 2474 [58] M. Oguni, H. Hikawa and H. Suga, *Thermochim. Acta* 158(1990)143.
- 2475 [59] S.Z.D. Cheng, D.P. Heberer, J.J. Janimak, S.I-1.-S. Lien and F.W. Harris, *Polymer* 32
2476 (1991) 2053.
- 2477 [60] C. Tsitsilianis and I. Mylonas, *Makromol. Chem. Rapid. Commun.* 13 (1992) 207.
- 2478 [61] W. Kauzmann, *Chem. Rev.* 43 (1948) 219.
- 2479 [62] C.A. Angell, in *Relaxations in Complex Systems*, ed. K.L. Ngai and G.B. Wright (Office
2480 of Naval Research, Arlington, VA, 1984) p. 3.
- 2481 [63] P. Richet and J. Bottinga, *Geochim. Cosmochim. Acta* 48 (1984) 453.
- 2482 [64] C.A. Angell and D.L. Smith, *J. Phys. Chem.* 86 (1982) 3845.

- 2483 [65] C.A. Angell and K.J. Rao, *J. Chem. Phys.* 57 (1972) 470, and references therein.
- 2484 [66] A.A. Miller, *Macromolecules* 11 (1978) 859.
- 2485 [67] F. Stillinger, *J. Chem. Phys.* 88 (1988) 7818.
- 2486 [68] C.A. Angell, D.R. MacFarlane and M. Oguni, *Proc. NY Acad. Sci.* 484 (1986) 241.
- 2487 [69] G. Vuillard, *Ann. Chim. (Paris)* 2 (1957) 223.
- 2488 [70] E.J. Sare, PhD thesis, Purdue University (1970).
- 2489 [71] J.H. Gibbs and E.A. DiMarzio, *J. Chem. Phys.* 23 (1958) 373.
- 2490 [72] P.D. Gujrati and M. Goldstein, *J. Chem. Phys.* 74 (1981) 2596.
- 2491 [73] E.A. DiMarzio and C.M. Guttman, *Macromolecules* 20 (1987) 1403.
- 2492 [74] A.J.-M. Yang and E.A. DiMarzio, *Macromolecules* 24 (1991) 6012.
- 2493 [75] P. Ehrenfest, *Commun., Kamerlingh Onnes Lab.*, U. Leiden (1933) 756.
- 2494 [76] C.A. Angell and W. Sichina, *Ann. NY Acad. Sci.* 279 (1976) 53.
- 2495 [77] J.M. O'Reilly, *J. Polym. Sci.* 57 (1962) 429.
- 2496 [78] G. McKenna, in: *Comprehensive Polymer Science*, Vol. 2, Polymer Properties, ed. C. Booth and C. Price (Pergamon, Oxford, 1989) Ch. 10.
- 2497 [79] C.T. Moynihan and A.V. Lesikar, *Ann. NY Acad. Sci.* 371 (1981) 152.
- 2499 [80] P.K. Gupta, *J. Non-Cryst. Solids* 102 (1988) 231.
- 2500 [81] B. Wunderlich and L.D. Jones, *J. Macromol. Sci. Phys.* B3 (1969) 67.
- 2501 [82] V.B.F. Mathot, *Polymer* 25 (1984) 579.
- 2502 [83] C. Alba, L.E. Busse and C.A. Angell, *J. Chem. Phys.* 92 (1990) 617.
- 2503 [84] P.B. Macedo and A. Napolitano, *J. Nat. Bur. Stand.* 71A (1967) 231.
- 2504 [85] Yu. Privalko, *J. Phys. Chem.* 84 (1980) 3307.
- 2505 [86] B.C. Sales, *J. Non-Cryst. Solids* 119 (1990) 136.
- 2506 [87] A.P. Gray, in *Analytical Calorimetry*, ed. R.S. Porter and J.F. Johnson (Plenum, New York, 1968).
- 2507 [88] M.A. DeBolt, PhD thesis, Catholic University of America (1976)
- 2509 [89] J.M. O'Reilly and I.M. Hodge, *J. Non-Cryst. Solids* 130-133 (1991) 451.
- 2510 [90] J.M. Hutchinson, M. Ruddy and M.R. Wilson, *Polymer* 29 (1983) 152.
- 2511 [91] J.M. Hutchinson and M. Ruddy, *J. Polym. Sci.* 26 (1988) 2341.
- 2512 [92] C.T. Moynihan, A.J. Easteal, J. Wilder and J. Tucker, *J. Phys. Chem.* 78 (1974) 2673.
- 2513 [93] R.R. Lagasse, *J. Polym. Sci. Polym. Phys. Ed.* 20 (1982) 279.
- 2514 [94] S.C. Mraw, *Rev. Sci. Instrum.* 53 (1982) 228.
- 2515 [95] M.J. Richardson and P. Burrington, *J. Therm. Anal.* 6 (1974) 345.
- 2516 [96] J.M. Hutchinson, *Progr. Coll. Polym. Sci.* 87 (1992) 69.
- 2517 [97] W.M. Prest Jr., unpublished results.
- 2518 [98] M.J. Richardson, *J. Polym. Sci.* C38 (1972) 251.
- 2519 [99] A.P. Gray, *Thermochim. Acta* 1 (1970) 563.
- 2520 [100] N.O. Birge and S.R. Nagel, *Phys. Rev. Lett.* 54 (1985) 2674.
- 2521 [101] N.O. Birge and S.R. Nagel, *Rev. Sci. Instrum.* 58 (1987) 1464.
- 2522 [102] N. Menon, K.P. O'Brien, P.K. Dixon, L. Wu, S.R. Nagel, B.D. Williams and J.P. Carini, *J. Non-Cryst. Solids* 141 (1992) 61.
- 2523 [103] N.O. Birge, *Phys. Rev.* B34 (1986) 1631.
- 2525 [104] R. Kohlrausch, *Pogg. Ann. Phys.* 91 (1854) 198.
- 2526 [105] R. Kohlrausch, *Pogg. Ann. Phys.* 119 (1863) 352.
- 2527 [106] G. Williams and D.C. Watts, *Trans. Faraday Soc.* 66 (1970) 80.
- 2528 [107] G. Williams, D.C. Watts, S.B. Dev and A.M. North, *Trans. Faraday Soc.* 67 (1971)

- 2529 1323.
- 2530 [108] M. Abramowitz and I.A. Stegun, Handbook of Mathematical Functions, (Dover, New
2531 York, 1965).
- 2532 [109] C.T. Moynihan, L.P. Boesch and N.L. Laberge, Phys. Chem. Glasses 14 (1973) 122.
- 2533 [110] C.P. Lindsey and G.D. Patterson, J. Chem. Phys. 73 (1980) 3348.
- 2534 [111] I.M. Hodge, unpublished calculations.
- 2535 [112] S. Opalka, PhD thesis, Rensselaer Polytechnic Institute (1987).
- 2536 [113] C.T. Moynihan, S.N. Crichton and S.M. Opalka, J. Non-Cryst. Solids 131-133 (1991)
2537 420.
- 2538 [114] D.W. Davidson and R.H. Cole, J. Chem. Phys. 18 (1951) 1417.
- 2539 [115] A.V. Tobolsky, Properties and Structure of Polymers (Wiley, New York, 1960).
- 2540 [116] H. Frohlich, Theory of Dielectrics (Oxford, Oxford, 1958).
- 2541 [117] K.S. Cole and R.H. Cole, J. Chem. Phys. 9 (1949) 341.
- 2542 [118] S. Havriliak and S. Negami, J. Polym. Sci. C14 (1966) 99.
- 2543 [119] S.H. Glarum, J. Chem. Phys. 33 (1960) 639, 1371.
- 2544 [120] In Ref. [41], Narayanaswamy introduced eq. (87) using a reference temperature, T_B ,
2545 which is rarely used nowadays.
- 2546 [121] P.B. Macedo and A. Napolitano, J. Chem. Phys. 49 (1963) 1837.
- 2547 [122] H. Tweer, N. Laberge and P.B. Macedo, J. Am. Ceram. Soc. 54 (1971) 121.
- 2548 [123] W.T. Laughlin and D.R. Uhlmann, J. Phys. Chem. 76 (1972) 2317.
- 2549 [124] M. Goldstein, J. Chem. Phys. 43 (1965) 1852.
- 2550 [125] A.J. Kovacs, J.M. Hutchinson and J.J. Aklonis, in The Structure of Non-Crystalline
2551 Materials, ed. P.H. Gaskell (Taylor and Francis, London, 1977) p. 153.
- 2552 [126] D.J. Plazek and J.H. Magill, J. Chem. Phys. 45 (1966) 3038.
- 2553 [127] J.H. Magill, J. Chem. Phys. 47 (1967) 2802.
- 2554 [128] F.S. Howell, P.A. Bose, P.B. Macedo and C.T. Moynihan, J. Phys. Chem. 78 (1974)
2555 639.
- 2556 [129] G.W. Scherer, J. Am. Ceram. Soc. 67 (1984) 504.
- 2557 [130] I.M. Hodge, Macromolecules 20 (1987) 2897.
- 2558 [131] J. Huang and PK. Gupta, J. Non-Cryst. Solids 139 (1992) 239.
- 2559 [132] C.A. Angell and R.D. Bressel, J. Phys. Chem. 76 (1972) 3244.
- 2560 [133] I.M. Hodge, J. Non-Cryst. Solids 131-133 (1991) 435.
- 2561 [134] J.P. Sethna, Europhys. Lett. 6 (1988) 529.
- 2562 [135] D.S. Fisher, Phys. Rev. Lett. 56 (1936) 416.
- 2563 [136] P.K. Dixon, S.R. Nagel and D.A. Weitz, J. Chem. Phys. 94 (1991) 6924.
- 2564 [137] R.M. Ernst, S.R. Nagel and G.S. Gresl, Phys. Rev. B43 (1991) 8070.
- 2565 [138] V.N. Lovikov and A.P. Sokolov, Solid State Commun. 77 (1991) 243.
- 2566 [139] L. Botjesson, A.K. Hassan, J. Swenson, L.M. Torell and A. Fontana, Phys. Rev. Lett. 70
2567 (1993) 1275.
- 2568 [140] G.H. Frederickson, Ann. Rev. Phys. Chem. 39 (1988) 149, and references therein.
- 2569 [141] H. Sasabe, M.A. DeBolt, P.B. Macedo and C.T. Moynihan, in Proc. of the 11th Int.
2570 Congr. on Glass, Prague (1977) p. 339.
- 2571 [142] A. Napolitano, J.H. Simmons, J.H. Blackburn and R.E. Chichester, J. Res. Natl. Bur.
2572 Stand. 78A (1974) 373.
- 2573 [143] M. Goldstein and M. Nakonecznyi, Phys. Chem. Glasses 6 (1965) 126.
- 2574 [144] P.B. Macedo and T.A. Litovitz, J. Chem. Phys. 62 (1965) Z45.

- 2575 [145] A.K. Doolittle, *J. Appl. Phys.* 22 (1951) 1471.
- 2576 [146] M.H. Cohen and D. Turnbull, *J. Chem. Phys.* 31 (1959) 1164.
- 2577 [147] G.J. Dienes, *J. Appl. Phys.* 24 (1953) 779.
- 2578 [148] O.V. Mazurin, V.P. Kluyer and S. Stlyar, *Glastech. Ber.* 56 (1983) 1148.
- 2579 [149] J.J. Trilbone, J.M. O'Reilly and J. Greener, *J. Polym. Sci. Polym. Phys. Ed.* 27 (1989)
2580 837.
- 2581 [150] C.T. Moynihan, P. Macedo, N. Saad, M. DeBolt, B. Dom, A. Easteal and J. Wilder, *Fiz. Khim. Stekla* 1 (1975) 420 (English translation: *Sov. J. Phys. Chem. Glasses* 1 (1975)
2582 392).
- 2583
- 2584 [151] O.V. Mazurin, S.M. Rekhson and Yu.K. Startsev, *Fiz. Khim. Stekla* 1 (1975) 438.
- 2585 [152] I.M. Hodge and A.R. Berens, *Macromolecules* 15 (1982) 762.
- 2586 [153] W.M. Prest .Jr., F.J. Roberts and I.M. Hodge, in: *Proc. 12th NATAS Conference*, ed.
2587 J.C. Buck (NATAS, 1983) p. 119.
- 2588 [154] G.W. Scherer, *J. Am. Ceram. Soc.* 69 (1986) 374.
- 2589 [155] S.M. Rekhson, *J. Non-Cryst. Solids* 84 (1986) 68.
- 2590 [156] S.M. Rekhson, A. Bulaeva and O.V. Mazurin, *Izv. Akad. Nauk. SSSR, Neorg. Mater.* 7
2591 (1971) 714.
- 2592 [157] S.M. Opalka and C.T. Moynihan, presented at *Int. Congress on Glasses, Leningrad*
2593 (1989).
- 2594 [158] R.W. Rendell and K.L. Ngai, in *Relaxations in Complex Systems*, ed. K.L. Ngai and
2595 G.B. Wright (Office of Naval Research, Arlington, VA, 1984) p. 309.
- 2596 [159] C.T. Moynihan, personal communication (to be published).
- 2597 [160] M.A. DeBolt, A.J. Easteal, P.B. Macedo and C.T. Moynihan, *J. Am. Ceram. Soc.* 59
2598 (1976) 16.
- 2599 [161] I.M. Hodge, *Macromolecules* 16 (1983) 898.
- 2600 [162] J.J. Tribone, J.M. O'Reilly and J. Greener, *Macromolecules* 19 (1986) 1732.
- 2601 [163] J.M. Hutchinson and M. Ruddy, *J. Polym. Sci. Polym. Sci. Ed.* 28 (1990) 2127
- 2602 [164] C.T. Moynihan, A.J. Bruce, D.L. Gavin, S.R. Loehr, S.M. Opalka and M.G. Drexhage,
2603 *Polym. Eng. Sci.* 24 (1984) 1117.
- 2604 [165] A.J. Kovacs and J.M. Hutchinson, *J. Polym. Sci. Polym. Phys.* 17 (1979) 2031.
- 2605 [166] J.M. Hutchinson and M. Ruddy, *Makromol. Chem. Macromol. Symp.* 27 (1989) 319.
- 2606 [167] J.M. Hutchinson and A.J. Kovacs, *Polym. Eng. Sci.* 24 (1984) 1087.
- 2607 [168] A.R. Ramos, J.M. Hutchinson and A.J. Kovacs, *J. Polym. Sci. Polym. Phys. Ed.* 22
2608 (1984) 1655.
- 2609 [169] R.R. Lagasse, R.E. Cohen and A. Letton, *J. Polym. Sci. Polym. Phys. Ed.* 20 (1982) 375.
- 2610 [170] J.M. Hutchinson and A.J. Kovacs, *J. Polym. Sci. Phys. Ed.* 21 (1983) 2415.
- 2611 [171] I. Avramov, E. Grantscharova and I. Gutzow, *J. Non-Cryst. Solids* 91 (1987) 386.
- 2612 [172] I. Avramov, E. Grantscharova and I. Gutzow, *J. Non-Cryst. Solids* 104 (1988) 148.
- 2613 [173] S.N. Crichton and C.T. Moynihan, *J. Non-Cryst. Solids* 99 (1988) 413.
- 2614 [174] J.M. Hutchinson and M. Ruddy, *J. Non-Cryst. Solids* 108 (1989) 225.
- 2615 [175] J.M. Hutchinson, *J. Polym. Sci. Polym. Phys. Ed.* 29 (1991) 1303.
- 2616 [176] D.M. Marquardt, *J. Soc. Indust. Appl. Math.* 11 (1963) 431.
- 2617 [177] I.M. Hodge and G.S. Huvad, *Macromolecules* 16 (1983) 371.
- 2618 [178] J.L. Kuester and J.H. Mize, *Optimization Techniques with Fortran* (McGraw-Hill, New
2619 York, 1973) PP. 240-250.
- 2620 [179] P.R. Bevington, *Data Reduction and Error Analysis for the Physical Sciences* (McGraw-

- 2621 Hill, New York, 1969).
- 2622 [180] I.M. Hodge and A.R. Berens, *Macromolecules* 18 (1985) 1980.
- 2623 [181] A.R. Ramos, A.J. Kovacs, J.M. O'Reilly, I.J. Tribone and J. Greener, *J. Polym. Sci. B26*
2624 (1988) 501.
- 2625 [182] M.V. Volkenstein and Yu.A. Sharonov, *Vysokomol. Soedin.* 3 (1961) 1739.
- 2626 [183] C.R. Foltz and P.V. McKinney, *J. Appl. Polym. Sci.* 13 (1969) 2235.
- 2627 [184] S.E.B. Petrie, *J. Polym. Sci. P311 A>2* 10 (1972) 1255.
- 2628 [185] R. Straff and D.R. Uhlmann, *J. Polym. Sci. Polym. Phys. Ed.* 14 (1975) 1087.
- 2629 [186] J.M. O'Reilly, *J. Appl. Phys.* 50 (1979) 6083.
- 2630 [187] M.S. Ali and R.P. Sheldon, *J. Appl. Polym. Sci.* 14 (1970) 2619.
- 2631 [188] Z.H. Ophir, J.A. Emerson and G.L. Wilkes, *J. Appl. Phys.* 69 (1978) 5032.
- 2632 [189] M. Bosma, G. ten Brinke and T.S. Ellis, *Macromolecules* 21 (1988) 1465.
- 2633 [190] R. Grooten and G. ten Brinke, *Macromolecules* 22 (1989) 1761.
- 2634 [191] X. Quan, H.E. Bair and G.E. Johnson, *Macromolecules* 22 (1989) 4631.
- 2635 [192] G. ten Brinke, *Macromolecules* 23 (1990) 1225.
- 2636 [193] J. Mijovic, T. Ho and T.K. Kwei, *Polym. Eng. Sci.* 29 (1989) 1604.
- 2637 [194] T. Ho and J. Mijovic, *Macromolecules* 23 (1990) 1411.
- 2638 [195] M.H. Lehr, R.G. Parker and R.A. Komoroski, *Macromolecules* 18 (1985) 1265.
- 2639 [196] A. Halbrucker and E. Mayer, *J. Phys. Chem.* 91 (1987) 503.
- 2640 [197] G.P. Johari, A. Halbrucker and E. Mayer, *Nature* 330 (1987) 552.
- 2641 [198] K. Hofer, A. Halbrucker, E. Mayer and G.P. Johari, *J. Phys. Chem.* 93 (1989) 4674.
- 2642 [199] P.K. Gupta and J. Huang, *J. Non-Cryst. Solids*, 151 (1992) 175.
- 2643 [200] S.B. Warner, *Macromolecules* 13 (1980) 450.
- 2644 [201] P.G. Hedmark, R.W.R. Dick and U.W. Gedde, *Polym. Bull.* 23 (1990) 83.
- 2645 [202] S.E.B. Petrie, in: *Polymeric Materials: Relationships Between Structure and Mechanical*
2646 *Behavior*, ed. E. Baer and S. Radcliffe (American Society for Metals, Metals Park, OH,
2647 1974) p. 55.
- 2648 [203] R. B. Stephens, *J. Appl. Phys.* 49 (1978) 5855.
- 2649 [204] H.-L. Ma, X.-H. Zhang, J. Lucas, H. Senapati, R. Bohmer and C.A. Angel], *J. Solid*
2650 *State Chem.* 96 (1992) 181.
- 2651 [205] M. Tatsumisago, B.L. Halfpap, J.L. Green, S.M. Lindsay and C.A. Angel], *Phys. Rev.*
2652 *Lett.* 64 (1990) 1549.
- 2653 [206] G.W. Koebrugge, J. Sietsma and A. van den Beukel, *Acta Metall. Mater.* 40 (1992) 753.
- 2654 [207] F. Sommer, H. Haas and B. Predel, *J. Non-Cryst. Solids* 618162 (1984) 793.
- 2655 [208] K.-H. Illers, *Makromol. Chem.* 127 (1969) 1.
- 2656 [209] A. Gray and M. Gilbert, *Polymer* 17 (1976) 44.
- 2657 [210] H.S. Chen and T.T. Wang, *J. Appl. Phys.* 52 (1981) 5898.
- 2658 [211] M. Ruddy and J.M. Hutchinson, *Polym. Commun.* 29 (1988) 132.
- 2659 [212] M.G. Wysgoski, *J. Appl. Polym. Sci.* 25 (1980) 1455.
- 2660 [213] A.R. Berens and I.M. Hodge, *Macromolecules* 15 (1982) 756.
- 2661 [214] H.S. Chen and C.R. Kurkjian, *J. Am. Ceram. Soc.* 66 (1983) 613.
- 2662 [215] J.L. Gomez Ribelles, A. Ribes Greus and R. Diaz Calleja, *Polymer* 31 (1990) 223.
- 2663 [216] R. Diaz Calleja, J. Perez, J.L. Gomez Ribelles, and A. Ribes Greus, *Makromol. Chem.*
2664 *Macromol. Symp.* 27 (1989) 289.
- 2665 [217] M. Ribas, *Progr. Colloid Polym. Sci.* 87 (1992) 78.
- 2666 [218] K. Hofer, E. Mayer and I.M. Hodge, *J. Non-Cryst. Solids* 139 (1992) 78.

- 2667 [219] H. Senapati and C.A. Angell, *J. Non-Cryst. Solids* 130 (1991) 53.
- 2668 [220] C.B. McGowan, D.Y. Kim and R.B. Blumstein, *Macromolecules* 25 (1992) 4658.
- 2669 [221] Z. Altounian, J.O. Strom-Olsen and M. Olivier, *J. Mater. Sci.* 2 (1987) 54.
- 2670 [222] H.S. Chen, *J. Non-Cryst. Solids* 46 (1981) 289.
- 2671 [223] H.S. Chen and A. Inoue, *J. Non-Cryst. Solids* 61&62 (1984) 805.
- 2672 [224] A. Inoue, T. Masumoto and H.S. Chen, *J. Mater. Sci.* 19 (1984) 3953.
- 2673 [225] A. Inoue, T. Masumoto and H.S. Chen, *J. Mater. Sci.* 20 (1985) 4057.
- 2674 [226] H.S. Chen, A. Inoue and T. Masumoto, *J. Mater. Sci.* 20 (1985) 2417.
- 2675 [227] M.J. Richardson and N.G. Savill, *Br. Polym. J.* 11 (1979) 123.
- 2676 [228] A. Weitz and B. Wunderlich, *J. Polym. Sci., Polym. Phys. Ed.* 12 (1974) 2473.
- 2677 [229] J.E. Yourtee and S.L. Cooper, *J. Appl. Polym. Sci.* 18 (1974) 897.
- 2678 [230] W.C. Dale and C.E. Rogers, *J. Appl. Phys.* 42 (1971) 4917.
- 2679 [231] R.G. Brown, R.E. Wetton, M.J. Richardson and N.G. Savill, *Polymer* 19 (1978) 659.
- 2680 [232] R.M. Kimmel and D.R. Uhlmann, *J. Appl. Polym. Phys.* 42 (1971) 4917.
- 2681 [233] C. Price, *Polymer* 16 (1975) 585.
- 2682 [234] R.E. Wetton and H.G. Money Penny, *Br. Polym. J.* 7 (1975) 51.
- 2683 [235] W.M. Prest Jr. and F.J. Roberts Jr., *Ann. N.Y. Acad. Sci.* 371 (1981) 67.
- 2684 [236] W.M. Prest Jr., J.M. O'Reilly, F.J. Roberts Jr. and R.A. Masher, *Polym. Eng. Sci.* 21 (1981) 1181.
- 2686 [237] J.M. Hutchinson, M.D. Ingram and A.1-1. Robertson, *Philos. Mag.* B66 (1992) 449.
- 2687 [238] A.R. Berens and I.M. Hodge, *Polym. Eng. Sci.* 24 (1984) 1123.
- 2688 [239] T.E. Brady and S.A. Jabarin, *Polym. Eng. Sci.* 17 (1977) 686.
- 2689 [240] A.R. Shultz and A.L. Young, *Macromolecules* 13 (1980) 663.
- 2690 [241] A.H. Chan and D.R. Paul, *J. Appl. Polym. Sci.* 24 (1979) 1539.
- 2691 [242] J.E. McKinney and R. Simha, *J. Res. Nat. Bur. Stand. Sect. A* 81A (1977) 283.
- 2692 [243] ZBLA is an acronym for zirconium-barium-lanthanum-aluminum.
- 2693 [244] J.M. Hutchinson, M.D. Ingram and A.J. Pappin, *J. Non-Cryst. Solids* 131-133 (1991) 483.
- 2694 [245] M.D. Ingram, J.M. Hutchinson and A.J. Pappin, *Phys. Chem. Glasses* 32 (1991) 121.
- 2696 [246] V.P. Privalko, S.S. Demchenko and Yu.S. Lipatov, *Macromolecules* 19 (1986) 901.
- 2697 [247] G.C. Stevens and M.J. Richardson, *Polym. Commun.* Z6 (1985) 77.
- 2698 [248] L. Aras and M.J. Richardson, *Polymer* 30 (1989) 2246.
- 2699 [249] B. Wunderlich, D.M. Bodily and M.H. Kaplan, *J. Appl. Phys.* 35 (1964) 95.
- 2700 [250] H. Sasabe and C.T. Moynihan, *J. Polym. Sci.* 16 (1978) 1447.
- 2701 [251] H.-J. Ott, *Colloid Polym. Sci.* Z57 (1979) 486.
- 2702 [252] I. Avramov, G. Gnappi and A. Montenero, *Phys. Chem. Glasses* 33 (1992) 140.
- 2703 [253] Y. Ishida and K. Yamafuji, *Kolloid Z.* 177 (1961) 7.
- 2704 [254] A.J. Pappin, J.M. Hutchinson and M.D. Ingram, *Macromolecules* 25 (1992) 1084.
- 2705 [255] M.R. Tant and G.L. Wilkes, *J. Appl. Polym. Sci.* 26 (1981) 2813.
- 2706 [256] J. Menczel and B. Wunderlich, *J. Polym. Sci. Polym. Lett. Ed.* 19 (1981) 261.
- 2707 [257] A.J. Easteal, J.A. Wilder, R.K. Mohr and C.T. Moynihan, *J. Am. Ceram. Soc.* 60 (1977) 134.
- 2708 [258] C.T. Moynihan, H. Sasabe and J. Tucker, in *Proc. Int. Symp. on Molten Salts* (Electrochemical Society, Pennington, NJ, 1976) p. 182.
- 2710 [259] C.T. Moynihan, A.J. Easteal, D.C. Tran, J.A. Wilder and E.P. Donovan, *J. Am. Ceram.*
- 2711

- 2712 Soc. 59 (1976) 137.
- 2713 [260] S.N. Crichton and C.T. Moynihan, *J. Non-Cryst. Solids* 102 (1988) 222.
- 2714 [261] 5P2E is an acronym for '5-phenyl 2-ether', the chemical formula of which
2715 $C_6H_5(OC_6H_4)_3OC_6H_5$.
- 2716 [262] C.A. Angell, *J. Non-Cryst. Solids* 102 (1988) 205.
- 2717 [263] J.M. O'Reilly, H.E. Bair and F.E. Karasz, *Macromolecules* 15 (1982) 1083.
- 2718 [264] F.E. Karasz, H.E. Bair and J.M. O'Reilly. *J. Phys. Chem.* 69 (1965) 2657.
- 2719 [265] A.A. Miller, *Macromolecules* 3 (1970) 674.
- 2720 [266] Y. Ishida, *Kolloid Z.* 168 (1960) 29.
- 2721 [267] N.G. McCrum, B.E. Read and G. Williams, *Anelastic and Dielectric Effects in*
2722 *Polymeric Solids* (Dover, New York, 1991).
- 2723 [268] E.V. Gouinlock, *J. Polym. Sci. Polym. Phys. Ed.* 13 (1975) 1533.
- 2724 [269] P.K. Dixon and S.R. Nagel, *Phys. Rev. Lett.* 61 (1988) 341.
- 2725 [270] S.R. Nagel and P.K. Dixon, *J. Chem. Phys.* 90 (1989) 3885.
- 2726 [271] P.K. Dixon, *Phys. Rev. B* 42 (1990) 8179.
- 2727 [272] R.J. Greet and D. Turnbull, *J. Chem. Phys.* 47 (1967) 2185.
- 2728 [273] K.L. Ngai and R.W. Rendell, in: *The Physics of Non-Crystalline Solids*, ed. L.D. Pye,
2729 W.C. La Course and H.J. Stevens (Taylor and Francis, London, 1992) p. 309.
- 2730 [274] C.T. Moynihan and J. Schroeder, *J. Non-Cryst. Solids* 160 (1993) 52.
- 2731 [275] C.T. Moynihan and S. Cantor, *J. Chem. Phys.* 48 (1968) 115, and references therein.
- 2732 [276] C.T. Moynihan, oral presentation at Int. Conf. on Relaxation in Complex Systems, Crete,
2733 June 1990.
- 2734 [277] S. Rekhson and J.-P. Ducroux, in: *The Physics of NonCrystalline Solids*, ed. L.D. Pye,
2735 W.C. La Course and H.J. Stevens (Taylor and Francis, London, 1992) p. 315.